Università degli Studi di Firenze

DOTTORATO DI RICERCA IN
"Oncologia Sperimentale e Clinica"

CICLO XXV

COORDINATORE Prof. Persio Dello Sbarba

# Identification and characterization of genes involved in the development and progression of colorectal and endometrial cancers

Settore Scientifico Disciplinare MED/04


**Dottorando**

Dott. Angelo Fortunato

**Tutore**

Prof. Annarosa Arcangeli


Anni 2010/2012

**TABLE OF CONTENTS**

# Chapter 1

## hERG1 ion channels are involved in the epithelial to mesenchymal transition in colorectal cancer

**ABSTRACT**

The transition between the epithelial to mesenchymal states (EMT) has a paramount role in carcinomas progression. The EMT allows cells to acquire mobility, stem-like behavior and resistance to apoptosis and consequently to drug treatments. These features make the EMT a central process in tumor biology. HCT116 colorectal cancer cell line show a mesenchymal molecular profile and hERG1 gene high expression. We knock-down the expression of hERG1 gene in the HCT116 cells by lentivirus mediated RNAi. The silencing of hERG1 gene has several consequences: a change on cell morphology, the reduction of the proliferative and tumorigenic capacity of the cells both *in vitro* and *in vivo* and a significant reduction of HCT116 cells cisplatin resistance. Notably, the knock-down of hERG1 determines a change in the molecular profile of HCT116 cells in the direction of a more epithelial profile confirmed by microarray analysis. Moreover, we identified several novel genetic interactions with hERG1 gene. Collectively our data suggesting an involvement of hERG1 ion channel in EMT. These data confirm previous studies that suggesting the involvement of hERG1 in tumor progression and identify one of the main biological process in which this gene is involved. This finding underlines the importance of hERG1 in colorectal cancer biology.

# INTRODUCTION

The transition between the epithelial to mesenchymal states (EMT) is a fundamental event in the acquisition of an invasive tumor phenotype and therefore constitutes a key event in tumor progression (Thiery, 2006; Hugo, 2007; Yang 2008; Baum, 2008; Polyak, 2009). EMT allows cells to acquire motility, invasiveness, resistance to apoptosis and stem-like characteristics.

EMT transition is accompanied by a profound reorganization of plasma membrane ion channels during development (Huber, 2000) and there are several reports suggesting the involvement of ion channels in EMT transition in cancer. For instance, $Ca^{2+}$ influx contribute to regulate EMT in human breast cancer cells (Hu, 2011; Davis, 2012) and the EAG1 potassium channel expression is up-regulated during EMT in lung cancer cells (Restrepo-Angulo, 2011).

Potassium channels are a large class of ion channels and are involved in diverse functions. They are abundant in excitable cells but they are also expressed in different tissues and physiological processes (Schwarz, 2004). Potassium channels contribute to regulate the membrane potential, cell volume and intracellular pH change during cell-cycle progression (Kunzelmann, 2005). $K^+$ channels are often deregulated in tumors and they contribute to the pathological behavior of cancer cells. In cancer, they are involved in signaling, evasion of apoptosis, proliferation, angiogenesis, tissue invasion and metastasis (Arcangeli, 2009; 2010). The blockage of $K^+$ channels has an antiproliferative effect in different types of cells (Arcangeli, 2010). hERG1 (other aliases: KCNH2, Kv11.1) potassium channels are over expressed in several types of tumors, including colorectal adenocarcinoma, assuming function not strictly related to the canonical ion flux function (Arcangeli, 2009; 2010). In particular, hERG1 channels can form macromolecular complexes with integrin receptors (Arcangeli, 2006; Bechetti, 2010). This protein-protein interaction has the function to modulate the adhesive interactions of cells with the extracellular matrix, promoting cell motility and

invasiveness but, the integrin-channel complex can also regulate downstream signaling pathways involving protein kinases (Becchetti, 2010).

Colorectal cancer is a molecularly heterogeneous tumor and currently there is not a specific molecular profile that characterize this disease (Laboda, 2011; Hogan, 2012). However, unsupervised gene expression analysis of colorectal cancer correlate the EMT molecular signature with poor surviving of patients (Laboda, 2011). For these reasons the identification of genes that regulate EMT in colorectal cancer could contribute to identify new molecular prognostic markers and therapeutic targets.

In this study we characterize the role of hERG1 potassium channel in the transition between the epithelial to mesenchymal states by using the HCT116 colorectal cancer cells as model.

## MATERIALS AND METHODS

### hERG1 lentivirus mediated interference of RNA (RNAi).

We used lentivirus vectors to transduce colorectal cancer cells with shRNA constructs capable of post-transcriptional silence specific genes. Each shRNA construct (commercially distributed by Open Biosystems) included a hairpin of 21 base pair sense and antisense stem and a 6 base pair loop cloned into the pLKO.1 lentiviral vector harboring a puromycin resistance gene. When the shRNA are processed by cellular enzymes they become activated (siRNA), eventually leading to the degradation of the complementary mRNAs by the RNA interference machinery. In order to test preliminarily the effectiveness of the shRNA commercially distributed by Open Biosystems, HCT116 cells were transfected by using Lipofectamine® 2000 Transfection Reagent (Invitrogen ™), according to the manufacturer's instructions. Then, we produced lentivirus particles by co-transfecting 2$^{nd}$ generation lentiviral plasmids and the transfer vector construct into the HEK293T packaging cell line. Successively, we transduced colorectal cancel HCT116 cells with virus at Multiplicity Of Infection (MOI)=3 and 5. Subsequently we selected stable silenced cell lines by using puromycin.

### Cell biology

HCT116, H630, HCT8, CACO2 and HT29 cell lines were purchased from the American Type Culture Collection (ATCC) (Rockville, MD). HCT116, H630 and HCT8 cells were grown in RPMI-1640 medium (EuroClone), CACO2 cells were grown in DMEM (EuroClone) and HT29 cells were grown in McCoy's medium (EuroClone) supplemented with 2% L-Glut, 10% fetal bovine serum (FBS) (Hyclone) and 1% penicillin/streptomycin at 37°C in a humidified 5% $CO_2$ atmosphere.

For soft agar colony forming assay, a bottom layer of 0.5% low melting agarose in RPMI medium, supplemented with 2% L-glu and 10% FBS was prepared in 60mm plates. After the bottom layer was solidified, cells were added in culture medium containing 0.35% agarose in RPMI medium supplemented with 2% L-glu, 10% FBS, 1% penicillin/streptomycin and puromicin (1.5µg/µl). After 30 minutes, plates were incubated 15 days at 37 °C in 5% CO2 atmosphere. The experiments were performed in triplicate for each cell lines used. Pictures of colonies of each plates were taken and the diameter of colonies measured.

To estimate the growth rate of cell lines over the time $5x10^3$ cells of the controls and experimental cell lines were sided in 6 well plates. Every day cells from a sub-set of wells were detached and counted for six consecutive days. To avoid any error in the cell counting during plates siding that could vitiates all subsequent counting, the value of the cell number obtained on the first day was used to normalize the number of cells of the following days.

To investigate whether the cell cycle was effected by hERG1 silencing, $3\ x10^5$ cells were seeded in 35mm multi-well plates in RPMI medium, supplemented with 2% L-glu, puromicin (1.5µg/µl) and 10% FBS. After 24 hours cells were washed with PBS and fresh medium without serum was added to synchronize the cell cycle. After 6 (t=6), 18 (t=18) and 24 (t=24) hours cells were washed in PBS and stained with PI in presence of TRITON. Subsequently cells were detached from plates by using a scraper, collected in polystyrene tubes and incubated at 4°C per 30 minutes. Cell cycle were analyzed with a cytoflorimeter. Each measurement was done twice.

***In vivo* experiments**

We injected $2\times10^6$ cells (pLKO.1 and sh7 cell lines) in nu/nu mice resuspended in 100 µl culture medium into the flanks of nude mice. The tumor masses development were monitorated for 18 days.

**Analysis of apoptosis by flow cytometry**

We investigated the sensitivity to cisplatin of 4 colorectal cancer cell lines: HCT116, HCT8, H630 and HT29 by flow cytometry. In order to perform this experiment, $1.5x10^5$ cells per well were seeded in 6-well plates (Costar, Corning). After 24 hours the cells were treated with 100 µM concentrations of cisplatin for 24h. Thus, we detected apoptotic and necrotic cells by FACSCanto flow cytometry (Becton Dickinson), using a Annexin-V-FLUOS staining kit (Roche). Then, we investigated the sensitivity to cisplatin of the control pLKO.1 and silenced (sh4 and sh7) cell lines (MOI=3) derived from HCT116 cells. Cells were treated with 3 different concentrations of cisplatin (124.5 µM, 174.3 µM, 224.1 µM) for 24h and analysed by using the protocol described above.

**Protein extraction and Western Blot**

Total protein extraction from controls and silenced cell lines and western blot analysis were carried out by standard methods as described in Lastraioli *et al*., 2004.

**Patch-clamp recording**

Cells were seeded on 35mm Petri dishes and traces were recorded with the amplifier Axopatch 700 A (Molecular devices), using the whole cell configuration. Measurements of $I_{HERG}$ was performed in voltage clamp. Pipettes resistances were between 3 and 5MΩ (borosilicate glass, Harvard Apparatus). Gigaseal resistances were in the range 1–2 GΩ. Input resistances of the cells were in the range 2–6GΩ. Whole cell currents were filtered at 1–3 kHz.

For data acquisition and analysis, the pClamp8.0 (Molecular Devices) and Origin6.0 (Microcal Software, Northampton, MA) were routinely used. For a precise measurement of the current gating parameters, pipette and cell capacitance and the series resistance (up to 70–80%) were carefully compensated before each voltage clamp protocol run.

The protocol used to measure the tail $I_{HERG}$ maximal current ($I_{MAX}$) started from a holding of 0 mV and tested the current at -120 mV, after preconditioning from 0 to -70 mV for 15 seconds with steps of 10mV. Finally, each current was normalized to the respective cell capacitance.

Solutions: the extracellular solution with low potassium (low $K_o$ solution) contained (mM): NaCl 130, KCl 5, $CaCl_2$ 2, $MgCl_2$ 2, Hepes–NaOH 10, and glucose 5, pH 7.4. The extracellular solution with high potassium (high $K_o$ solution) contained (mM): NaCl 95, KCl 40, $CaCl_2$ 2, $MgCl_2$ 2, Hepes–NaOH 10, and glucose 5, pH 7.4. The standard pipette solution at $[Ca^{2+}]$ $10^{-7}$ M contained (mM): 130 $K^+$ aspartate, 10 NaCl, 2 $MgCl_2$, 2 $CaCl_2$, 10 EGTA–KOH and 10 Hepes–KOH, pH 7.4.

**Gene expression analysis: real time PCR**

Cells were homogenised in TRIzol® Reagent (Invitrogen™) to isolate total RNA according to manufactorer's protocol. The RNA integrity was assessed on the Agilent 2100 Bioanalyzer. One µg of RNA of each specimens was retrotranscribed using random primers and SuperScript™ II Reverse Transcriptase (Invitrogen™) according to manufacturer's protocol. SYBR green fluorescent dye (Power SYBR® Green, PCR master mix, Applied Biosystems) was used to monitor DNA synthesis. The expression levels of the genes of interest were normalized to the levels of the GAPDH reference gene using the method of Pfaffl, for quantification (Pfaffl, 2001). hERG1 3.1 isoform gene expression levels were normalized to MYH11 gene expression (see Fortunato et al., in press).

The primers for the genes of interest were designed using the software Primer3 (http://frodo.wi.mit.edu/) or selected from literature (Tab.1).

**Table 1. Primer sequences**

| Gene | | Sequence (5'-3') | Source |
|---|---|---|---|
| **FAM96A** | Forward | CGGATCATGGAAGAGAAAGC | Primer3 |
| | Reverse | CTTTCCGAGACCACTTCCAG | |
| **GAPDH** | Forward | ATGGGGAAGGTGAAGGTCG | Primer Bank |
| | Reverse | GGGGTCATTGATGGCAACAATA | |
| **CDKN2A** | Forward | ACCAGAGGCAGTAACCATGC | Primer3 |
| | Reverse | CCTGTAGGACCTTCGGTGAC | |
| **VIM** | Forward | CCTTGAACGCAAAGTGGAAT | Primer3 |
| | Reverse | TTTGGACATGCTGTTCCTGA | |
| **CXCR4** | Forward | CAGCAGGTAGCAAAGTGACG | Primer3 |
| | Reverse | ATAGTCCCCTGAGCCCATTT | |
| **LAX1** | Forward | TGAGAGCCTCCTCTCCAGAA | Primer3 |
| | Reverse | GATGTGGGCTGTATGCTCCT | |
| **LCK** | Forward | TCTTTTGGGATCCTGCTGAC | Primer3 |
| | Reverse | GCTCCAGGTTCTGAATCACC | |
| **TNFRSF1A** | Forward | CCTTCAGAAGTGGGAGGACA | Primer3 |
| | Reverse | GAATTCCTTCCAGCGCAAC | |
| **SLC20A1** | Forward | GCCTCGATCTCCTCGTCTC | Primer3 |
| | Reverse | GCTAAAAGCACGGAGCAGAA | |
| **RHOA** | Forward | CAGAAAAGTGGACCCCAGAA | Primer3 |
| | Reverse | TGCCTTCTTCAGGTTTCACC | |
| **SGK** | Forward | CCCCCTTTTAACCCAAATGT | Primer3 |
| | Reverse | GGGACTTGCCAATGGAGTT | |
| **TMEM158** | Forward | CTGCATTTCTGCTGCCTAGA | Primer3 |
| | Reverse | CCACACCACGATGACCAG | |
| **DCAMKL1** | Forward | ACCACGGGTTTACCATCAAG | Primer3 |
| | Reverse | CTTGTACCGGCTCCTCACAT | |
| **DUSP4** | Forward | AGAGGCTGGAGATTGGGAAT | Primer3 |
| | Reverse | GTCCCCCACCTAGAATTGGT | |
| **SYBL1** | Forward | TCCCATTGCAGTTGATTTGA | Primer3 |
| | Reverse | CCCCACCCCCTCTACTACAT | |
| **CDH1** | Forward | GAGTGCCAACTGGACCATTC | Hur, 2012 |
| | Reverse | ACCCACCTCTAAGGCCATCT | |
| **CDH2** | Forward | AGCCAACCTTAACTGAGGAGT | Primer Bank |
| | Reverse | GGCAAGTTGATTGGAGGGATG | |
| **FOXC2** | Forward | CCTCCTGGTATCTCAACCACA | Primer Bank |
| | Reverse | GAGGGTCGAGTTCTCAATCCC | |
| **MMP1** | Forward | GGGGCTTTGATGTACCCTAGC | Primer Bank |
| | Reverse | TGTCACACGCTTTTGGGGTTT | |
| **hERG1** | Forward | ATGGGGAAGGTGAAGGTCG | Primer3 |
| | Reverse | GGGGTCATTGATGGCAACAATA | |
| **hERG1 3.1** | Forward | CAACATCACTGTGTACCCCATAA | Primer3 |
| | Reverse | TTTTCCATCTATAAAATGGGAAGAAT | |

**Table 1. Primer sequences of studied genes.**

**Gene expression analysis: microarray**

Expression profiling analysis was performed using Agilent Oligo Microarray Kit according to Agilent One-Colour Microarray based Gene Expression Analysis Protocol. RNA was amplified and labeled using Agilent Quick Amp Labelling Kit. The amplified fragmented RNA was hybridized on a 4 × 44K Whole Human Genome Oligo Microarray Chip (Agilent Technologies) then scanned with an Agilent DNA microarray scanner. Feature Extraction Software Version 9.5 (Agilent Technologies), was used to extract and analyze the signals.

**Statistical analysis of microarray**

Data analysis was performed using R software version 2.15.0 (http://www.r-project.org) by Bioconductor Packages using row images (dat files), as obtained from the Feature extraction analysis. Data were normalized using "scale" normalization (Smyth and Speed, 2003) as implemented in “limma” package, made available on Bioconductor. To perform differential expression analysis, aimed at identifying deregulated genes between controls and silenced cell lines, we started from the $\log_2$ of normalized intensity values of each gene. Then, we used ANOVA test to identify for each gene significant changes in expression values between controls and silenced cell lines. *P* value was calculated for each gene. To select the differentially expressed genes (DEGs) we considered a threshold of P=0.01.

**Functional annotation analysis**

We used Cytoscape software (Maere, 2005) and the BiNGO plugin (Smoot, 2011) to analyze Gene Ontology terms significantly enriched in the DEGs. The enrichment for each term has been tested using hypergeometric test. All terms with a $p<0.05$ were considered enriched. To identify the KEGG pathways significantly enriched in the DEGs, we used NIH-DAVID software (version 6.7). All pathways with a $p<0.05$ were considered enriched.

**Functional annotation analysis**

We used Cytoscape software (Maere et al., 2005) and the BiNGO plugin (Smoot et al.,2011) to analyze Gene Ontology terms significantly enriched in the DEGs. The enrichment for each term has been tested using hypergeometric test. All terms with a $p<0.05$ were considered enriched. To identify the KEGG pathways significantly enriched in the DEGs, we used NIH-DAVID software (version 6.7). All pathways with a $p<0.05$ were considered enriched.

## RESULTS

### Colorectal cell lines EMT status and hERG1 gene expression

We investigated the expression of several gene markers (VIM, CDH1, CDH2, MMP1, FOXC2) of EMT in 5 cell lines of colorectal cancer to determine their EMT status (Fig. 1A). This analysis revealed that HCT116 cells have the higher level of mesenchymal status between the cell lines tested. Moreover, the hERG1 gene is expressed at different levels in the colorectal cell lines analysed. In particular, HCT116 and H630 cell lines express hERG1 gene at high levels (Fig. 1B).

### RNAi

We selected the HCT116 cell line to be transduced with shRNA constructs capable of post-transcriptional silence hERG1 gene by using a lentiviral vector, because this cell line has strongest mesenchymal molecular profile and express at high level the hERG1 gene. If the hERG1 gene has a role in EMT we can predict that the silenced HCT116 cells will modify the expression profile of EMT molecular markers from mesenchymal to a more epithelial profile. Moreover, in consideration that EMT alter the relative abundance of the proteins involved in cytosckeleton organization we should detect also a phenotypic change in the morphology of the silenced cells in the direction of the re-acquisition of an epithelial-like phenotype.

Five different shRNA constructs were available for the gene of interest. In order to select the most effective shRNA constructs to knock-down hERG1 gene expression, by transfecting each shRNA in HEK293 over-expressing hERG1 ion channels by employing conventional (Lipofectamine) delivery methods. The expression of hERG1 in the transfected cells were measured by real time PCR. The two shRNAs (named sh4 and sh7) with the highest gene knock-down were selected for further experiments (Tab. 2). The two shRNAs recognize the

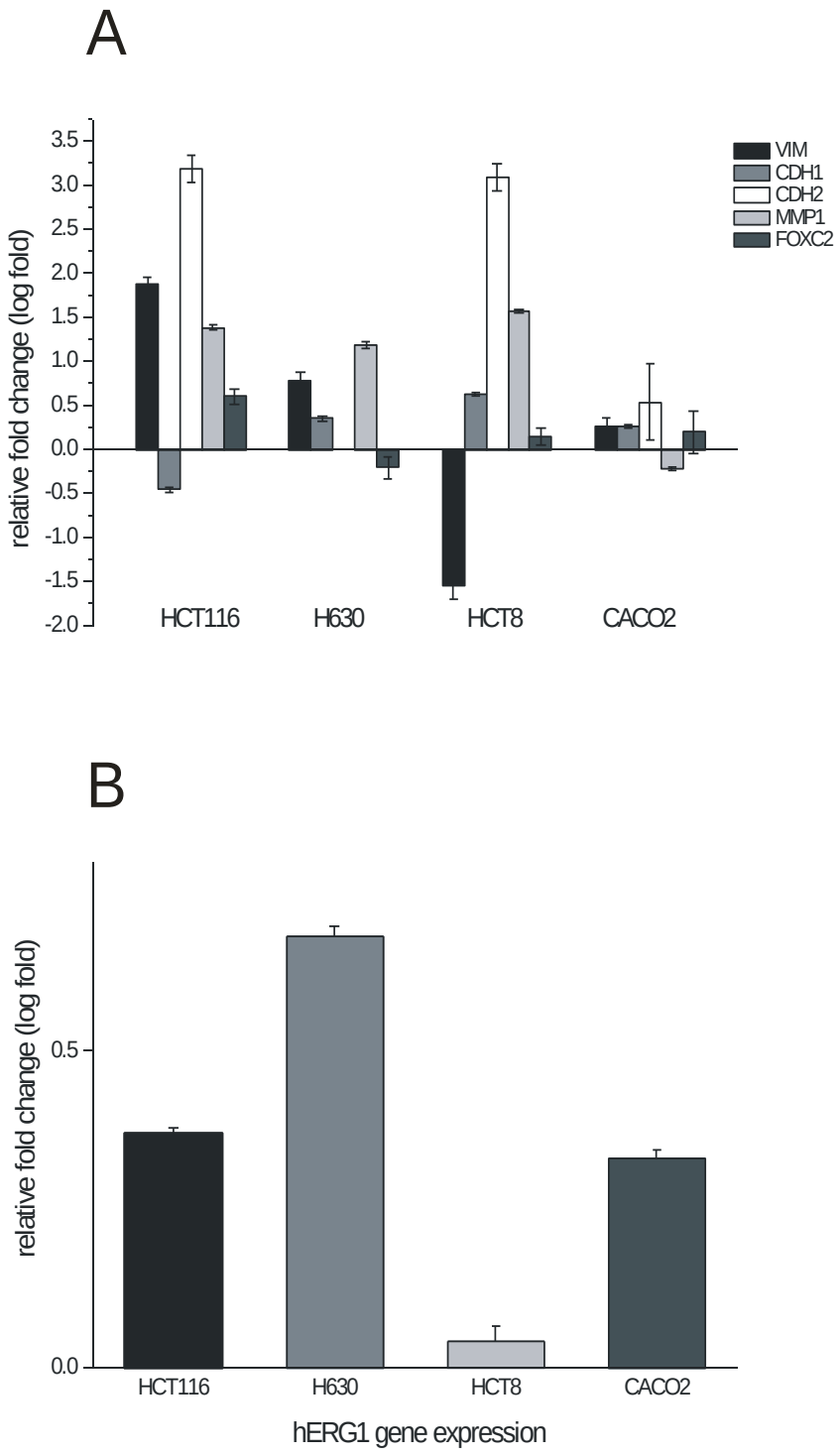


**Figure 1. EMT status and hERG1 gene expression analysis of colorectal cell lines**
(A) The analysis of gene expression of mesenchymal (VIM, CDH2, MMP1, FOXC2) and epithelial (CDH1) markers, shows that the HCT116 cells possess a high expression of mesenchymal markers and a simultaneous low expression of the epithelial marker therefore, HCT116 cells have the stronger mesenchymal profile between the HCT116, HCT8, CACO2 and H630 cell lines tested. (B) hERG1 is expressed in HCT116, HCT8, CACO2, H630 and HT29 colorectal cancer cell lines. HCT116 and H630 cell lines express at high levels hERG1 gene. Data were normalized to HT29 cell line. Histograms represent the fold-mean ± s.e.m (error bars).

| **Table 2. shRNA sequences** | |
|---|---|
| **sh7** (TRCN0000021717) | **Sequences** |
| Hairpin | CCGGCCTCATGTATGCTAGCATCTTCTCGAGAAGATGCTAGCATACATGAGGTTTTT |
| Mature Sense | CCTCATGTATGCTAGCATCTT |
| Mature Antisense | AAGATGCTAGCATACATGAGG |
| | |
| **sh4** (TRCN0000021714) | **Sequences** |
| Hairpin | CCGGCCTGCGAGATACCAACATGATCTCGAGATCATGTTGGTATCTCGCAGGTTTTT |
| Mature Sense | CCTGCGAGATACCAACATGAT |
| Mature Antisense | ATCATGTTGGTATCTCGCAGG |

**Table 2. shRNA sequences.** Selected from the TRC shRNA library.

target sequence of different isoforms. sh4 recognizes only the hERG1Al, hERG1B and hERG1 3.1 isoforms instead the sh7 recognizes all the isoforms (Fig. 2). Interestingly, the hERG1 3.1 isoform previously described in brain and heart, and associated with risk for schizophrenia (Huffaker, 2009) is expressed in both HCT116 cell line and bioptic samples of colorectal cancer (Fig. 3). Then, we produced lentivirus particles by co-transfecting 2$^{nd}$ generation lentiviral plasmids and the transfer vector construct into the HEK293T packaging cell line. Thus, we transduced colorectal cancer HCT116 cells at MOI=3 and 5 with the lentivirus vectors. Subsequently, we used puromycin selection to generate stable-silenced cell lines (named sh4 and sh7) and control cell lines (named pLKO.1). By implementing this technical platform we strongly suppressed the expression of hERG1 of both transcripts (Fig. 4A) and proteins (Fig. 4B, 5) in the silenced cell lines in comparison with the control cell lines transduced with the empty vector pLKO.1. The two silenced cell lines have different levels of hERG1 knockdown (Fig. 4A, B); the sh4 cell lines has higher hERG1 gene knock-down both at transcriptional and protein levels.

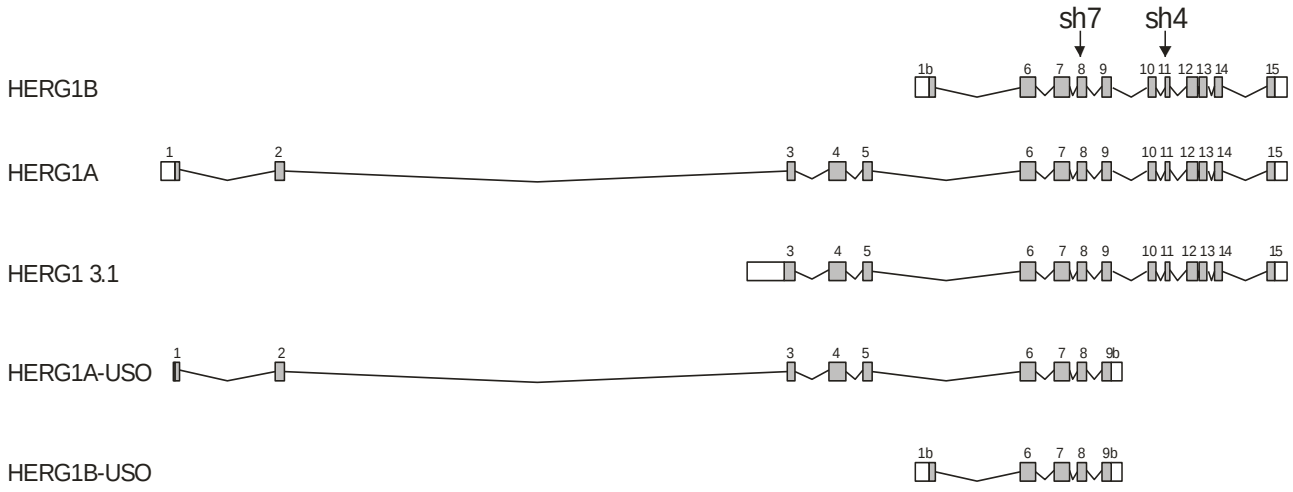


**Figure 2. HERG1 isoforms**
Protein coding isoforms of the hERG1 gene. Box: exon; grey box: protein coding sequence; box not filled: untranslate sequence; line between boxes: intron.

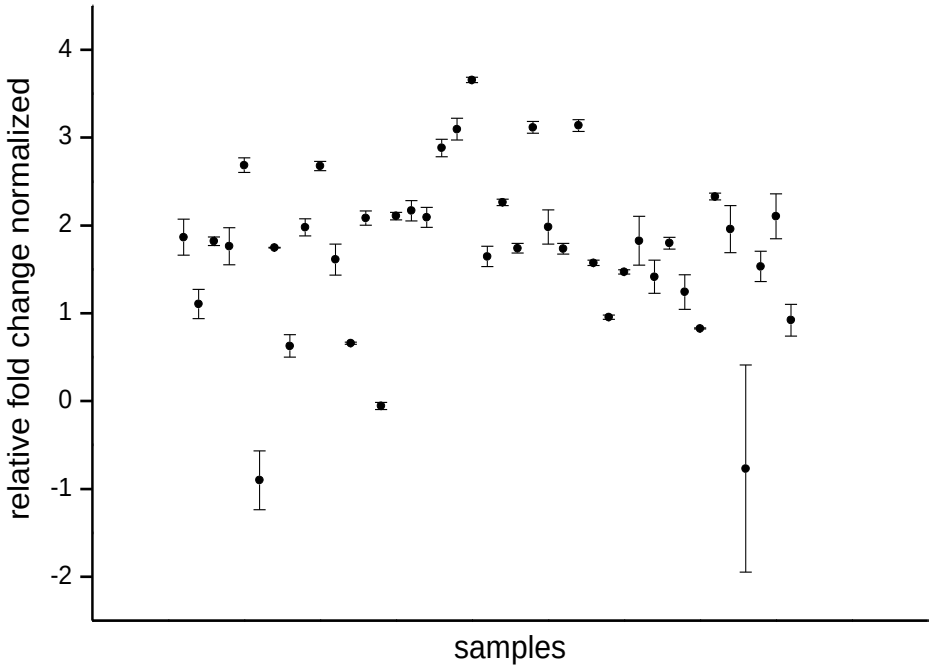


**Figure 3. Analysis of hERG1 3.1 isoform gene expression.**
Relative expression values for hERG1 3.1 gene isoform. Data were normalized to the value of expression of HT116 cell line and to a stroma-myofibroblast marker.

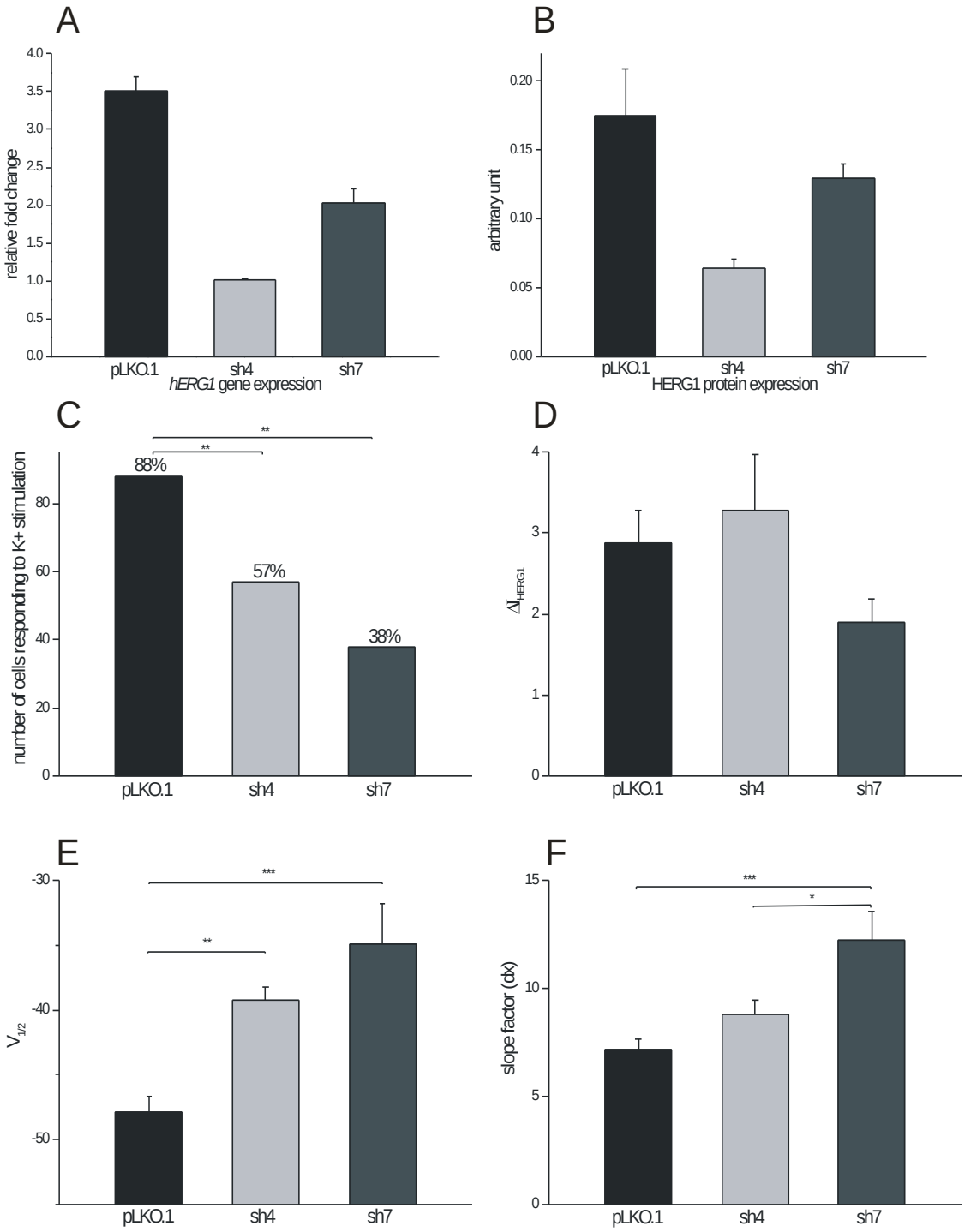


**Figure 4. Validation of hERG1 gene silencing and consequences of its knock-down**

(A) The expression of hERG1 of both transcripts and proteins (B) were strongly reduced by RNAi (pLKO.1: control cells transduced with the empty pLKO.1 vector; sh4 and sh7: silenced cell lines transduced with two distinct shRNAs). The sh4 cell lines has the higher hERG1 knock-down both at transcriptional and protein levels compared with control and sh7 cells. (C-F) Electrophysiological measurements (whole-cell clamp) shown that the silenced cells have reduced their ability to respond to $K^+$ stimulation (C). It means that the physiological function of hERG1 ion channels is strongly decreased and impaired in both silenced cells. Sh7 cells have the stronger hERG1 ion channels physiological impairment. We reported the characteristic parameters of HERG1 currents described by the Boltzmann equation. (D): $I_{HERG1=}$ current; (E): $V_{1/2}$= the voltage at which the current is half inactivated; (F): dx= slope factor. Histograms represent the mean ± s.e.m (error bars). *=p<0.05, p<0.05<**<p<0.01, ***p<0.01

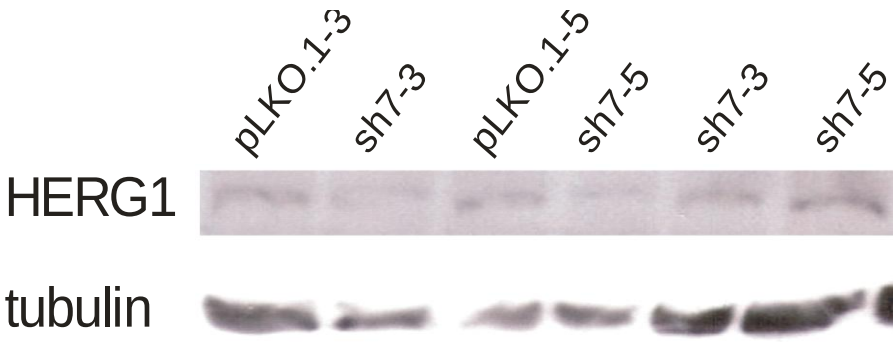


**Figure 5. Western Blot Analysis**
Western blot image of total protein analysis of control (pLKO) and silenced (sh7) cells.

**Electrophysiology**

We verified by electrophysiological measurements (whole-cell clamp) that the silenced cells have reduced their ability to respond to $K^+$ stimulation ($\chi^2$ test, pLKO.1 (control) vs. sh7 cells, p=0.014; pLKO.1 (control) vs. sh4, p=0.023) (Fig. 4C-F). Moreover, the HERG1 currents, described by the Boltzmann equation, in their characteristic parameters: $V_{1/2}$, the voltage at which the current is half inactivated, and the slope factor *dx,* are affected by hERG1 knock-down (ANOVA tests, $V_{1/2}$: p<0.0001, Dunn's multiple comparison test, pLKO.1 vs sh7, P<0.001; sh4 vs sh7, p<0.01; ANOVA tests, slope factor *dx*: p<0.0006, Dunn's multiple comparison test, pLKO.1 vs sh7, P<0.001; sh4 vs sh7, p<0.05). According to these results we can conclude that the hERG1 gene silencing not only reduce the hERG1 transcripts and proteins but most importantly the physiological function of the channel is
impaired. Interestingly, the sh7 cell line, despite a minor knock-down of the hERG1 gene, has a stronger functional impairment of the channel.

**Cell biology**

We characterized the silenced cell lines to highlight the role of hERG1 gene in cancer cells. Notably, the silenced cells lines (sh4 and sh7) shown a different morphology when compared with controls (Fig. 6). Both silenced cell lines appeared to have a reduced number of membrane

protrusions making the shape of cells, adherent to Petri dish surface, much more roundish and are visible cohesive groups of cells. This phenotype is particularly evident in the sh7 cells line (Fig. 6). The actin cytoskeleton of sh7 cells compared to control cells appears to be disorganized and the focal adhesions with the substratum are rare (Fig. 7). To characterized the physiological effect of hERG1 knock-down, we investigated the

proliferative capacity of the transduced cell lines by soft agar colony formation assay. We found that the silenced cells forms smaller colony in comparison with control cells transduced with the empty vector (pLKO.1 (controls) vs. sh7 silenced cells, Kruskal-wallis test, $P<0.0001$, Dunn's multiple comparison test) (Fig. 8A). Moreover, also the size of the colonies of sh7 cells were smaller then sh4 colonies (Dunn's multiple comparison test, $P<0.001$) (Fig. 8A). In addition, we calculated the cell growth rate over the time in control and experimental cell lines for six consecutive days. We found that the proliferation rate of sh4 and sh7 cell lines is lower compared to controls (ANOVA, $p=0.0145$) (Fig. 8B). The reduction of the proliferation rate could be explained by cell cycle slow down, in fact, we detected a delay into S phase entry of the silenced sh7 cells compared to both control and sh4 cells (Paired t-test, control vs. sh7, $p=0.031$; sh4 vs. sh7, $p=0.038$) (Fig. 9). Collectively, these experiments confirm that, despite the minor level of hERG1 knock-down of the sh7 cells in comparison with the sh4 cells, the sh7 cells show a stronger phenotype, for this reason we selected sh7 cells for *in vivo* experiments.

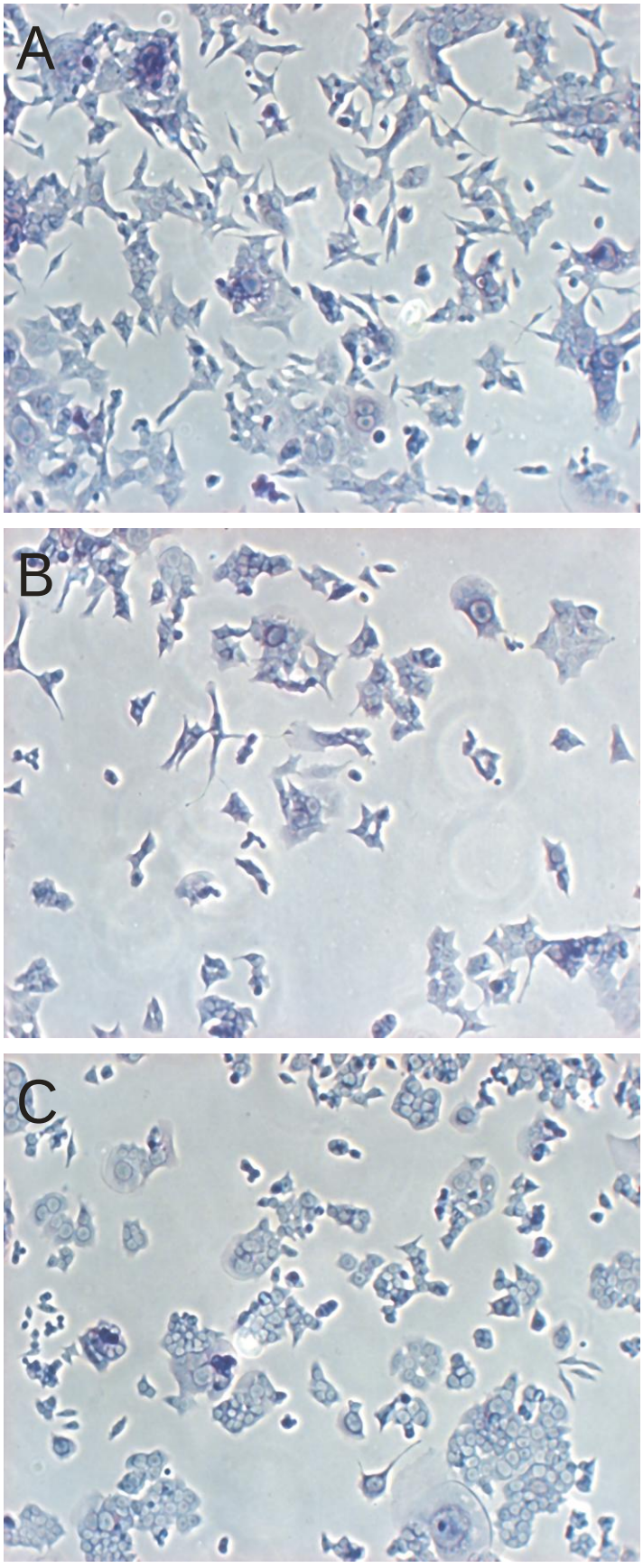


**Figure 6. Phenotypic effect of hERG1 gene silencing.**The silenced cells lines (sh4 and sh7) show a different morphology if compared with controls. Both silenced cell lines have a reduced number of membrane protrusions. This phenotype is particularly evident in the sh7 cells line. (A): pLKO.1 control cells; (B): sh4 silenced cells; (C): sh7 silenced cells.

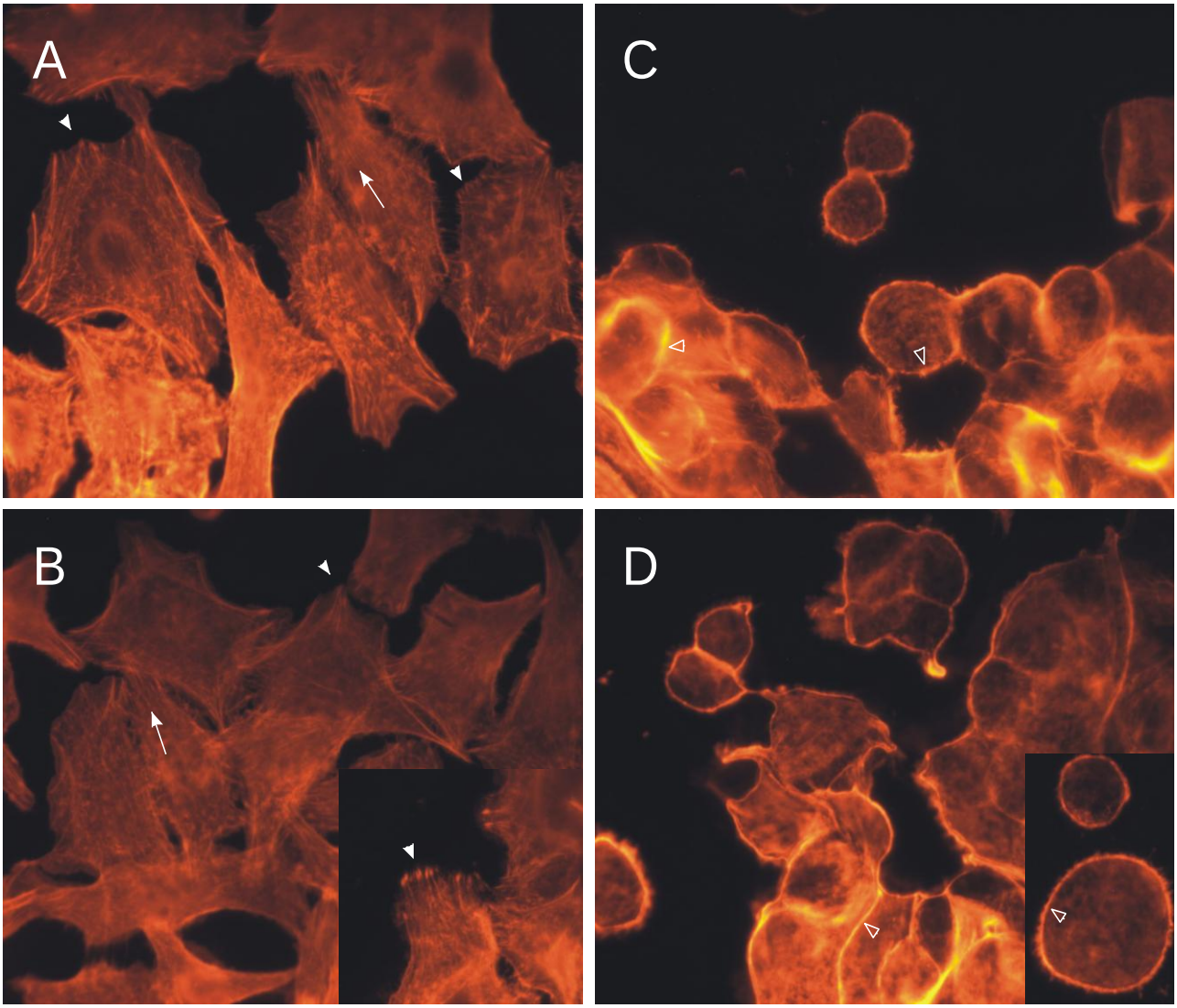


**Figure 7. Visualization of actin cytoskeleton in control and hERG1 silenced cells.**
The actin cytoskeleton (red stained) and focal adhesion contacts in control pLKO.1 (A,B) and sh7 (C,D) silenced cells. Control cells show actin stress fibers aligned with the direction of cell migration (arrows) and the filopoda, focal adhesions with the substratum (head arrows). Instead, in the silenced cells the actin cytoskeleton are not oriented and filopoda are strongly reduced. The actin cytoskeleton is mainly localized at the cell surface in the silenced cells (head arrows not filled). Actin proteins were visualized with rhodamine-conjugate phalloidin. Magnification 1000x.

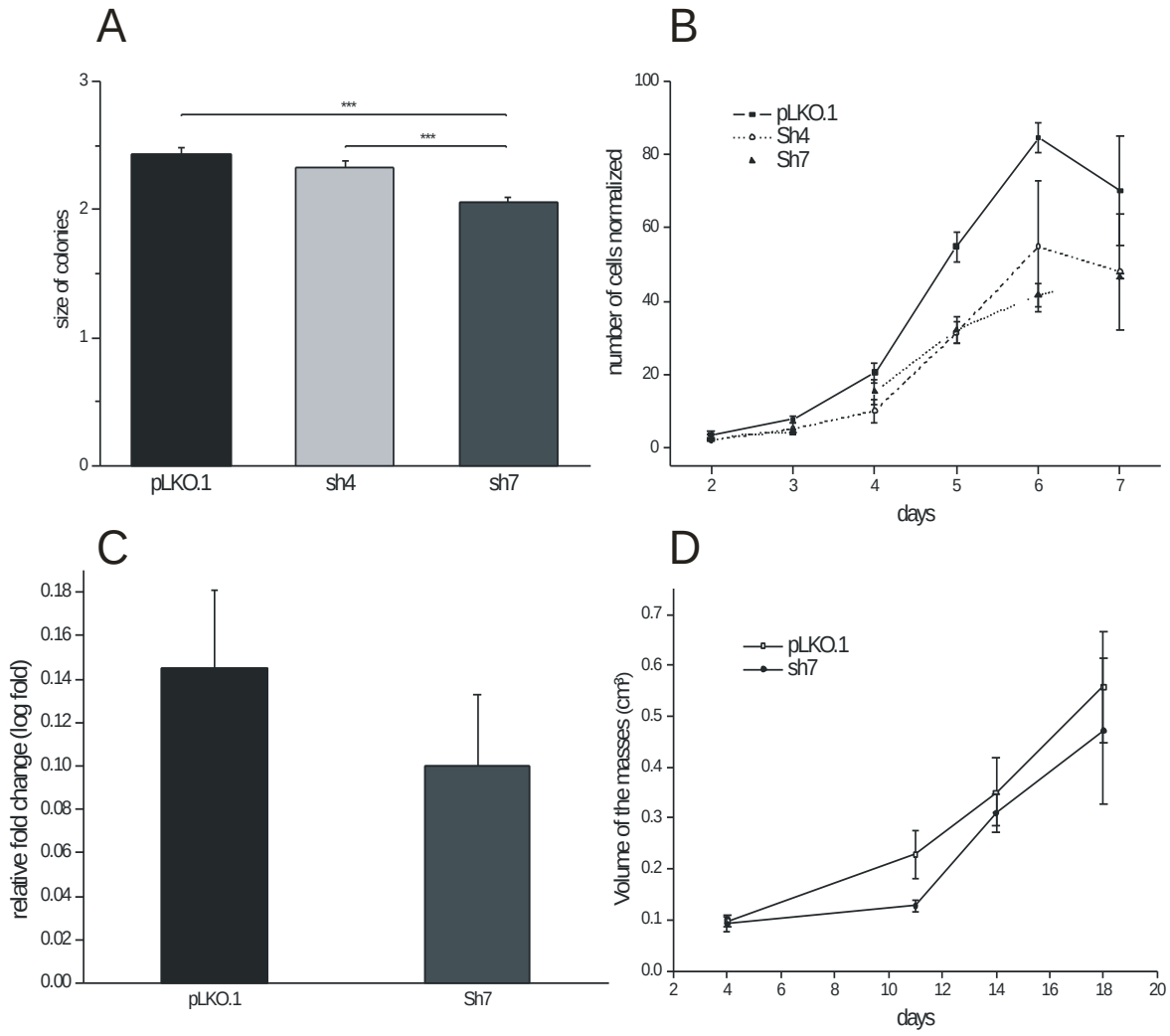


**Figure 8. Characterization of silenced cell lines.**
(A) Soft agar colony formation assay. The silenced cells forms smaller colony in comparison with control cells showing a reduced proliferative capacity. Moreover, also the size of the colonies of sh7 cells were smaller then the sh4 colonies. Histograms represent the mean ± s.e.m (error bars). (B) The proliferation rate of sh4 and sh7 cell lines is lower compared to controls. Cells were counted for six consecutive days. Mean ± s.e.m (error bars). (C,D) *In vivo* experiments. After **s**ubcutaneous injection of control and sh7 silenced cells in nu/nu mice, tumor masses were measured after 4, 11, 14 and 18 days after the cells injection. The volume of the masses originated by silenced cells were significantly smaller compared to controls. The hERG1 gene silencing was maintained until the mice sacrifice (C).

***In vivo* experiments**

We carried on *in vivo* experiments by subcutaneous injection of control and sh7 silenced cells in mice. $2x10^6$ cells were injected in both side of nu/nu mice then, the tumor masses development were monitorated for 18 days. Tumor masses were measured and compared with those of the controls after 4, 11, 14 and 18 days after the cells injection and we verified that the hERG1 silencing was maintained until the mice sacrifice (Fig. 8C). We found that the volume of the masses originated by silenced cells were significantly smaller compared to controls (paired t-test, p=0.0363) (Fig. 8D).

**Testing the role of hERG1 in EMT**

In order to further validate the involvement of hERG1 in the EMT we selected a group of genes that are described in the literature as being biomarkers of epithelial and mesenchymal cells thus, able to discriminate between the two states: VIM, CDH1, CDH2, FOXC2 and MMP1 (also used to characterize the EMT status of the colorectal cell lines, see figure 1).

Then, we analyzed the expression value of these genes in both silenced and control cells. If hERG1 is involved in EMT, the silenced cells that have a reduced expression of hERG1, should re-acquire an epithelial molecular profile instead the control cells should maintain a mesenchymal profile. As predicted, the analysis of gene markers expression show an epithelial-like molecular profile of the silenced cells, validating our hypothesis (Fig. 10).

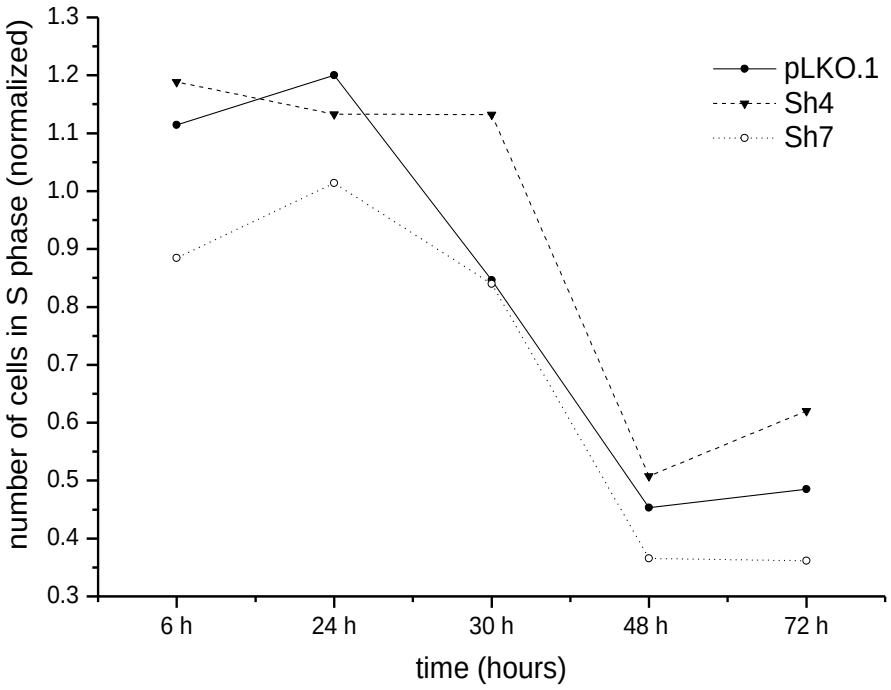


**Figure 9. Cell cycle analysis.**
Graph of cell cycle analysis shows a delay into S phase entry of the silenced sh7 cells compared to both control and sh4 cells. (Paired t-test, control vs. sh7, p=0.031; sh4 vs. sh7, p=0.038).

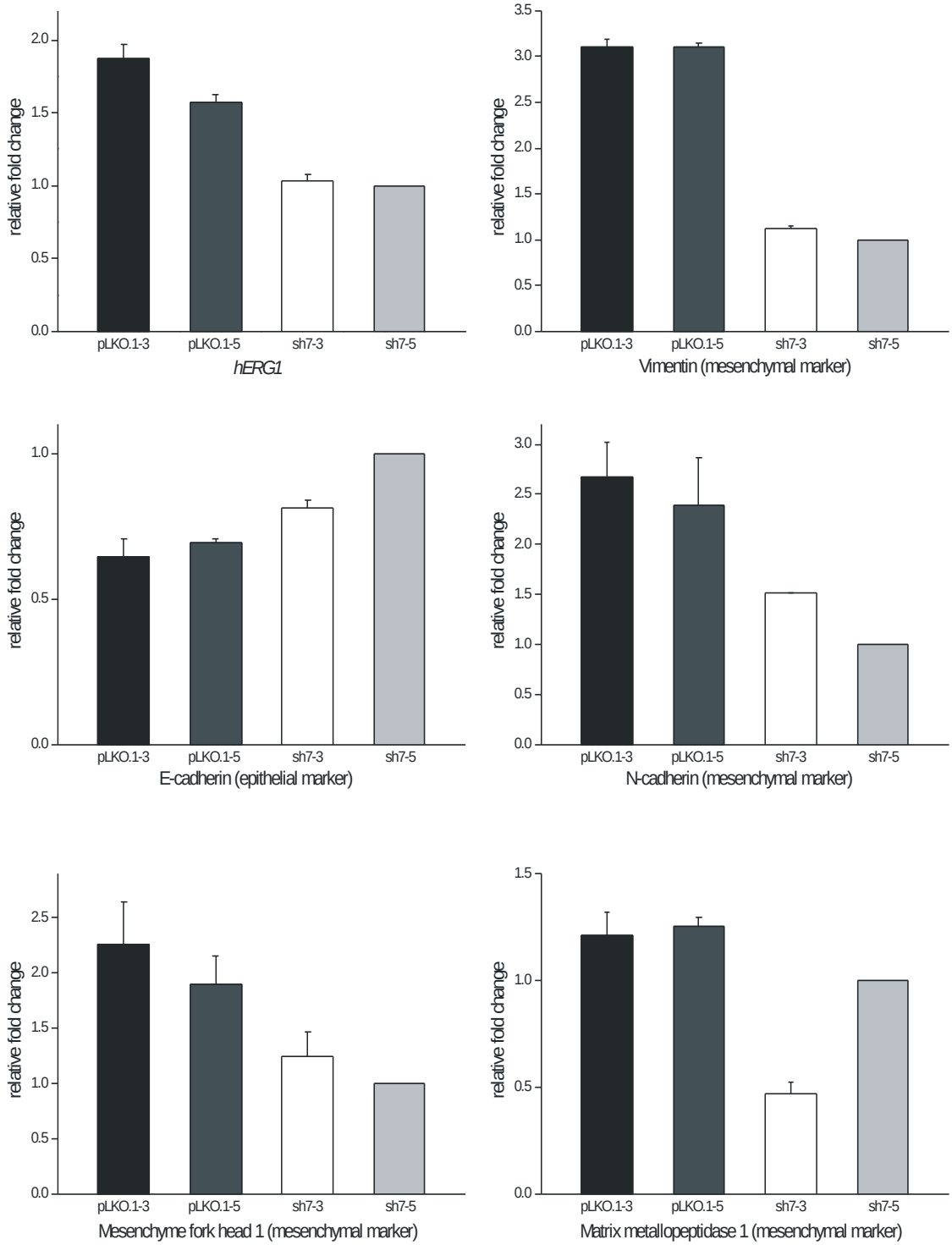


**Figure 10. EMT status of silenced cells and hERG1 expression.**
The expression of hERG1 is reduced in the silenced cells (sh7-3 and sh7-5) compared to control cells (pLKO.1-3 and pLKO.1-5). In order to investigate the EMT status of silenced (sh7-3 and sh7-5) cells, we analyzed the gene expression of mesenchymal (VIM, CDH2, MMP1, FOXC2) and epithelial (CDH1) markers. The silenced cells have a stronger epithelial-like molecular profile compared to controls that have a mesenchymal-like profile.

**Gene expression analysis by microarrays**

In order to investigated the genetic interactions of hERG1 with other genes and to further validate the role of hERG1 in EMT we performed a microarray experiment confronting the two silenced cell lines sh7-3 and sh7-5, respectively trasduced at MOI=3 and MOI=5 with the corresponding control cell lines, pLKO.1-3 and pLKO.1-5 (Fig. 11).

We found 307 genes were deregulated in the silenced cells (Tab. 3). We validated by real time PCR a sub set of these genes focusing mainly on the genes most down regulated in silenced cell lines. We tested 9 genes between the top 15 genes and we verified that 8 of these were fully validate in both cell lines (sh7-3 and sh7-5 compared to controls). We consider the genes truly differentially expressed only if both silenced cell lines (sh7-3 and sh7-5) have a value of gene expression greater or lesser than both control cell lines (pLKO.1-3 and pLKO.1-5). By using this approach, the effect observed is independent of the MOI values used minimizing false positive gene detection due to an eventual unspecific reaction to viral infection (Tab. 4). By introducing these validation criteria we found that among the validated genes several of them are involved in cytoskeleton rearrangement and/or signaling, confirming a role of hERG1 ion channels in the transition between the epithelial to mesenchymal states in HCT116 colorectal cancer cells (Tab. 4, see Discussion). Moreover, we attempted to identify the transcriptional factors (TF) that can bind to genes differentially expressed (DF) between the controls and silenced cells (Tab. 3) by bioinformatics analysis. First, we determined the number predicted interactions with DF consensus sites for each TF identified. Thus, we obtained the number of genes that can bind each TF selected at genomic level and finally we analyzed statistically the data to assess whether for each selected TF the number of genes that have the consensus binding site is enriched between the DF genes with respect to the whole genome. After multiple testing correction, we obtained a list of TFs that are associated in a statistically significant manner to the genes DF (Tab. 5).

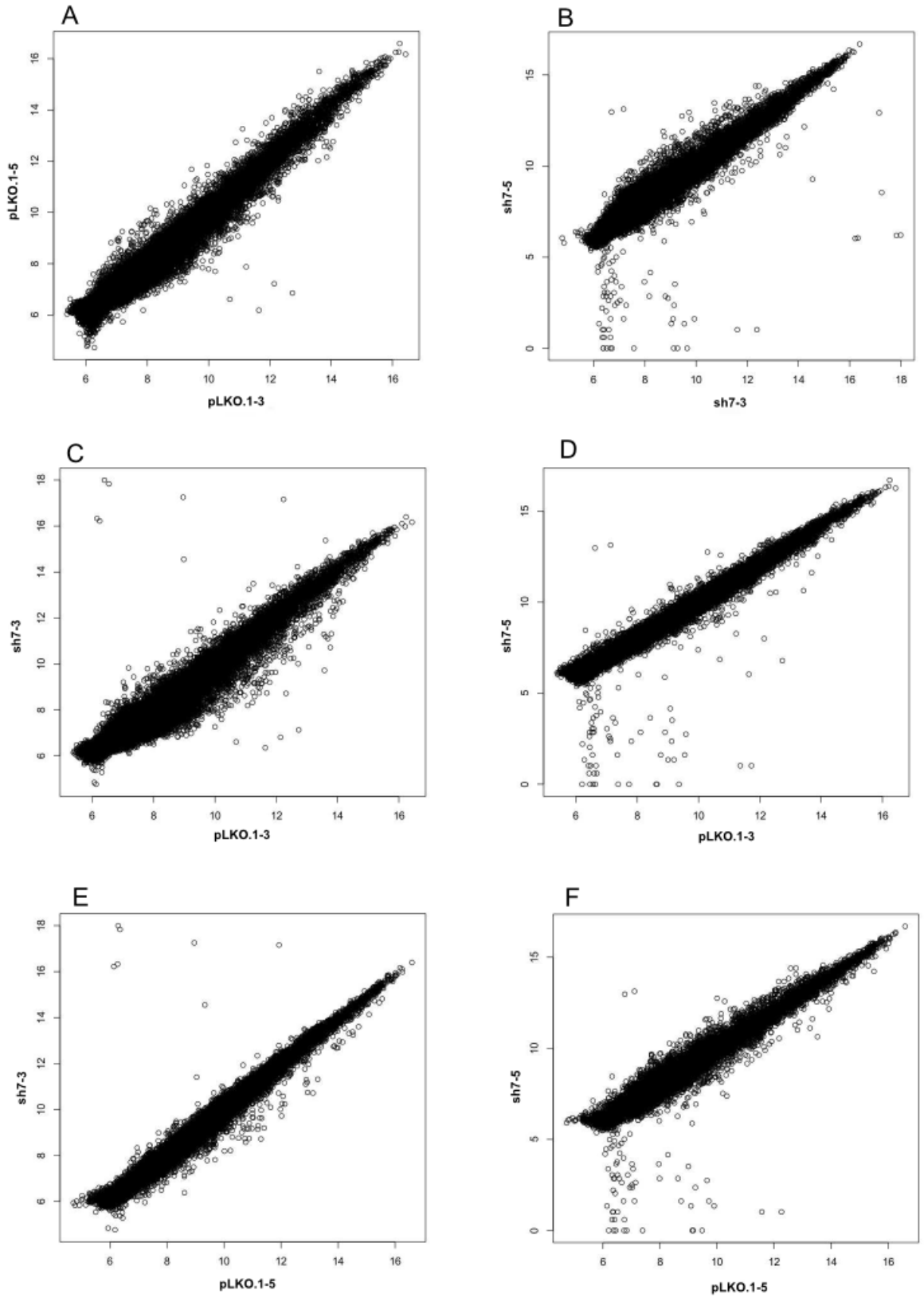


**Figure 11. Comparison of genome-wide gene expression profiles of control and silenced cell lines**
Plot of log2 normalized values for each gene of pLKO.1-3, pLKO.1-5 (controls) and sh7-3 and sh7-5 cells (silenced). The degree of similarity between controls and between silenced cells, Pearson's correlation coefficients: (A)=0.99; (B)=0.98; (C)=0.98; (D)=0.99; (E)=0.99; (F)=0.98.

**Table 3. Differentially expressed genes**

| | control pLKO.1-3 | control pLKO.1-5 | RNAi sh7-3 | RNAi sh7-5 | diff. mean | *p* value |
|---|---|---|---|---|---|---|
| **CAPN2** | 13.889 | 13.843 | 12.744 | 12.524 | 1.232 | 0.008 |
| **VIM** | 8.672 | 8.624 | 7.581 | 7.542 | 1.087 | 0.001 |
| **TMEM158** | 9.367 | 9.369 | 8.373 | 8.500 | 0.931 | 0.005 |
| **SGK** | 9.243 | 9.382 | 8.448 | 8.405 | 0.886 | 0.007 |
| **FAM64A** | 11.475 | 11.394 | 10.626 | 10.473 | 0.885 | 0.009 |
| **FAM64A** | 11.659 | 11.580 | 10.839 | 10.698 | 0.851 | 0.009 |
| **DCAMKL1** | 7.572 | 7.563 | 6.701 | 6.755 | 0.840 | 0.001 |
| **AL833005** | 7.817 | 7.802 | 7.011 | 7.094 | 0.757 | 0.003 |
| **SYBL1** | 9.808 | 9.896 | 9.178 | 9.091 | 0.718 | 0.007 |
| **DUSP4** | 10.897 | 10.885 | 10.205 | 10.179 | 0.699 | 0.000 |
| **NPAS3** | 7.799 | 7.874 | 7.158 | 7.249 | 0.633 | 0.009 |
| **PLA2G4D** | 7.316 | 7.247 | 6.720 | 6.740 | 0.552 | 0.004 |
| **NAV3** | 8.240 | 8.185 | 7.668 | 7.661 | 0.548 | 0.003 |
| **NAV2** | 7.646 | 7.617 | 7.101 | 7.100 | 0.531 | 0.001 |
| **OBFC1** | 10.566 | 10.564 | 10.044 | 10.069 | 0.509 | 0.001 |
| **SLC20A1** | 14.146 | 14.068 | 13.648 | 13.617 | 0.474 | 0.008 |
| **FRMD1** | 6.905 | 6.894 | 6.418 | 6.455 | 0.463 | 0.002 |
| **THC2279352** | 8.163 | 8.141 | 7.681 | 7.716 | 0.454 | 0.002 |
| **HTR7** | 8.049 | 8.067 | 7.645 | 7.637 | 0.417 | 0.001 |
| **TRIM47** | 10.175 | 10.199 | 9.739 | 9.803 | 0.415 | 0.007 |
| **CD109** | 7.826 | 7.848 | 7.432 | 7.490 | 0.376 | 0.007 |
| **HSD17B1** | 9.588 | 9.651 | 9.263 | 9.223 | 0.376 | 0.010 |
| **A_24_P921036** | 6.408 | 6.408 | 6.045 | 6.030 | 0.371 | 0.000 |
| **SLC39A13** | 11.267 | 11.249 | 10.853 | 10.921 | 0.370 | 0.009 |
| **MAST1** | 8.518 | 8.526 | 8.135 | 8.196 | 0.357 | 0.007 |
| **RAB8B** | 7.611 | 7.640 | 7.274 | 7.280 | 0.349 | 0.002 |
| **ENST00000371189** | 8.213 | 8.146 | 7.825 | 7.843 | 0.345 | 0.010 |
| **CPD** | 8.015 | 8.050 | 7.674 | 7.704 | 0.343 | 0.004 |
| **LOC286254** | 9.713 | 9.698 | 9.395 | 9.331 | 0.343 | 0.009 |
| **A_24_P127517** | 7.554 | 7.543 | 7.230 | 7.211 | 0.328 | 0.001 |
| **GSTT2** | 10.545 | 10.505 | 10.186 | 10.212 | 0.326 | 0.005 |
| **PALMD** | 6.432 | 6.426 | 6.095 | 6.112 | 0.326 | 0.001 |
| **A_23_P143676** | 10.325 | 10.314 | 10.035 | 9.975 | 0.315 | 0.009 |
| **MSTP9** | 11.539 | 11.509 | 11.221 | 11.203 | 0.312 | 0.003 |
| **LGR6** | 6.392 | 6.408 | 6.105 | 6.100 | 0.297 | 0.001 |
| **RARRES3** | 7.026 | 7.031 | 6.758 | 6.710 | 0.294 | 0.006 |
| **C14orf139** | 9.002 | 9.003 | 8.726 | 8.702 | 0.289 | 0.002 |
| **OPA3** | 6.840 | 6.837 | 6.560 | 6.551 | 0.283 | 0.000 |
| **HCRTR1** | 7.057 | 7.109 | 6.812 | 6.791 | 0.281 | 0.010 |
| **BC031319** | 6.254 | 6.300 | 6.004 | 5.993 | 0.278 | 0.007 |
| **BC015351** | 6.141 | 6.130 | 5.872 | 5.851 | 0.274 | 0.002 |
| **THC2400593** | 6.456 | 6.460 | 6.199 | 6.189 | 0.264 | 0.000 |
| **DMRTA1** | 6.408 | 6.443 | 6.181 | 6.146 | 0.262 | 0.009 |
| **THC2439202** | 6.307 | 6.318 | 6.075 | 6.030 | 0.260 | 0.008 |
| **PDPR** | 6.502 | 6.477 | 6.217 | 6.253 | 0.255 | 0.007 |
| **D83692** | 6.472 | 6.434 | 6.199 | 6.200 | 0.254 | 0.005 |
| **THC2442107** | 6.307 | 6.309 | 6.065 | 6.054 | 0.248 | 0.001 |
| **ENST00000186436** | 9.713 | 9.692 | 9.451 | 9.457 | 0.248 | 0.002 |
| **TNFRSF1A** | 7.690 | 7.698 | 7.466 | 7.426 | 0.248 | 0.007 |
| **ATP2B4** | 9.478 | 9.461 | 9.244 | 9.212 | 0.241 | 0.006 |
| **MRPS2** | 13.059 | 13.079 | 12.846 | 12.817 | 0.237 | 0.005 |

| | | | | | | |
|---|---|---|---|---|---|---|
| **C10orf62** | 6.533 | 6.502 | 6.270 | 6.293 | 0.235 | 0.007 |
| **HIST2H2AB** | 7.908 | 7.896 | 7.687 | 7.649 | 0.234 | 0.007 |
| **THC2444522** | 6.324 | 6.355 | 6.124 | 6.089 | 0.233 | 0.010 |
| **A_24_P118719** | 6.307 | 6.300 | 6.075 | 6.066 | 0.233 | 0.001 |
| **H19** | 6.740 | 6.763 | 6.524 | 6.517 | 0.232 | 0.003 |
| **AJ295984** | 6.456 | 6.477 | 6.217 | 6.253 | 0.231 | 0.008 |
| **LOC442247** | 6.235 | 6.222 | 6.004 | 5.993 | 0.230 | 0.001 |
| **AK098835** | 6.160 | 6.119 | 5.918 | 5.905 | 0.229 | 0.009 |
| **CHST7** | 7.814 | 7.842 | 7.598 | 7.601 | 0.228 | 0.004 |
| **TG** | 6.487 | 6.518 | 6.287 | 6.263 | 0.227 | 0.007 |
| **THC2406514** | 6.254 | 6.281 | 6.035 | 6.054 | 0.223 | 0.005 |
| **UBE2F** | 10.727 | 10.750 | 10.505 | 10.527 | 0.222 | 0.005 |
| **DYSF** | 6.766 | 6.770 | 6.538 | 6.559 | 0.219 | 0.002 |
| **BCAN** | 6.605 | 6.604 | 6.387 | 6.391 | 0.216 | 0.000 |
| **ADIPOR2** | 6.922 | 6.931 | 6.726 | 6.695 | 0.216 | 0.006 |
| **CSF2** | 6.432 | 6.443 | 6.235 | 6.211 | 0.215 | 0.004 |
| **SDK2** | 6.375 | 6.373 | 6.143 | 6.178 | 0.213 | 0.007 |
| **HRASLS2** | 6.547 | 6.573 | 6.363 | 6.333 | 0.213 | 0.008 |
| **AQP8** | 6.562 | 6.558 | 6.338 | 6.362 | 0.210 | 0.003 |
| **MOCS1** | 6.472 | 6.477 | 6.279 | 6.253 | 0.208 | 0.004 |
| **A_32_P78876** | 6.350 | 6.346 | 6.134 | 6.146 | 0.208 | 0.001 |
| **LOC723809** | 6.217 | 6.242 | 6.025 | 6.030 | 0.202 | 0.004 |
| **FLJ40194** | 6.307 | 6.281 | 6.085 | 6.100 | 0.201 | 0.006 |
| **A_24_P383934** | 6.803 | 6.804 | 6.608 | 6.600 | 0.199 | 0.000 |
| **EPB41L4B** | 6.922 | 6.949 | 6.751 | 6.725 | 0.197 | 0.009 |
| **LOC200261** | 6.226 | 6.232 | 6.025 | 6.042 | 0.196 | 0.002 |
| **C1orf118** | 6.298 | 6.300 | 6.085 | 6.123 | 0.195 | 0.009 |
| **SLC25A22** | 9.630 | 9.640 | 9.444 | 9.440 | 0.193 | 0.001 |
| **FNDC3B** | 9.327 | 9.343 | 9.150 | 9.135 | 0.193 | 0.003 |
| **A_24_P926720** | 6.440 | 6.426 | 6.235 | 6.253 | 0.189 | 0.004 |
| **CTSF** | 6.235 | 6.242 | 6.065 | 6.042 | 0.185 | 0.004 |
| **BST1** | 6.502 | 6.502 | 6.321 | 6.313 | 0.185 | 0.000 |
| **RAVER2** | 6.358 | 6.337 | 6.171 | 6.168 | 0.178 | 0.004 |
| **CNTNAP4** | 6.358 | 6.373 | 6.199 | 6.178 | 0.177 | 0.005 |
| **RNH1** | 6.424 | 6.434 | 6.253 | 6.253 | 0.177 | 0.001 |
| **VGF** | 7.052 | 7.042 | 6.876 | 6.868 | 0.175 | 0.001 |
| **CXCR4** | 6.316 | 6.300 | 6.134 | 6.146 | 0.168 | 0.003 |
| **PRODH** | 7.020 | 7.037 | 6.864 | 6.861 | 0.166 | 0.002 |
| **ENST00000378679** | 7.142 | 7.130 | 6.980 | 6.966 | 0.163 | 0.003 |
| **AA180985** | 6.080 | 6.076 | 5.929 | 5.905 | 0.162 | 0.006 |
| **THC2326033** | 6.472 | 6.493 | 6.330 | 6.313 | 0.161 | 0.007 |
| **C20orf91** | 6.440 | 6.443 | 6.270 | 6.293 | 0.160 | 0.005 |
| **GUSB** | 11.047 | 11.039 | 10.878 | 10.891 | 0.158 | 0.002 |
| **THC2313673** | 6.502 | 6.485 | 6.338 | 6.333 | 0.158 | 0.003 |
| **CBWD3** | 6.358 | 6.355 | 6.208 | 6.189 | 0.158 | 0.004 |
| **PHKG1** | 6.472 | 6.460 | 6.304 | 6.313 | 0.157 | 0.002 |
| **COPZ2** | 6.341 | 6.318 | 6.181 | 6.168 | 0.156 | 0.007 |
| **DBC1** | 6.307 | 6.300 | 6.162 | 6.134 | 0.155 | 0.008 |
| **BX110856** | 7.636 | 7.644 | 7.477 | 7.498 | 0.152 | 0.006 |
| **PLEKHA8** | 6.701 | 6.693 | 6.553 | 6.551 | 0.145 | 0.001 |
| **KIAA1462** | 6.518 | 6.534 | 6.371 | 6.391 | 0.145 | 0.008 |
| **C3orf18** | 9.896 | 9.924 | 9.764 | 9.766 | 0.145 | 0.010 |
| **THC2442647** | 6.141 | 6.119 | 5.983 | 5.993 | 0.142 | 0.007 |
| **A_24_P118512** | 6.272 | 6.290 | 6.134 | 6.146 | 0.141 | 0.006 |
| **LOC653056** | 6.694 | 6.722 | 6.567 | 6.568 | 0.141 | 0.009 |

| | | | | | | |
|---|---|---|---|---|---|---|
| **THC2432688** | 6.350 | 6.355 | 6.217 | 6.211 | 0.139 | 0.001 |
| **AA449494** | 6.307 | 6.318 | 6.181 | 6.168 | 0.139 | 0.004 |
| **RND1** | 6.281 | 6.271 | 6.143 | 6.134 | 0.137 | 0.002 |
| **DIO1** | 6.324 | 6.318 | 6.181 | 6.200 | 0.131 | 0.006 |
| **HGS** | 14.203 | 14.215 | 14.083 | 14.074 | 0.130 | 0.003 |
| **PFTK1** | 6.518 | 6.526 | 6.387 | 6.400 | 0.128 | 0.004 |
| **FGA** | 6.367 | 6.373 | 6.244 | 6.242 | 0.127 | 0.001 |
| **OR4C3** | 6.674 | 6.693 | 6.567 | 6.551 | 0.125 | 0.010 |
| **ENST00000355278** | 6.245 | 6.232 | 6.105 | 6.123 | 0.124 | 0.008 |
| **SLC12A3** | 6.797 | 6.804 | 6.688 | 6.664 | 0.124 | 0.010 |
| **ZNF471** | 6.101 | 6.098 | 5.972 | 5.981 | 0.123 | 0.001 |
| **A_24_P897062** | 6.179 | 6.182 | 6.055 | 6.066 | 0.120 | 0.002 |
| **AF400500** | 6.289 | 6.300 | 6.171 | 6.178 | 0.120 | 0.003 |
| **ENST00000378204** | 6.198 | 6.182 | 6.065 | 6.077 | 0.119 | 0.007 |
| **A_24_P942798** | 6.307 | 6.318 | 6.199 | 6.189 | 0.118 | 0.004 |
| **AW874698** | 6.416 | 6.400 | 6.296 | 6.283 | 0.118 | 0.008 |
| **MGC20470** | 6.367 | 6.373 | 6.262 | 6.242 | 0.118 | 0.007 |
| **ENST00000382611** | 6.341 | 6.337 | 6.226 | 6.221 | 0.115 | 0.001 |
| **LOC644374** | 6.487 | 6.502 | 6.387 | 6.372 | 0.115 | 0.008 |
| **THC2285720** | 6.472 | 6.460 | 6.354 | 6.352 | 0.112 | 0.003 |
| **A_32_P91156** | 7.218 | 7.237 | 7.115 | 7.117 | 0.112 | 0.007 |
| **A_24_P136299** | 6.840 | 6.830 | 6.720 | 6.733 | 0.109 | 0.005 |
| **A_32_P14737** | 7.031 | 7.037 | 6.926 | 6.928 | 0.107 | 0.001 |
| **ENST00000331447** | 6.432 | 6.443 | 6.338 | 6.323 | 0.107 | 0.007 |
| **RAB27B** | 6.456 | 6.460 | 6.354 | 6.352 | 0.105 | 0.000 |
| **A_24_P918694** | 6.358 | 6.355 | 6.262 | 6.253 | 0.100 | 0.002 |
| **EP300** | 6.440 | 6.426 | 6.338 | 6.333 | 0.098 | 0.006 |
| **C21orf62** | 6.141 | 6.141 | 6.035 | 6.054 | 0.096 | 0.010 |
| **NYD-SP26** | 6.235 | 6.232 | 6.134 | 6.146 | 0.094 | 0.004 |
| **IGHD** | 6.392 | 6.391 | 6.304 | 6.293 | 0.092 | 0.004 |
| **HOXC5** | 6.525 | 6.518 | 6.434 | 6.428 | 0.091 | 0.003 |
| **SLC6A4** | 6.591 | 6.604 | 6.509 | 6.517 | 0.085 | 0.008 |
| **A_24_P715434** | 7.232 | 7.233 | 7.153 | 7.151 | 0.080 | 0.000 |
| **BC036431** | 6.933 | 6.919 | 6.847 | 6.847 | 0.079 | 0.008 |
| **PKNOX1** | 6.887 | 6.888 | 6.812 | 6.813 | 0.075 | 0.000 |
| **AY040225** | 6.289 | 6.281 | 6.217 | 6.211 | 0.071 | 0.006 |
| **VWF** | 7.073 | 7.076 | 7.011 | 6.998 | 0.070 | 0.009 |
| **TLR4** | 6.307 | 6.300 | 6.235 | 6.232 | 0.070 | 0.003 |
| **LOXHD1** | 6.341 | 6.337 | 6.270 | 6.273 | 0.067 | 0.002 |
| **THC2374512** | 6.870 | 6.869 | 6.800 | 6.805 | 0.066 | 0.002 |
| **LOC283177** | 7.706 | 7.698 | 7.635 | 7.637 | 0.066 | 0.004 |
| **AF113698** | 6.179 | 6.182 | 6.134 | 6.134 | 0.047 | 0.001 |
| **ELL3** | 8.308 | 8.308 | 8.258 | 8.265 | 0.047 | 0.006 |
| **LOC653579** | 6.612 | 6.604 | 6.567 | 6.568 | 0.041 | 0.009 |
| **IL18BP** | 6.510 | 6.510 | 6.538 | 6.534 | -0.026 | 0.007 |
| **KLHL5** | 7.931 | 7.930 | 7.961 | 7.961 | -0.030 | 0.000 |
| **ZNF547** | 6.341 | 6.337 | 6.371 | 6.372 | -0.032 | 0.005 |
| **DNALI1** | 6.333 | 6.337 | 6.371 | 6.372 | -0.036 | 0.003 |
| **A_24_P11980** | 6.208 | 6.202 | 6.244 | 6.242 | -0.038 | 0.005 |
| **BU681613** | 6.472 | 6.477 | 6.524 | 6.517 | -0.046 | 0.009 |
| **DSCAM** | 6.487 | 6.485 | 6.531 | 6.534 | -0.046 | 0.001 |
| **CD1E** | 6.018 | 6.009 | 6.065 | 6.066 | -0.052 | 0.008 |
| **SLC29A3** | 7.329 | 7.333 | 7.381 | 7.388 | -0.054 | 0.006 |
| **AF116641** | 6.495 | 6.493 | 6.553 | 6.559 | -0.062 | 0.003 |
| **A_23_P71179** | 6.753 | 6.749 | 6.818 | 6.813 | -0.064 | 0.003 |

| | | | | | | |
|---|---|---|---|---|---|---|
| **A2ML1** | 6.955 | 6.955 | 7.021 | 7.035 | -0.073 | 0.009 |
| **PDE7A** | 6.367 | 6.373 | 6.442 | 6.455 | -0.078 | 0.009 |
| **AF086013** | 6.456 | 6.468 | 6.545 | 6.542 | -0.082 | 0.006 |
| **PLXNC1** | 6.198 | 6.202 | 6.287 | 6.293 | -0.090 | 0.002 |
| **THC2288322** | 6.272 | 6.262 | 6.363 | 6.352 | -0.091 | 0.006 |
| **ENST00000334564** | 6.179 | 6.182 | 6.270 | 6.273 | -0.091 | 0.000 |
| **AK125173** | 6.189 | 6.182 | 6.270 | 6.283 | -0.091 | 0.006 |
| **BX457454** | 7.604 | 7.594 | 7.694 | 7.689 | -0.092 | 0.004 |
| **IL6** | 6.876 | 6.869 | 6.964 | 6.966 | -0.093 | 0.002 |
| **LOC400451** | 6.753 | 6.756 | 6.841 | 6.854 | -0.093 | 0.005 |
| **EDNRB** | 6.121 | 6.119 | 6.217 | 6.211 | -0.094 | 0.001 |
| **BC034817** | 6.208 | 6.202 | 6.304 | 6.293 | -0.094 | 0.004 |
| **A_24_P925678** | 6.502 | 6.518 | 6.608 | 6.600 | -0.094 | 0.008 |
| **VAPA** | 9.457 | 9.443 | 9.546 | 9.543 | -0.095 | 0.006 |
| **THC2455681** | 6.101 | 6.098 | 6.199 | 6.189 | -0.095 | 0.003 |
| **C17orf25** | 9.858 | 9.872 | 9.954 | 9.965 | -0.095 | 0.009 |
| **GJA10** | 6.341 | 6.355 | 6.449 | 6.446 | -0.099 | 0.005 |
| **KPNA6** | 8.070 | 8.062 | 8.158 | 8.176 | -0.101 | 0.010 |
| **KRT27** | 6.131 | 6.141 | 6.235 | 6.242 | -0.103 | 0.003 |
| **SLC31A1** | 7.392 | 7.383 | 7.488 | 7.494 | -0.104 | 0.003 |
| **PTHLH** | 7.123 | 7.114 | 7.230 | 7.217 | -0.105 | 0.006 |
| **COL4A5** | 6.392 | 6.391 | 6.494 | 6.508 | -0.110 | 0.004 |
| **C4orf7** | 6.502 | 6.493 | 6.602 | 6.617 | -0.111 | 0.006 |
| **AA617765** | 6.049 | 6.043 | 6.171 | 6.157 | -0.118 | 0.005 |
| **WNK3** | 6.208 | 6.202 | 6.313 | 6.333 | -0.118 | 0.008 |
| **NUP160** | 7.312 | 7.300 | 7.420 | 7.431 | -0.119 | 0.004 |
| **AK025573** | 6.018 | 6.031 | 6.143 | 6.146 | -0.120 | 0.003 |
| **A_23_P206741** | 6.727 | 6.722 | 6.836 | 6.854 | -0.120 | 0.007 |
| **KCNH6** | 7.308 | 7.314 | 7.428 | 7.435 | -0.121 | 0.002 |
| **CACNG2** | 6.254 | 6.262 | 6.387 | 6.372 | -0.122 | 0.005 |
| **A_32_P406186** | 6.121 | 6.119 | 6.253 | 6.232 | -0.122 | 0.007 |
| **KIAA0256** | 6.408 | 6.426 | 6.545 | 6.534 | -0.123 | 0.007 |
| **A_24_P922430** | 6.091 | 6.098 | 6.226 | 6.211 | -0.124 | 0.005 |
| **WIT1** | 6.424 | 6.426 | 6.560 | 6.542 | -0.126 | 0.005 |
| **A_24_P460405** | 6.121 | 6.141 | 6.262 | 6.263 | -0.132 | 0.006 |
| **THC2425210** | 6.060 | 6.054 | 6.199 | 6.178 | -0.132 | 0.007 |
| **LOC148203** | 6.208 | 6.222 | 6.354 | 6.343 | -0.134 | 0.005 |
| **SIKE** | 6.217 | 6.222 | 6.354 | 6.352 | -0.134 | 0.000 |
| **ENST00000377233** | 7.255 | 7.237 | 7.381 | 7.379 | -0.134 | 0.004 |
| **CR590180** | 6.408 | 6.400 | 6.545 | 6.534 | -0.136 | 0.003 |
| **ENST00000263739** | 6.060 | 6.076 | 6.208 | 6.200 | -0.136 | 0.004 |
| **LOC284998** | 6.208 | 6.202 | 6.330 | 6.352 | -0.136 | 0.007 |
| **MED12L** | 6.049 | 6.031 | 6.181 | 6.178 | -0.139 | 0.004 |
| **ENTPD3** | 6.198 | 6.202 | 6.346 | 6.333 | -0.139 | 0.002 |
| **SLC39A12** | 6.440 | 6.460 | 6.581 | 6.600 | -0.141 | 0.010 |
| **PLAC1** | 6.668 | 6.679 | 6.806 | 6.827 | -0.143 | 0.007 |
| **TLR2** | 6.170 | 6.161 | 6.304 | 6.313 | -0.143 | 0.002 |
| **PASD1** | 5.952 | 5.962 | 6.105 | 6.100 | -0.146 | 0.001 |
| **PCDHGB3** | 6.101 | 6.119 | 6.262 | 6.253 | -0.147 | 0.005 |
| **AF007193** | 6.289 | 6.281 | 6.418 | 6.446 | -0.147 | 0.009 |
| **ENST00000361565** | 6.893 | 6.881 | 7.046 | 7.022 | -0.147 | 0.008 |
| **CCDC99** | 8.801 | 8.792 | 8.946 | 8.951 | -0.152 | 0.001 |
| **KIAA1328** | 6.591 | 6.604 | 6.751 | 6.748 | -0.152 | 0.002 |
| **AL581249** | 6.479 | 6.493 | 6.649 | 6.633 | -0.154 | 0.005 |
| **ENST00000370363** | 6.502 | 6.493 | 6.642 | 6.664 | -0.155 | 0.006 |

| | | | | | | |
|---|---|---|---|---|---|---|
| **THC2404242** | 7.098 | 7.125 | 7.265 | 7.269 | -0.156 | 0.007 |
| **TAS2R8** | 6.392 | 6.391 | 6.553 | 6.542 | -0.156 | 0.001 |
| **AGXT** | 6.341 | 6.337 | 6.494 | 6.499 | -0.158 | 0.000 |
| **VPS13A** | 7.152 | 7.151 | 7.320 | 7.300 | -0.158 | 0.004 |
| **KLHL7** | 7.802 | 7.816 | 7.971 | 7.964 | -0.159 | 0.002 |
| **FLJ39660** | 9.141 | 9.164 | 9.307 | 9.323 | -0.163 | 0.008 |
| **C10orf128** | 6.358 | 6.373 | 6.524 | 6.542 | -0.167 | 0.005 |
| **THC2412999** | 6.350 | 6.382 | 6.538 | 6.534 | -0.170 | 0.009 |
| **POTE14** | 6.208 | 6.192 | 6.371 | 6.372 | -0.171 | 0.002 |
| **C9orf90** | 10.073 | 10.052 | 10.231 | 10.247 | -0.176 | 0.005 |
| **PTPN4** | 6.408 | 6.382 | 6.560 | 6.584 | -0.177 | 0.010 |
| **LANCL3** | 6.464 | 6.460 | 6.655 | 6.625 | -0.178 | 0.007 |
| **A_24_P356304** | 6.416 | 6.408 | 6.581 | 6.600 | -0.178 | 0.003 |
| **CHEK2** | 8.728 | 8.707 | 8.885 | 8.908 | -0.179 | 0.007 |
| **AK091348** | 6.456 | 6.477 | 6.649 | 6.656 | -0.186 | 0.004 |
| **BQ674642** | 6.392 | 6.408 | 6.574 | 6.600 | -0.187 | 0.007 |
| **SLC26A7** | 6.226 | 6.252 | 6.418 | 6.437 | -0.189 | 0.007 |
| **C1orf162** | 6.518 | 6.502 | 6.714 | 6.687 | -0.191 | 0.006 |
| **AF130053** | 6.080 | 6.098 | 6.270 | 6.293 | -0.193 | 0.006 |
| **OR52A1** | 6.612 | 6.635 | 6.830 | 6.805 | -0.194 | 0.007 |
| **A_24_P933305** | 6.647 | 6.620 | 6.824 | 6.834 | -0.195 | 0.006 |
| **AF118084** | 6.472 | 6.477 | 6.675 | 6.664 | -0.196 | 0.001 |
| **XRN1** | 6.111 | 6.130 | 6.330 | 6.303 | -0.196 | 0.007 |
| **FLJ32206** | 6.518 | 6.485 | 6.688 | 6.710 | -0.198 | 0.010 |
| **EMG1** | 12.646 | 12.637 | 12.825 | 12.854 | -0.198 | 0.006 |
| **SNX5** | 8.440 | 8.439 | 8.625 | 8.650 | -0.198 | 0.004 |
| **FAM70A** | 6.028 | 6.020 | 6.217 | 6.232 | -0.200 | 0.002 |
| **ZNFN1A1** | 6.039 | 6.065 | 6.253 | 6.253 | -0.201 | 0.004 |
| **LOC646990** | 6.424 | 6.426 | 6.635 | 6.617 | -0.201 | 0.002 |
| **ZNF175** | 6.316 | 6.337 | 6.545 | 6.517 | -0.205 | 0.008 |
| **ZFP28** | 6.198 | 6.182 | 6.403 | 6.391 | -0.207 | 0.002 |
| **BC042517** | 6.281 | 6.262 | 6.465 | 6.491 | -0.207 | 0.006 |
| **FLJ25371** | 6.160 | 6.161 | 6.387 | 6.352 | -0.209 | 0.007 |
| **AL834140** | 6.121 | 6.109 | 6.304 | 6.343 | -0.209 | 0.009 |
| **PRO2214** | 5.860 | 5.864 | 6.055 | 6.089 | -0.210 | 0.006 |
| **LCK** | 6.727 | 6.715 | 6.948 | 6.928 | -0.217 | 0.003 |
| **TMEM111** | 11.256 | 11.254 | 11.495 | 11.457 | -0.221 | 0.007 |
| **AK092594** | 6.049 | 6.054 | 6.253 | 6.293 | -0.221 | 0.008 |
| **A_32_P59990** | 6.254 | 6.271 | 6.487 | 6.482 | -0.222 | 0.002 |
| **UBE2D2** | 9.273 | 9.271 | 9.508 | 9.484 | -0.223 | 0.003 |
| **A_32_P136614** | 6.263 | 6.281 | 6.480 | 6.517 | -0.226 | 0.008 |
| **AK094424** | 6.028 | 6.020 | 6.235 | 6.273 | -0.230 | 0.007 |
| **KIN** | 7.471 | 7.465 | 7.697 | 7.700 | -0.230 | 0.000 |
| **AMD1** | 11.599 | 11.580 | 11.800 | 11.841 | -0.231 | 0.010 |
| **FAM18B** | 10.579 | 10.585 | 10.804 | 10.821 | -0.231 | 0.001 |
| **THC2314039** | 6.341 | 6.355 | 6.567 | 6.600 | -0.235 | 0.006 |
| **THC2307989** | 7.152 | 7.187 | 7.420 | 7.398 | -0.239 | 0.008 |
| **IL1R2** | 6.080 | 6.098 | 6.338 | 6.323 | -0.241 | 0.002 |
| **ENST00000373644** | 6.456 | 6.468 | 6.714 | 6.695 | -0.242 | 0.002 |
| **AF035297** | 5.952 | 5.914 | 6.162 | 6.189 | -0.243 | 0.009 |
| **PMS2CL** | 8.347 | 8.322 | 8.577 | 8.578 | -0.243 | 0.003 |
| **MTHFR** | 6.307 | 6.337 | 6.574 | 6.559 | -0.245 | 0.005 |
| **ZNF490** | 6.392 | 6.364 | 6.615 | 6.633 | -0.246 | 0.004 |
| **A_24_P736638** | 10.676 | 10.659 | 10.933 | 10.895 | -0.246 | 0.007 |
| **MPHOSPH6** | 8.939 | 8.949 | 9.205 | 9.179 | -0.248 | 0.003 |

| | | | | | | |
|---|---|---|---|---|---|---|
| **LAX1** | 6.217 | 6.212 | 6.457 | 6.473 | -0.250 | 0.001 |
| **LHPP** | 8.262 | 8.245 | 8.485 | 8.528 | -0.253 | 0.008 |
| **CDKL5** | 7.321 | 7.314 | 7.581 | 7.567 | -0.257 | 0.001 |
| **CYP2J2** | 6.708 | 6.707 | 6.980 | 6.954 | -0.259 | 0.003 |
| **C9orf85** | 7.162 | 7.156 | 7.432 | 7.407 | -0.261 | 0.002 |
| **ACTL6A** | 11.019 | 11.051 | 11.295 | 11.304 | -0.264 | 0.004 |
| **DDX1** | 12.598 | 12.616 | 12.864 | 12.880 | -0.265 | 0.002 |
| **THC2307226** | 6.111 | 6.087 | 6.387 | 6.343 | -0.266 | 0.009 |
| **A_24_P195724** | 11.641 | 11.662 | 11.941 | 11.894 | -0.266 | 0.009 |
| **LOC653374** | 7.067 | 7.114 | 7.357 | 7.369 | -0.272 | 0.008 |
| **THC2268343** | 6.307 | 6.346 | 6.615 | 6.584 | -0.273 | 0.008 |
| **AK098699** | 5.930 | 5.950 | 6.217 | 6.211 | -0.274 | 0.001 |
| **ENST00000370892** | 6.281 | 6.232 | 6.524 | 6.542 | -0.277 | 0.009 |
| **ENST00000319043** | 6.392 | 6.417 | 6.695 | 6.672 | -0.279 | 0.004 |
| **AA490192** | 9.291 | 9.277 | 9.584 | 9.574 | -0.295 | 0.001 |
| **RGPD2** | 6.141 | 6.141 | 6.449 | 6.428 | -0.298 | 0.001 |
| **BI752712** | 6.281 | 6.242 | 6.567 | 6.584 | -0.314 | 0.004 |
| **THC2332128** | 6.502 | 6.493 | 6.812 | 6.813 | -0.314 | 0.000 |
| **SAMD9** | 6.887 | 6.894 | 7.230 | 7.184 | -0.317 | 0.005 |
| **LTBP1** | 6.562 | 6.534 | 6.893 | 6.840 | -0.319 | 0.009 |
| **RAB3IP** | 5.963 | 5.950 | 6.304 | 6.253 | -0.322 | 0.007 |
| **RHOA** | 12.627 | 12.601 | 12.919 | 12.966 | -0.329 | 0.006 |
| **C14orf48** | 6.091 | 6.119 | 6.457 | 6.418 | -0.333 | 0.005 |
| **PDZRN4** | 6.263 | 6.202 | 6.581 | 6.559 | -0.337 | 0.009 |
| **PCGF3** | 8.827 | 8.801 | 9.138 | 9.165 | -0.338 | 0.003 |
| **RABGGTB** | 10.833 | 10.852 | 11.205 | 11.196 | -0.358 | 0.001 |
| **UXS1** | 8.952 | 8.898 | 9.319 | 9.286 | -0.378 | 0.007 |
| **CLEC2D** | 11.595 | 11.546 | 11.963 | 11.934 | -0.378 | 0.006 |
| **OXCT1** | 8.127 | 8.135 | 8.686 | 8.593 | -0.508 | 0.008 |
| **WWOX** | 9.523 | 9.612 | 10.137 | 10.142 | -0.572 | 0.006 |
| **IFI44** | 7.991 | 7.972 | 8.534 | 8.609 | -0.590 | 0.004 |
| **FABP5** | 10.694 | 10.730 | 11.370 | 11.320 | -0.633 | 0.002 |
| **LOC346887** | 9.450 | 9.517 | 10.145 | 10.152 | -0.665 | 0.003 |
| **CPVL** | 7.031 | 6.955 | 8.002 | 8.051 | -1.034 | 0.002 |
| **ANK3** | 6.688 | 6.810 | 7.865 | 7.772 | -1.069 | 0.005 |

**Table 3. Differentially expressed genes.**
307 statistically significant different genes differentially expressed between controls and silenced cell lines were selected by ANOVA analysis. A threshold of $p<0.01$ were introduced to select the differentially expressed genes.

| Table 4. Real time PCR validated gene | | | |
|---|---|---|---|
| **Group** | **Gene** | **Expression** | **Description** |
| Top15 | **VIM** | **down** | vimentin |
| Top15 | **TMEM158** | **down** | transmembrane protein 158 |
| Top15 | **SGK1** | **down** | serum/glucocorticoid regulated kinase |
| Top15 | **DCAMKL1** | **down** | doublecortin and CaM kinase-like 1 |
| Top15 | **SYBL1** | **down** | synaptobrevin-like 1 |
| Top15 | **DUSP4** | **down** | dual specificity phosphatase 4 |
| Top15 | **SLC20A1** | **down** | solute carrier family 20 (phosphate transporter), member 1 |
| Top15 | **CXCR4** | **down** | chemokine (C-X-C motif) receptor 4 |
| other | **CDKN2A** | **down** | cyclin-dependent kinase inhibitor 2A |
| other | **LAX1** | **down** | lymphocyte transmembrane adaptor 1 |
| other | **LCK** | **down** | lymphocyte-specific protein tyrosine kinase |
| other | **TNFRSF1A** | **down** | tumor necrosis factor receptor superfamily, member 1A |
| EMT | **CDH2** | **down** | N-cadherin |
| EMT | **FOXC2** | **down** | mesenchyme forkhead 1 |
| EMT | **MMP1** | **down** | matrix metallopeptidase 1 |
| EMT | **ITGB1** | **down** | integrin, beta 1 |
| EMT | **RHOA** | **up** | ras homolog gene family, member A |
| other | **ALPP** | **up** | alkaline phosphatase, placental (Regan isozyme) |
| other | **FAM96A** | **up** | family with sequence similarity 96 |
| EMT | **CDH1** | **up** | E-cadherin (epithelial) |

**Table 4. Real time PCR validated genes.**
Each gene is considered differentially expressed only if both silenced cell lines (sh7-3 and sh7-5) have a value of gene expression greater or lesser than both control cell lines (pLKO.1-3 and pLKO.1-5). By using this approach, we validated 8 of the 9 genes selected between the top 15 genes selected by microarrays analysis (Top15). Moreover, we validated EMT genes (EMT) and genes involved in various biological processes (other).

Interestingly, the TFs selected belong to homebox and HMG-box gene types or anyway are involved in cell differentiation, development and EMT.

Moreover, previuos studies have identified many genes involved in EMT in different cancer types, thus, we verified if a sub set of genes identified to be involved in EMT in colorectal cancer (Loboda, 2011) could be used to cluster controls and silenced cell lines. We found that among those, 21 genes are associated to hERG1 silencing (down-regulated or up-regulated) identifying a genetic EMT signature of the silenced cells (Fig. 12). These genes are directly or indirectly associated to TGF-beta signaling pathway suggesting a key role of hERG1 in regulating this pathway in colorectal cancer.

Bioinformatic analysis of differentially expressed genes identifies 4 gene clusters (Fig. 13). In table 6 are reported the functional biological process statistically enriched in these clusters.

**Table 5. Transcription factor associated with differential expressed genes**

| ID | Base ID | pwm Length | Gene | pValue | Description |
|---|---|---|---|---|---|
| 9394 | MA0156 | 8 | FEV | 0.031 | FEV (ETS oncogene family) |
| 10204 | PB0082 | 17 | TCF3 | 0.031 | transcription factor 3 (E2A immunoglobulin enhancer binding factors) |
| 10266 | PB0144 | 16 | LEF1 | 0.031 | lymphoid enhancer-binding factor 1 |
| 10300 | PB0178 | 14 | SOX8 | 0.031 | SRY (sex determining region Y)-box 8 |
| 10305 | PB0183 | 17 | SRY | 0.031 | SRY (sex determining region Y)-box 17 |
| 10310 | PB0188 | 16 | TCF7L2 | 0.031 | transcription factor 7-like 2 (T-cell specific, HMG-box) |
| 10494 | PH0164 | 17 | SIX4 | 0.031 | sine oculis homeobox homolog 4 (Drosophila) |
| 10205 | PB0083 | 17 | TCF7 | 0.035 | transcription factor 7 (T-cell specific, HMG-box) |
| 10264 | PB0142 | 16 | JUNDM2 | 0.035 | Jun dimerization protein 2 |
| 10292 | PB0170 | 17 | SOX17 | 0.035 | SRY (sex determining region Y)-box 17 |
| 10341 | PH0011 | 17 | ALX1 | 0.035 | ALX homeobox 1 |
| 10504 | PH0174 | 16 | VAX1 | 0.035 | ventral anterior homeobox 1 |
| 9230 | MA0002 | 11 | RUNX1 | 0.039 | mRNA for an acute myeloid leukaemia protein |
| 10183 | PB0061 | 17 | SOX11 | 0.039 | SRY (sex determining region Y)-box 11 |
| 10201 | PB0079 | 16 | SRY | 0.039 | SRY (sex determining region Y)-box 17 |
| 10296 | PB0174 | 16 | SOX30 | 0.039 | SRY (sex determining region Y)-box 30 |
| 10491 | PH0161 | 17 | SIX1 | 0.039 | sine oculis homeobox homolog 1 (Drosophila) |
| 9301 | MA0073 | 20 | RREB1 | 0.042 | ras responsive element binding protein 1 |
| 10186 | PB0064 | 16 | SOX14 | 0.042 | SRY (sex determining region Y)-box 14 |
| 10237 | PB0115 | 16 | EHF | 0.042 | ets homologous factor |
| 10252 | PB0130 | 16 | GM397 | 0.042 | zinc finger and SCAN domain containing 4C |
| 10293 | PB0171 | 16 | SOX18 | 0.042 | SRY (sex determining region Y)-box 18 |
| 10383 | PH0053 | 16 | HOXA6 | 0.042 | homeobox A6 |

**Table 5. Transcription factor associated with differential expressed genes.**
List of transcription factors that can bind the genes differentially expressed (Tab. 3) selected by bioinformatics analysis. After multiple testing correction, we identified the transcription factors statistically significantly associated with the genes differentially expressed. The transcription factors selected belong to homeobox and HMG-box gene groups or are involved in cell differentiation, development and EMT. pwm Length=length of binding motifs.

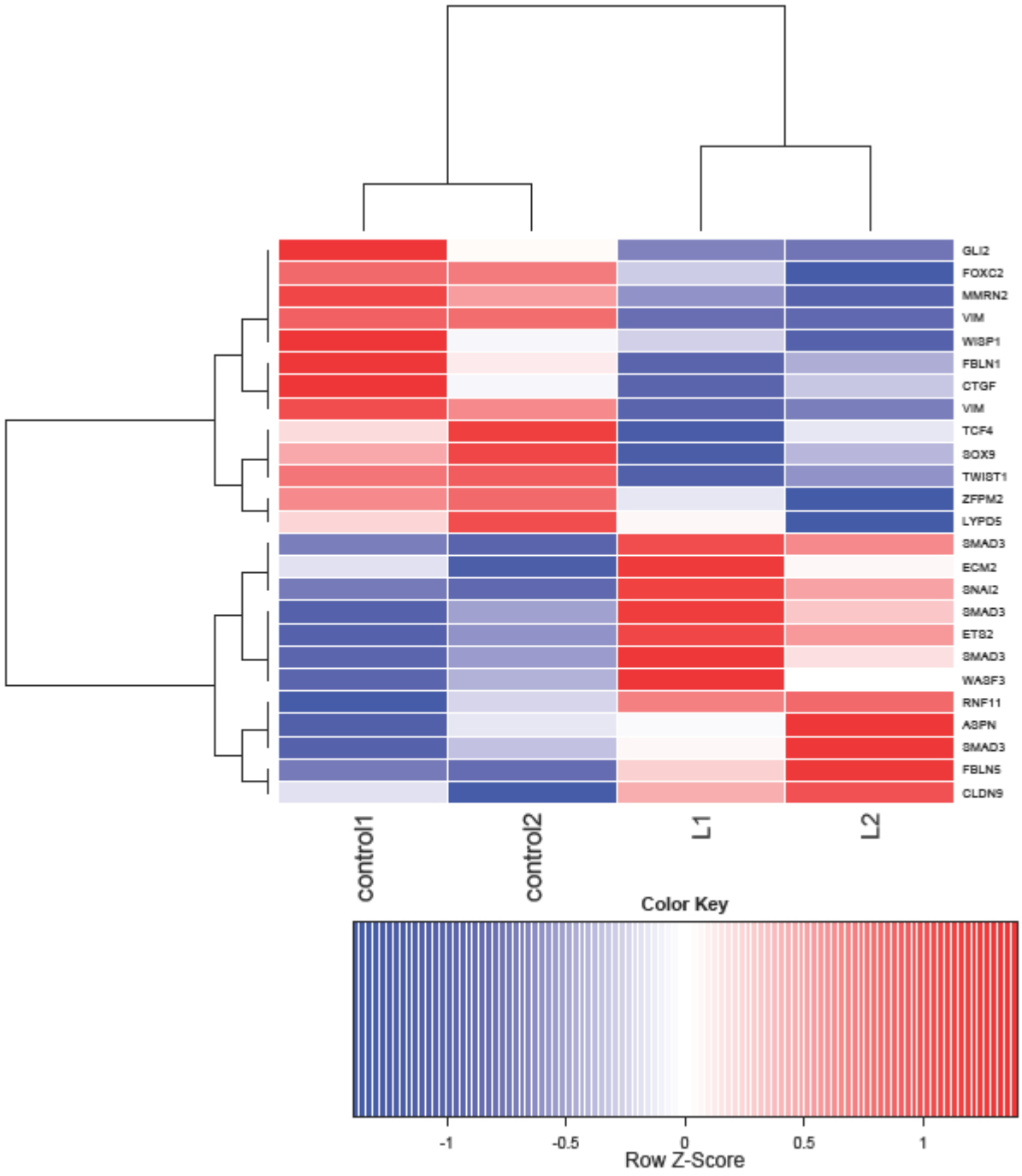


**Figure 12. Hierarchical cluster analysis of EMT associates genes.**
Hierarchical cluster analysis of EMT colorectal cancer associate genes detected 21 genes associated to hERG1 silencing (red: up-regulated; blue: down-regulated) describing a genetic EMT signature of the silenced cells. These genes are directly or indirectly associated to TGF-beta pathway (control1:pLKO.1-3; control2:pLKO.1-5; L1: sh7-3; L2:sh7-5).

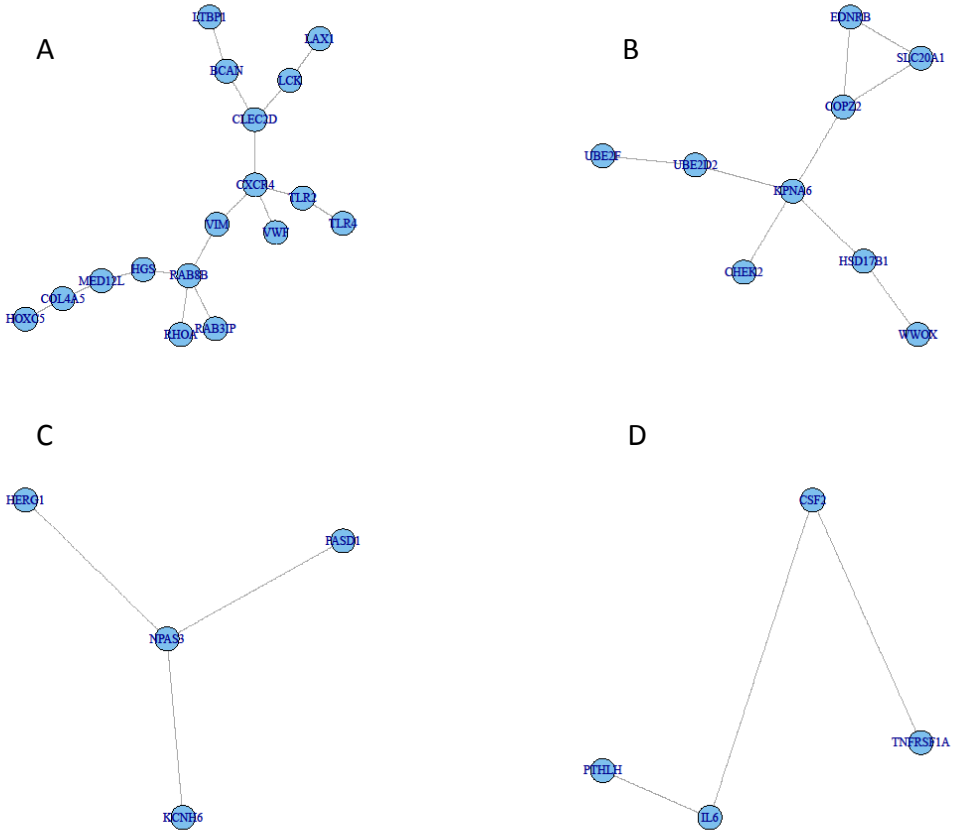


**Figure 13. Bioinformatic analysis of DF genes identifies 4 gene clusters.**

**Table 6. Functional annotation clustering**

**CLUSTER A**

| | | | | | | |
|---|---|---|---|---|---|---|
| Annotation Cluster 1 | Enrichment Score: 2.67 | | | | | |
| **Category** | **Term** | **PValue** | **Fold Enric.** | **Bonferroni** | **Benjamini** | **FDR** |
| GOTERM_BP_FAT | cell activation | 0.000 | 18.854 | 0.003 | 0.003 | 0.010 |
| GOTERM_BP_FAT | leukocyte activation | 0.000 | 18.634 | 0.040 | 0.020 | 0.124 |
| GOTERM_MF_FAT | enzyme binding | 0.000 | 8.761 | 0.028 | 0.028 | 0.343 |
| GOTERM_MF_FAT | kinase binding | 0.001 | 17.066 | 0.110 | 0.057 | 1.373 |
| GOTERM_BP_FAT | positive regulation of immune system process | 0.002 | 15.157 | 0.551 | 0.148 | 2.395 |
| GOTERM_CC_FAT | membrane raft | 0.012 | 16.760 | 0.610 | 0.145 | 11.887 |
| GOTERM_BP_FAT | regulation of cell activation | 0.014 | 15.461 | 0.998 | 0.478 | 17.850 |
| GOTERM_MF_FAT | protein kinase binding | 0.014 | 15.586 | 0.721 | 0.346 | 14.057 |
| GOTERM_BP_FAT | lymphocyte activation | 0.017 | 13.596 | 1.000 | 0.499 | 22.224 |
| GOTERM_BP_FAT | cell surface receptor linked signal transduction | 0.114 | 2.430 | 1.000 | 0.824 | 82.310 |
| | | | | | | |
| Annotation Cluster 2 | Enrichment Score: 2.22 | | | | | |
| GOTERM_CC_FAT | plasma membrane part | 0.002 | 3.264 | 0.117 | 0.117 | 1.650 |
| GOTERM_CC_FAT | plasma membrane | 0.003 | 2.327 | 0.224 | 0.119 | 3.352 |
| SP_PIR_KEYWORDS | membrane | 0.043 | 1.809 | 0.984 | 0.402 | 38.156 |
| | | | | | | |
| Annotation Cluster 3 | Enrichment Score: 1.91 | | | | | |
| GOTERM_BP_FAT | cell activation | 0.000 | 18.854 | 0.003 | 0.003 | 0.010 |
| GOTERM_BP_FAT | leukocyte activation | 0.000 | 18.634 | 0.040 | 0.020 | 0.124 |
| GOTERM_BP_FAT | positive regulation of immune system process | 0.002 | 15.157 | 0.551 | 0.148 | 2.395 |
| UP_SEQ_FEATURE | mutagenesis site | 0.005 | 3.848 | 0.489 | 0.489 | 5.347 |
| GOTERM_BP_FAT | positive regulation of molecular function | 0.021 | 6.156 | 1.000 | 0.530 | 25.713 |
| GOTERM_BP_FAT | positive regulation of signal transduction | 0.036 | 9.172 | 1.000 | 0.642 | 41.016 |
| GOTERM_BP_FAT | positive regulation of cell communication | 0.044 | 8.224 | 1.000 | 0.638 | 47.613 |
| GOTERM_BP_FAT | regulation of apoptosis | 0.047 | 4.487 | 1.000 | 0.641 | 49.395 |
| GOTERM_BP_FAT | regulation of programmed cell death | 0.048 | 4.443 | 1.000 | 0.634 | 50.275 |
| GOTERM_BP_FAT | regulation of cell death | 0.048 | 4.426 | 1.000 | 0.621 | 50.604 |
| GOTERM_BP_FAT | positive regulation of apoptosis | 0.071 | 6.292 | 1.000 | 0.713 | 65.233 |
| GOTERM_BP_FAT | positive regulation of programmed cell death | 0.072 | 6.248 | 1.000 | 0.705 | 65.697 |
| GOTERM_BP_FAT | positive regulation of cell death | 0.073 | 6.220 | 1.000 | 0.695 | 66.004 |
| GOTERM_BP_FAT | regulation of transcription | 0.275 | 1.734 | 1.000 | 0.984 | 98.997 |
| | | | | | | |
| Annotation Cluster 4 | Enrichment Score: 1.53 | | | | | |
| GOTERM_BP_FAT | cell activation | 0.000 | 18.854 | 0.003 | 0.003 | 0.010 |
| GOTERM_BP_FAT | leukocyte activation | 0.000 | 18.634 | 0.040 | 0.020 | 0.124 |
| GOTERM_BP_FAT | Imm. response-activating reg. signal transd. | 0.001 | 52.031 | 0.454 | 0.183 | 1.813 |
| GOTERM_BP_FAT | transduction | 0.001 | 48.314 | 0.504 | 0.161 | 2.098 |
| GOTERM_BP_FAT | positive regulation of immune system process | 0.002 | 15.157 | 0.551 | 0.148 | 2.395 |
| GOTERM_BP_FAT | activation of immune response | 0.004 | 28.783 | 0.857 | 0.277 | 5.723 |
| UP_SEQ_FEATURE | disulfide bond | 0.005 | 3.191 | 0.520 | 0.308 | 5.840 |
| GOTERM_CC_FAT | proteinaceous extracellular matrix | 0.006 | 9.986 | 0.361 | 0.106 | 5.837 |
| GOTERM_BP_FAT | protein kinase cascade | 0.006 | 9.750 | 0.939 | 0.329 | 8.108 |
| SP_PIR_KEYWORDS | disulfide bond | 0.006 | 3.096 | 0.432 | 0.246 | 6.392 |
| GOTERM_BP_FAT | intracellular signaling cascade | 0.007 | 4.308 | 0.958 | 0.328 | 9.168 |
| GOTERM_CC_FAT | extracellular matrix | 0.007 | 9.262 | 0.424 | 0.105 | 7.147 |
| GOTERM_BP_FAT | positive regulation of immune response | 0.010 | 18.659 | 0.989 | 0.395 | 12.799 |
| SP_PIR_KEYWORDS | immune response | 0.015 | 15.154 | 0.748 | 0.368 | 14.853 |
| GOTERM_BP_FAT | response to wounding | 0.016 | 6.807 | 0.999 | 0.494 | 20.302 |
| GOTERM_CC_FAT | external side of plasma membrane | 0.016 | 14.098 | 0.731 | 0.171 | 16.158 |
| SP_PIR_KEYWORDS | extracellular matrix | 0.017 | 14.085 | 0.795 | 0.232 | 16.878 |
| GOTERM_BP_FAT | positive regulation of molecular function | 0.021 | 6.156 | 1.000 | 0.530 | 25.713 |
| GOTERM_BP_FAT | positive regulation of response to stimulus | 0.024 | 11.464 | 1.000 | 0.559 | 29.341 |
| GOTERM_BP_FAT | immune response | 0.032 | 5.228 | 1.000 | 0.612 | 36.747 |

| | | | | | | |
|---|---|---|---|---|---|---|
| UP_SEQ_FEATURE | glycosylation site:N-linked (GlcNAc...) | 0.039 | 2.178 | 0.997 | 0.856 | 37.920 |
| GOTERM_BP_FAT | inflammatory response | 0.043 | 8.325 | 1.000 | 0.648 | 46.849 |
| SP_PIR_KEYWORDS | glycoprotein | 0.048 | 2.096 | 0.990 | 0.399 | 41.432 |
| GOTERM_CC_FAT | cell surface | 0.061 | 6.887 | 0.993 | 0.465 | 48.958 |
| GOTERM_MF_FAT | carbohydrate binding | 0.069 | 6.472 | 0.999 | 0.733 | 54.306 |
| GOTERM_BP_FAT | regulation of phosphorylation | 0.082 | 5.806 | 1.000 | 0.728 | 70.540 |
| GOTERM_BP_FAT | regulation of phosphate metabolic process | 0.088 | 5.579 | 1.000 | 0.742 | 73.111 |
| GOTERM_BP_FAT | regulation of phosphorus metabolic process | 0.088 | 5.579 | 1.000 | 0.742 | 73.111 |
| GOTERM_CC_FAT | extracellular region part | 0.098 | 3.329 | 1.000 | 0.594 | 66.349 |
| GOTERM_BP_FAT | cell surface receptor linked signal transduction | 0.114 | 2.430 | 1.000 | 0.824 | 82.310 |
| SP_PIR_KEYWORDS | signal | 0.119 | 2.089 | 1.000 | 0.628 | 74.957 |
| UP_SEQ_FEATURE | signal peptide | 0.121 | 2.076 | 1.000 | 0.976 | 78.398 |
| GOTERM_BP_FAT | defense response | 0.131 | 4.399 | 1.000 | 0.858 | 86.541 |
| SP_PIR_KEYWORDS | receptor | 0.140 | 2.859 | 1.000 | 0.663 | 80.768 |
| GOTERM_CC_FAT | integral to plasma membrane | 0.157 | 2.690 | 1.000 | 0.742 | 83.742 |
| SP_PIR_KEYWORDS | Secreted | 0.161 | 2.680 | 1.000 | 0.691 | 85.351 |
| GOTERM_CC_FAT | intrinsic to plasma membrane | 0.165 | 2.630 | 1.000 | 0.727 | 85.269 |
| UP_SEQ_FEATURE | topological domain:Extracellular | 0.184 | 2.067 | 1.000 | 0.993 | 91.006 |
| UP_SEQ_FEATURE | topological domain:Cytoplasmic | 0.309 | 1.666 | 1.000 | 1.000 | 98.752 |
| SP_PIR_KEYWORDS | transmembrane | 0.401 | 1.365 | 1.000 | 0.941 | 99.636 |
| GOTERM_CC_FAT | extracellular region | 0.427 | 1.590 | 1.000 | 0.913 | 99.729 |
| UP_SEQ_FEATURE | transmembrane region | 0.620 | 1.145 | 1.000 | 1.000 | 99.999 |
| GOTERM_CC_FAT | integral to membrane | 0.815 | 0.905 | 1.000 | 0.999 | 100.000 |
| GOTERM_CC_FAT | intrinsic to membrane | 0.844 | 0.874 | 1.000 | 0.999 | 100.000 |
| | | | | | | |
| Annotation Cluster 5 | Enrichment Score: 1.12 | | | | | |
| GOTERM_BP_FAT | GO:0015031~protein transport | 0.041 | 4.734 | 1.000 | 0.663 | 44.741 |
| GOTERM_BP_FAT | GO:0045184~establishment of protein localization | 0.042 | 4.691 | 1.000 | 0.652 | 45.520 |
| GOTERM_BP_FAT | GO:0008104~protein localization | 0.059 | 4.090 | 1.000 | 0.666 | 57.796 |
| SP_PIR_KEYWORDS | protein transport | 0.060 | 6.999 | 0.997 | 0.443 | 49.458 |
| SP_PIR_KEYWORDS | transport | 0.411 | 2.033 | 1.000 | 0.937 | 99.697 |
| | | | | | | |
| Annotation Cluster 6 | Enrichment Score: 0.82 | | | | | |
| GOTERM_CC_FAT | internal side of plasma membrane | 0.005 | 10.112 | 0.351 | 0.134 | 5.642 |
| SP_PIR_KEYWORDS | lipoprotein | 0.015 | 7.050 | 0.758 | 0.299 | 15.260 |
| SP_PIR_KEYWORDS | cell membrane | 0.029 | 3.094 | 0.934 | 0.322 | 27.241 |
| SP_PIR_KEYWORDS | nucleotide-binding | 0.415 | 2.013 | 1.000 | 0.930 | 99.723 |
| GOTERM_MF_FAT | ribonucleotide binding | 0.683 | 1.248 | 1.000 | 1.000 | 100.000 |
| GOTERM_MF_FAT | purine ribonucleotide binding | 0.683 | 1.248 | 1.000 | 1.000 | 100.000 |
| GOTERM_MF_FAT | purine nucleotide binding | 0.708 | 1.195 | 1.000 | 1.000 | 100.000 |
| GOTERM_MF_FAT | nucleotide binding | 0.792 | 1.021 | 1.000 | 1.000 | 100.000 |
| | | | | | | |
| Annotation Cluster 7 | Enrichment Score: 0.76 | | | | | |
| SP_PIR_KEYWORDS | host-virus interaction | 0.002 | 15.880 | 0.137 | 0.137 | 1.701 |
| GOTERM_CC_FAT | cytosol | 0.200 | 2.403 | 1.000 | 0.691 | 90.593 |
| GOTERM_CC_FAT | cytoskeleton | 0.216 | 2.314 | 1.000 | 0.699 | 92.403 |
| GOTERM_CC_FAT | cytoskeletal part | 0.309 | 2.517 | 1.000 | 0.820 | 98.009 |
| SP_PIR_KEYWORDS | cytoplasm | 0.542 | 1.358 | 1.000 | 0.970 | 99.981 |
| GOTERM_CC_FAT | intracellular non-membrane-bounded organelle | 0.614 | 1.231 | 1.000 | 0.981 | 99.996 |
| GOTERM_CC_FAT | non-membrane-bounded organelle | 0.614 | 1.231 | 1.000 | 0.981 | 99.996 |
| | | | | | | |
| Annotation Cluster 8 | Enrichment Score: 0.34 | | | | | |
| GOTERM_BP_FAT | regulation of transcription | 0.275 | 1.734 | 1.000 | 0.984 | 98.997 |
| GOTERM_BP_FAT | regulation of transcription, DNA-dependent | 0.565 | 1.526 | 1.000 | 1.000 | 99.999 |
| GOTERM_BP_FAT | regulation of RNA metabolic process | 0.578 | 1.492 | 1.000 | 1.000 | 100.000 |
| | | | | | | |
| Annotation Cluster 9 | Enrichment Score: 0.007432102946880186 | | | | | |
| GOTERM_MF_FAT | metal ion binding | 0.982 | 0.553 | 1.000 | 1.000 | 100.000 |

| | | | | | | |
|---|---|---|---|---|---|---|
| GOTERM_MF_FAT | cation binding | 0.983 | 0.548 | 1.000 | 1.000 | 100.000 |
| GOTERM_MF_FAT | ion binding | 0.984 | 0.540 | 1.000 | 1.000 | 100.000 |

**CLUSTER B**

| | | | | | | |
|---|---|---|---|---|---|---|
| Annotation Cluster 1 | Enrichment Score: 0.83 | | | | | |
| **Category** | **Term** | **PValue** | **Fold Enric.** | **Bonferroni** | **Benjamini** | **FDR** |
| UP_SEQ_FEATURE | mutagenesis site | 0.006 | 5.192 | 0.261 | 0.261 | 5.930 |
| UP_SEQ_FEATURE | active site:Proton acceptor | 0.029 | 9.682 | 0.748 | 0.498 | 24.289 |
| GOTERM_BP_FAT | regulation of apoptosis | 0.078 | 5.609 | 1.000 | 1.000 | 63.826 |
| GOTERM_BP_FAT | regulation of programmed cell death | 0.079 | 5.553 | 1.000 | 1.000 | 64.493 |
| GOTERM_BP_FAT | regulation of cell death | 0.080 | 5.533 | 1.000 | 0.996 | 64.741 |
| SP_PIR_KEYWORDS | disease mutation | 0.137 | 4.030 | 0.999 | 0.973 | 75.695 |
| SP_PIR_KEYWORDS | alternative splicing | 0.662 | 1.142 | 1.000 | 0.999 | 99.997 |
| UP_SEQ_FEATURE | splice variant | 0.664 | 1.139 | 1.000 | 1.000 | 99.997 |
| SP_PIR_KEYWORDS | polymorphism | 0.951 | 0.740 | 1.000 | 1.000 | 100.000 |
| UP_SEQ_FEATURE | sequence variant | 0.965 | 0.708 | 1.000 | 1.000 | 100.000 |
| | | | | | | |
| Annotation Cluster 2 | Enrichment Score: 0.68 | | | | | |
| SP_PIR_KEYWORDS | atp-binding | 0.101 | 4.835 | 0.995 | 0.995 | 63.874 |
| SP_PIR_KEYWORDS | nucleotide-binding | 0.151 | 3.803 | 1.000 | 0.865 | 79.178 |
| GOTERM_MF_FAT | ATP binding | 0.185 | 3.296 | 1.000 | 1.000 | 85.207 |
| GOTERM_MF_FAT | adenyl ribonucleotide binding | 0.189 | 3.252 | 1.000 | 0.990 | 85.878 |
| GOTERM_MF_FAT | adenyl nucleotide binding | 0.205 | 3.087 | 1.000 | 0.965 | 88.323 |
| GOTERM_MF_FAT | purine nucleoside binding | 0.210 | 3.041 | 1.000 | 0.925 | 88.986 |
| GOTERM_MF_FAT | nucleoside binding | 0.212 | 3.020 | 1.000 | 0.878 | 89.279 |
| GOTERM_MF_FAT | ribonucleotide binding | 0.259 | 2.652 | 1.000 | 0.890 | 93.984 |
| GOTERM_MF_FAT | purine ribonucleotide binding | 0.259 | 2.652 | 1.000 | 0.890 | 93.984 |
| GOTERM_MF_FAT | purine nucleotide binding | 0.277 | 2.538 | 1.000 | 0.870 | 95.194 |
| GOTERM_MF_FAT | nucleotide binding | 0.348 | 2.169 | 1.000 | 0.905 | 98.166 |
| | | | | | | |
| Annotation Cluster 3 | Enrichment Score: 0.37 | | | | | |
| GOTERM_CC_FAT | plasma membrane part | 0.207 | 2.901 | 1.000 | 0.996 | 89.102 |
| GOTERM_CC_FAT | plasma membrane | 0.463 | 1.692 | 1.000 | 1.000 | 99.733 |
| SP_PIR_KEYWORDS | membrane | 0.791 | 1.025 | 1.000 | 1.000 | 100.000 |

**CLUSTER C**

| | | | | | | |
|---|---|---|---|---|---|---|
| Annotation Cluster 1 | Enrichment Score: 3.07 | | | | | |
| **Category** | **Term** | **PValue** | **Fold Enrich.** | **Bonferroni** | **Benjamini** | **FDR** |
| UP_SEQ_FEATURE | domain:PAC | 0.000 | 551.337 | 0.000 | 0.000 | 0.004 |
| INTERPRO | IPR013767:PAS fold | 0.000 | 499.770 | 0.000 | 0.000 | 0.004 |
| INTERPRO | IPR001610:PAC motif | 0.000 | 480.548 | 0.000 | 0.000 | 0.005 |
| SMART | SM00086:PAC | 0.000 | 261.894 | 0.000 | 0.000 | 0.009 |
| GOTERM_BP_FAT | regulation of transcription, DNA-dependent | 0.017 | 7.630 | 0.455 | 0.455 | 14.221 |
| GOTERM_BP_FAT | regulation of RNA metabolic process | 0.018 | 7.462 | 0.470 | 0.272 | 14.825 |
| GOTERM_BP_FAT | regulation of transcription | 0.037 | 5.201 | 0.732 | 0.356 | 28.362 |
| SP_PIR_KEYWORDS | alternative splicing | 0.059 | 2.569 | 0.753 | 0.753 | 38.237 |
| UP_SEQ_FEATURE | splice variant | 0.059 | 2.563 | 0.755 | 0.375 | 38.453 |
| | | | | | | |
| Annotation Cluster 2 | Enrichment Score: 2.56 | | | | | |
| UP_SEQ_FEATURE | domain:PAS | 0.000 | 955.650 | 0.000 | 0.000 | 0.001 |
| INTERPRO | IPR000014:PAS | 0.000 | 378.614 | 0.000 | 0.000 | 0.007 |
| SMART | SM00091:PAS | 0.000 | 206.341 | 0.000 | 0.000 | 0.015 |
| SP_PIR_KEYWORDS | alternative splicing | 0.059 | 2.569 | 0.753 | 0.753 | 38.237 |
| UP_SEQ_FEATURE | splice variant | 0.059 | 2.563 | 0.755 | 0.375 | 38.453 |
| SP_PIR_KEYWORDS | polymorphism | 0.649 | 1.249 | 1.000 | 1.000 | 99.975 |
| UP_SEQ_FEATURE | sequence variant | 0.687 | 1.195 | 1.000 | 0.999 | 99.990 |

**CLUSTER D**

| Annotation Cluster 1 | Enrichment Score: 2.30 | | | | | |
|---|---|---|---|---|---|---|
| **Category** | **Term** | **PValue** | **Fold Enric.** | **Bonferroni** | **Benjamini** | **FDR** |
| GOTERM_BP_FAT | positive reg. of nucleic acid metab. process | 0.000 | 21.679 | 0.034 | 0.034 | 0.134 |
| GOTERM_BP_FAT | positive reg. of nitrogen comp. metab. process | 0.000 | 21.006 | 0.037 | 0.019 | 0.147 |
| GOTERM_BP_FAT | positive reg. of cellular biosynthetic process | 0.000 | 19.749 | 0.044 | 0.015 | 0.177 |
| GOTERM_BP_FAT | positive regulation of biosynthetic process | 0.000 | 19.465 | 0.046 | 0.012 | 0.185 |
| GOTERM_BP_FAT | positive regulation of protein kinase cascade | 0.000 | 60.754 | 0.146 | 0.031 | 0.615 |
| SP_PIR_KEYWORDS | Secreted | 0.001 | 11.388 | 0.023 | 0.023 | 0.597 |
| GOTERM_BP_FAT | regulation of protein kinase cascade | 0.001 | 40.747 | 0.296 | 0.057 | 1.360 |
| GOTERM_BP_FAT | positive regulation of developmental process | 0.001 | 36.496 | 0.354 | 0.061 | 1.690 |
| GOTERM_BP_FAT | positive regulation of signal transduction | 0.001 | 34.393 | 0.389 | 0.060 | 1.900 |
| GOTERM_BP_FAT | positive regulation of cell communication | 0.002 | 30.839 | 0.457 | 0.066 | 2.355 |
| KEGG_PATHWAY | hsa04060:Cytokine-cytokine receptor interact. | 0.003 | 19.408 | 0.049 | 0.049 | 1.965 |
| GOTERM_BP_FAT | positive regulation of cell proliferation | 0.003 | 24.507 | 0.619 | 0.092 | 3.693 |
| GOTERM_CC_FAT | extracellular region | 0.004 | 6.359 | 0.046 | 0.046 | 2.472 |
| SP_PIR_KEYWORDS | signal | 0.005 | 5.918 | 0.156 | 0.081 | 4.189 |
| UP_SEQ_FEATURE | signal peptide | 0.005 | 5.881 | 0.116 | 0.116 | 3.917 |
| GOTERM_BP_FAT | positive regulation of gene expression | 0.005 | 17.463 | 0.849 | 0.158 | 7.098 |
| GOTERM_BP_FAT | positive reg. of macromol. biosynthetic process | 0.007 | 15.514 | 0.908 | 0.180 | 8.884 |
| GOTERM_BP_FAT | immune response | 0.008 | 14.704 | 0.930 | 0.185 | 9.825 |
| GOTERM_CC_FAT | extracellular space | 0.008 | 13.995 | 0.095 | 0.049 | 5.219 |
| GOTERM_BP_FAT | regulation of cell proliferation | 0.010 | 12.892 | 0.968 | 0.218 | 12.545 |
| GOTERM_BP_FAT | positive reg. of macromolecule metab. process | 0.012 | 11.839 | 0.983 | 0.237 | 14.661 |
| GOTERM_CC_FAT | extracellular region part | 0.016 | 9.986 | 0.177 | 0.063 | 9.893 |
| UP_SEQ_FEATURE | disulfide bond | 0.059 | 5.085 | 0.780 | 0.531 | 38.855 |
| SP_PIR_KEYWORDS | disulfide bond | 0.062 | 4.934 | 0.895 | 0.528 | 43.427 |
| GOTERM_BP_FAT | regulation of transcription | 0.097 | 3.901 | 1.000 | 0.892 | 75.117 |
| UP_SEQ_FEATURE | glycosylation site:N-linked (GlcNAc...) | 0.120 | 3.472 | 0.959 | 0.655 | 64.497 |
| SP_PIR_KEYWORDS | glycoprotein | 0.129 | 3.341 | 0.992 | 0.700 | 70.439 |
| SP_PIR_KEYWORDS | polymorphism | 0.216 | 1.665 | 1.000 | 0.819 | 88.478 |
| UP_SEQ_FEATURE | sequence variant | 0.247 | 1.594 | 0.999 | 0.830 | 89.988 |

**Table 6. Functional annotation clustering.** Bioinformatic analysis of clusters A, B, C and D. Term=Enrichment of functional process, Fold enrich.= Fold enrichment

## DISCUSSION

The epithelium-mesenchymal transition plays a key role in tumor progression, allowing cells to invade surrounding tissues and intravasate into lymph and blood vessels leading to the formation of distant metastases. The activation of complex signaling processes and the rearrangement of cytoskeleton are at the molecular basis of phenotypic and behavior changes of cells that undergoing EMT process. Hence, genes that acting on the regulation of EMT have a key role in tumor biology therefore the discovery of novel genes involved in EMT potentially has a prognostic and therapeutic relevance.

We knock-down the expression of hERG1 ion channel gene in HCT116 cells by lentivirus mediated RNAi because HCT116 cell line show a mesenchymal molecular profile and in the same time has a high expression of hERG1 gene. We verified that the transcripts and the proteins of hERG1 are reduced in the silenced cells. Most importantly, the silenced cells have lost their ability to respond to $K^+$ stimulation confirming a functional knock-down and impairment of hERG1 ion channels. The two shRNAs selected have a different level of hERG1 silencing: the sh4 shRNA have a stronger effect on transcript and protein knock-down compared to sh7 shRNA but the last have a stronger phenotypic effect. This could be caused by the fact that sh4 recornize only 3 isoforms (the most abundant) conversely the sh7 recornize all the known isoforms. In fact, the hERG1 isoforms orchestrate the correct delivery and assembly of hERG1 channel in the plasmambrane (Guasti, 2008). Thus, the silencing of all isoforms could be the reason of the stronger phenotypic effect registered in our experiments. The silencing of hERG1 gene has several different consequences: a change of cell morphology, the reduction of the proliferative and tumorigenic capacity of the cells both *in vitro* and *in vivo* and a significant reduction of cisplatin resistance. Moreover, we selected a panel of genes able to discriminate either an epithelial or a mesenchymal phenotype and we tested the silenced and control cells for the expression of these genes. Clearly the knock down of hERG1 genes

determine a change in the molecular profile of HCT116 cells in the direction of a more epithelial profile. This suggest that hERG1 gene has a relevant role in EMT. Moreover, we found that the silenced cells (cells that have re-acquired an epithelial-like phenotype) when treated with cisplatin, a drug that act inducing apoptosis, become more sensitive to cisplatin. Also this observation fit with the model that hERG1 expression contribute to the mesenchymal status of HCT116 cells.

Microarray analysis of control vs. silenced cells has identified novel genetic interactions of hERG1 with several different genes involved in cytosckeloton rearrangement and signalling (Tab. 4, 6). The deregulation of these genes could explain the phenotypic and behavior changes observed in silenced cells. For instance, vimentin is involved in cell mobility and lamella and lamellipodia formation and is one of the principal cytoskeletal component of motile mesenchymal and tumor cells. Moreover, vimentin is well known to be involved in the morphology changes of epithelial cells during epithelial to mesenchymal transition.

DCLK1 gene encodes a protein kinase that contains a C-terminal serine/threonine protein kinase domain and two N-terminal doublecortin domains which bind microtubules, regulate tubulin polymerization and have a role in cytoskeleton stability. The microtubules regulation of polymerization is independent of the kinase activity. In addition, it contains a serine/proline-rich domain which mediates protein-protein interactions. Moreover, DCLK1 colocalizes with vimentin and regulate epithelial-mesenchymal transition in human pancreatic adenocarcinoma. Interestingly, DCLK1 is also an intestinal and pancreatic stem cell marker (Sureban, 2009).

VAMP7 is involved in the fusion of transport vesicles to the membrane and is deregulated in the silenced cells. Its knockdown reduce the number of invadopodia as observed in VAMP7- and MT1-MMP-depleted breast cancer cells. Blocking the function of these proteins, cell migration and invasion it will be reduced. Moreover, several kinases are deregulated in silenced cells (Tab. 4). For instance, serum/glucocorticoid regulated kinase 1 gene (SGK1), encodes a serine/threonine protein kinase that activates potassium, sodium, and chloride ion channels,

carriers and Na+/+-ATPase. It regulates the activity of several enzymes and transcription factors and it is involved in numerous function including cell proliferation and apoptosis. SGK1 is up-regulated in several tumors and have a role of tumor growth, in particular in colorectal tumors and it could also has a role in chemoresistance. The TMEM158 gene is an other example of a signaling component affected by hERG1 silencing. TMEM158 is a transmembrane protein, termed also RIS-1 (for Ras-induced senescence 1) that is upregulated in response to activation of the Ras pathway and is often deregulated in cancer. Interestingly, protein kinases not only are involved in signalling but are also involved in initiating the formation of lamellipodia.

Collectively, these data, could explain the morphological change in silenced cells because several of these genes are is involved in cytoskeleton rearrangement and thus their reduction could explain the morphologic changes of the silenced cells. Previous studies have already shown a physical relationship of hERG1 ion channels with proteins involved with cell-cell and cell substrate interactions, such as integrins (Bechetti, 2010). The interaction of hERG1 with integrins has not only a mere mechanical function but determines the activation of signaling mechanisms that appear to activate key mechanisms of the physiology of tumors such as angiogenesis (Pillozzi, 2010). Our results not only confirm that hERG1 interact with genes that are involved in citoskeleton organization but collocate these finding in the contest of EMT processes. The morphological change in the shape of silenced cells as the reduction of the lamellipodia are a clear indication of the reduction of the mesenchymal phenotype of cells and fit very well with the molecular change above described in particular with EMT. Notably, the TFs identified to interact with the genes selected by microarray analysis belong to homebox and HMG-box class of genes or anyway are involved in cell differentiation and development suggesting that hERG1 is involved in cell differentiation. In addition, the silenced cells have a molecular profile congruent with a reduction of the mesenchymal phenotype in favor of an epithelial phenotype. Moreover the analysis of previous described genes involved in EMT of

colorectal cancer indicates an enrichment of deregulated genes directly or indirectly involved with the TGF-beta pathway, a pathways well known to regulate EMT, suggesting a role of hERG1 gene in the modulation of this pathway in colorectal cancer. Collectively, our data, provides evidences of a key role of hERG1 in EMT in colorectal cancer.

## REFERENCES


Arcangeli A, Becchetti A. Complex functional interaction between integrin receptors and ion channels. Trends Cell Biol 2006;16:631-639.

Arcangeli A, Crociani O, Lastraioli E, et al.Targeting ion channels in cancer: a novel frontier in antineoplastic therapy. *Curr Med Chem.* 2009;16:66-93.

Arcangeli A, Becchetti A. New trends in cancer therapy: targeting ion channels and transporters. Pharmaceuticals 2010;3:1202-1224.

Baum B, Settleman J, Quinlan MP. Transitions between epithelial and mesenchymal states in development and disease. Semin Cell Dev Biol. 2008 Jun;19(3):294-308.

Becchetti A, Pillozzi S, Morini R, Nesti E, Arcangeli A. New insights into the regulation of ion channels by integrins. In: Elsevier ed. Int Rev Cell Mol Biol, K. Jeon; 2010.279:135-190.

Davis FM, Peters AA, Grice DM, Cabot PJ, Parat MO, Roberts-Thomson SJ, Monteith GR. Non-stimulated, agonist-stimulated and store-operated Ca2+ influx in MDA-MB-468 breast cancer cells and the effect of EGF-induced EMT on calcium entry. PLoS One. 2012;7(5):e36923.

Fortunato A., Gasparoli L., Falsini S., Boni L., Arcangeli A. An analytical method for the quantification of *hERG1* channel gene expression in human colorectal cancer. Diagnostic Molecular Phatology, 2013, in press.

Guasti L, Crociani O, Redaelli E, Pillozzi S, Polvani S, Masselli M, Mello T, Galli A, Amedei A, Wymore RS, Wanke E, Arcangeli A. Identification of a posttranslational mechanism for the regulation of hERG1 K+ channel expression and hERG1 current density in tumor cells. Mol Cell Biol. 2008 Aug;28(16):5043-60.

Hogan NM, Dwyer RM, Joyce MR, Kerin MJ. Mesenchymal stem cells in the colorectal tumor microenvironment: recent progress and implications. Int J Cancer. 2012 Jul 1;131(1):1-7.

Hu J, Qin K, Zhang Y, Gong J, Li N, Lv D, Xiang R, Tan X. Downregulation of transcription factor Oct4 induces an epithelial-to-mesenchymal transition via enhancement of Ca2+ influx in breast cancer cells. Biochem Biophys Res Commun. 2011 Aug 12;411(4):786-91.

Huber SM, Braun GS, Segerer S, Veh RW, Horster MF. Metanephrogenic mesenchyme-to-epithelium transition induces profound expression changes of ion channels. Am J Physiol Renal Physiol. 2000

Huffaker SJ, Chen J, Nicodemus KK, Sambataro F, Yang F, Mattay V, Lipska BK, Hyde TM, Song J, Rujescu D, Giegling I, Mayilyan K, Proust MJ, Soghoyan A, Caforio G, Callicott JH, Bertolino A, Meyer-Lindenberg A, Chang J, Ji Y, Egan MF, Goldberg TE, Kleinman JE, Lu B, Weinberger DR. A primate-specific, brain isoform of KCNH2 affects cortical physiology, cognition, neuronal repolarization and risk of schizophrenia. Nat Med. 2009 May;15(5):509-18.

Hugo H, Ackland ML, Blick T, Lawrence MG, Clements JA, Williams ED, Thompson EW. Epithelial--mesenchymal and mesenchymal--epithelial transitions in carcinoma progression. J Cell Physiol. 2007 Nov;213(2):374-83.

Kunzelmann K. Ion channels and cancer. J.Membrane Biol. 2005, 205,159-173.

Loboda A, Nebozhyn MV, Watters JW, Buser CA, Shaw PM, Huang PS, Van't Veer L, Tollenaar RA, Jackson DB, Agrawal D, Dai H, Yeatman TJ. EMT is the dominant program in human colon cancer. BMC Med Genomics. 2011 Jan 20;4:9.

Restrepo-Angulo I, Sánchez-Torres C, Camacho J. Human EAG1 potassium channels in the epithelial-to-mesenchymal transition in lung cancer cells. Anticancer Res. 2011, 31(4):1265-70.

Schwarz JR, Bauer CK. Functions of erg K+ channels in excitable cells. J Cell Mol Med. 2004;8:22-30.

Sureban SM, May R, Ramalingam S, Subramaniam D, Natarajan G, Anant S, Houchen CW. Selective blockade of DCAMKL-1 results in tumor growth arrest by a Let-7a MicroRNA-dependent mechanism. Gastroenterology. 2009 Aug;137(2):649-59, 659.e1-2.

Thiery JP. Epithelial-mesenchymal transitions in tumour progression. Nat Rev Cancer. 2002 Jun;2(6):442-54.

Thiery JP, Sleeman JP. Complex networks orchestrate epithelial-mesenchymal transitions. Nat Rev Mol Cell Biol. 2006 Feb;7(2):131-42.

Pfaffl, M.W. A new mathematical model for relative quantification in real-time RT-PCR. Nucleic Acids Research. 2001;29:2002-2007.

Pillozzi S, Arcangeli A. Physical and functional interaction between integrins and hERG1 channels in cancer cells. Adv Exp Med Biol 2010;674:55-67.

Polyak K, Weinberg RA. Transitions between epithelial and mesenchymal states: acquisition of malignant and stem cell traits. Nat Rev Cancer. 2009 Apr;9(4):265-73.

Yang J, Weinberg RA. Epithelial-mesenchymal transition: at the crossroads of development and tumor metastasis. Dev Cell. 2008 Jun;14(6):818-29.

# Chapter 2

## An analytical method for the quantification of hERG1 channel gene expression in human colorectal cancer

## ABSTRACT

Cancer molecular investigation revealed a huge molecular heterogeneity between different types of cancers as well as among cancer patients affected by the same cancer type. This implies the necessity of a personalized approach for cancer diagnosis and therapy, based on the development of standardized protocols to facilitate the application of molecular techniques in the clinical decision making process.

Ion channels encoding genes are acquiring increasing relevance in oncological translational studies, representing new candidates for molecular diagnostic and therapeutic purposes. Hence, the development of molecular protocols for the quantification of ion channels encoding genes in tumor specimens may have relevance for diagnostic and prognostic investigation.

Two main hindrances must be overcome for these purposes: the use of formalin-fixed and paraffin-embedded (FFPE) samples for gene expression analysis and the physiologic expression of ion channels in excitable cells, potentially present in the tumor sample.

We here propose a method for hERG1 gene quantification in colorectal cancer samples in both cryopreserved and FFPE samples. An analytical method was developed to estimate hERG1 gene expression exclusively in epithelial cancer cells. Indeed we found that the hERG1 gene was expressed at significant levels by myofibroblats present in the tumor stroma This method was based on the normalization on a smooth muscle-myofibroblast specific gene, MYH11, with no need of microdissection. By applying this method, hERG1 expression turned out to correlate with VEGF-A expression, confirming previous immunohistochemical data.

## INTRODUCTION

The molecular profiling of cancer has unraveled an extensive molecular heterogeneity not only between different types of tumors but also among patients affected by the same histological tumor type. Hence, the identification and validation of new molecular biomarkers, which can integrate histopathological analysis, for the development of a personalized approach to cancer diagnosis and therapy are urgently needed (Sawyers, 2008; van't Veer, 2008).

Gene expression analysis of primary tumor samples is one of the main techniques applied for identifying genes which are deregulated in cancer and, hence, can represent new biomarkers and drug targets.

To accomplish gene expression analyses, RNA can be extracted from bioptic samples either immediately after surgical excision or from formalin-fixed and paraffin-embedded (FFPE) specimens which are usually used for pathological analyses. FFPE blocks can be also employed for molecular analyses of archival samples, to perform retrospective studies (Farragher, 2008). For these purposes, specific methods must be applied to extract nucleic acid from FFPE samples, since RNA extraction, purification and amplification are hampered by the formalin fixation process (Huijsmans, 2010).

One of the main hindrances to accomplish valuable gene expression analyses of tumor samples is the fact that tumors are composed by several cell types, either in the proper tumor mass or in the tumor microenvironment, each contributing to cancer establishment and progression (Joyce, 2009). In order to gather true and reproducible gene expression data, each bioptic sample should be analyzed at the single cellular level, such as by using microdissection techniques. Alternatively, a bioptic sample can be processed *in toto* and the abundance of the transcript(s) of interest in each cellular type estimated by analytical analyses (Erkkilä, 2010).

Among the genes de-regulated in cancer, those encoding ion channels or transporters are acquiring increasing relevance (Arcangeli, 2009; Masselli, 2012). Among them, hERG1 (other

aliases: KCNH2, Kv11.1) potassium channels are emerging as regulators of tumor growth and progression, in different cancer types, through the exploitation of different mechanisms, such as the regulation of the expression of one of the main regulator of tumor angiogenesis, i.e. VEGF-A (Ferrara, 2003).

Hence, the screening for hERG1 expression in tumor specimens is acquiring a more and more relevant diagnostic and prognostic valence. When searching for hERG1 expression in solid cancers, such as epithelial cancers, the physiologic expression of the hERG1 transcript in non epithelial stromal excitable cells (Tomasek, 2002), such as smooth muscle cells (Shoeb, 2003; Schwarz, 2004) must be taken into account. To this purpose, immunohistochemical techniques are employed, which allow the visualization of single tumor cells, but which do not allow a precise quantification of the expression of the molecule under study. These concepts were exploited in patients with non metastatic colorectal cancer, where hERG1 expression, as from immunohistochemical analysis, turned out to correlate with the expression of angiogenic factors, such as VEGF-A. Moreover, hERG1 positivity, along with a concomitant negative GLUT-1 expression, identified a subgroup of patient with worse prognosis (Lastraioli, 2012).

On the whole, a molecular protocol to quantify hERG1 transcript expression in cancer specimens processed *in toto* by analytical analysis is currently lacking. This could allow to reach a quantitative estimate of hERG1 expression to be exploited for diagnostic and prognostic purposes.

In this chapter, we provide a protocol for the quantitative analysis of hERG1 gene expression in both fresh and FFPE samples of colorectal cancer patients.

## MATERIALS AND METHODS

### Sample handling procedures.

We collected 40 cancer specimens and the corresponding normal mucosa (collected at least 10 cm away from the tumor site) as well as two adenomatous polyps, immediately after surgical resection of tumors from different patients. Samples were collected after obtaining an informed written consent from all the patients. Specimens were collected in order to minimize possible contamination by muscle tissue. Tumor samples were stored at -80° C. We then adopted a procedure aimed at reproducing the variability of fixing procedures which can occur in the different Pathology Departments, as well as at verifying whether formalin-fixed-paraffin embedded (FFPE) blocks could be usable for molecular investigation, per se and despite their heterogeneity in fixation time. Therefore, a subset of 20 specimens were randomly selected. The histological features of the samples are reported in table 1. Each of the 20 specimens was divided into three aliquots: one was fixed in 4% formaldehyde in PBS for 24h, the second was fixed in the same way for longer times (average=21.15 days, ranging from 11 to 49 days). Both aliquots were subsequently embedded in paraffin, according to standard protocols. The third aliquot was directly processed for RNA extraction.

### Preparation and immunohistochemical staining of histological specimens.

The samples were formalin fixed for 24h, dehydrated with graded series of ethanol and toluene before being embedded in paraffin. Subsequently, the samples were cut into 7 μm sections. Paraffin sections were dewaxed and dehydrated with graded ethanol. Endogenous peroxidases were blocked with a 1% $H_2O_2$ solution in phosphate-buffered saline. Antigen retrieval was performed by treatment with proteinase K (5 μg/ml) at 37°C. The following antibodies were used: i) hERG monoclonal antibody (Enzo Life Science) was diluted 1:200 and incubated 16 hours at 4°C; ii) VEGF rabbit polyclonal antibody (Santa Cruz Biotechnology, CA, U.S.A.)

was diluted 1:100 and incubated 16 hours at 4°C; iii) anti-α smooth muscle actin monoclonal (Sigma, product No. A 2547) was diluted 1:4000 and incubated 2 hours at room temperature. Immunostaining was performed with a PicTure Plus kit and DAB; Zymed, Carlsbad, CA kit, according to the manufacturer's instructions.

**Cell culture**

The human CCD-18Co, HCT116, H630 and HT29 cell lines were purchased from the American Type Culture Collection (ATCC) (Rockville, MD). CCD-18Co cells were grown in DMEM High Glucose (DMEM) (EuroClone) medium, HT29 in McCoy's medium (EuroClone) and HCT116 and H630cells were grown in RPMI-1640 medium (EuroClone) supplemented with 2% L-Glut, 10% fetal bovine serum (FBS) (Hyclone) and 1% penicillin/streptomycin under standard cell culture condition.

**Measurements of secreted VEGF**

VEGF was quantified using the DuoSet® ELISA (enzyme-linked immunoabsorbent assay) Development Systems (R&D Systems®) kit following manufacturer's instructions.

**Real time PCR**

Cryopreserved colorectal-cancer specimens (CRC) and cell lines were dipped in TRIzol® Reagent (Invitrogen™) and homogenized with a homogenizer to isolate total RNA according to manufactorer's protocol. RNA from formalin-fixed, paraffin-embedded tissues (FFPE) was extracted from 5 μm sections of tissue blocks using the PureLink™ FFPE isolation kit (Invitrogen™ cat.no. K1560-02), according to manufacturer's protocol. RNA was quantified by spectrophotometer and stored at -80° C. RNA integrity was assessed through the Agilent 2100 Bioanalyzer. One μg of RNA of each specimens was retrotranscribed (RT) in a 20 μl reaction mixture using random primers and SuperScript™ II Reverse Transcriptase (Invitrogen™)

according to manufacturer's protocol. To evaluate the presence of genomic DNA contamination, total RNA of each sample, was splitted into two reactions: one with reverse transcriptase and one without the enzyme (negative control). Then, the samples were tested by PCR for the GAPDH gene. The lack of any amplification PCR product in the RT negative control confirmed the absence of significant contaminating genomic DNA. RNA samples isolated from FFPE were subjected to DNase I treatment. cDNA was diluted 1:3 with sterile bidistilled water to be used as the template for real-time PCR analysis. SYBR green fluorescent dye (Power SYBR® Green, PCR master mix, Applied Biosystems) was used to monitor DNA synthesis. The amplicons size of the target and housekeeping genes and the sequence of primers are reported in Table 1. All primer pairs span intron/exon boundaries. Primers relative to hERG1 and myosin heavy chain 11 (MYH11) were designed using the software Primer3 (http://frodo.wi.mit.edu/); primers relative to GAPDH have been previously described in PrimerBank (http://pga.mgh.harvard.edu/primerbank/). VEGF-A primers were the same as in (Simpson, 2000).

Two µl of the prediluted cDNA were used as template for the PCR in a final volume of 25 µl. The PCR conditions were set as follows: a first denaturation step of 10 minutes at 95° C followed by 40 cycles of denaturation at 95° C for 15 seconds, annealing gene specific primers at 56° C for 1 minute. Melting curves from 60.0° C to 95.0° C, read every 0.5° C. The expression levels of hERG1, MYH11and VEGFA were normalized to the levels of the GAPDH housekeeping gene using the method of Pfaffl, for quantification (Pfaffl, 2001). In order to validate the efficiency of the primers a 10-fold serial dilution of cDNA, generated from a colorectal cancer sample was used to generate a linear regression equation for the target genes and GAPDH. All equations have a coefficient of correlation ($R^2$) greater than 0.990 and a slope coefficient included between -3.1 and -3.6 showing an optimal efficiency of the primers used. The slope coefficients were used to determine the efficiency (E) parameter and to calculate the expression values for both target gene and housekeeping gene after real time PCR analysis.

Melting curve analysis of the amplicons was performed to exclude the amplification of unspecific products or primer-dimer artefacts. Relative expression values for each target gene were expressed as a ratio of target gene expression level to GAPDH expression value in the same specimen and normalized for the value of expression of normal colonic tissue or HT29 cell line. To quantify the expression of hERG1 in the epithelial cancer cells, the expression value of each sample, calculate as described above, was normalized to the expression of MYH11 gene: hERG1 (relative fold value)/MYH11 (relative fold value). MYH11 is a gene expressed in the myofibloblasts but not significantly in the epithelial cancer cells instead, hERG1 is expressed in both myofibroblasts and epithelial cancer cells (see Results). Thus, this normalization allows to estimate the expression of hERG1 in the epithelial cancer cells by removing the contribute of myofibroblasts to hERG1 expression in samples processed *in toto*. Each sample was analysed in triplicate for the target gene and the housekeeping gene. The average measurements were used to generate the data of relative expression of the genes studied in the different specimens. All statistical analyses were performed using commercially available softwares**.**

TABLE 1. Primers sequences

| Gene | | Sequence | Amplificon Size | Source |
|---|---|---|---|---|
| GAPDH | Forward | ACGTCTCTCCCAACACCAAC | 108 | Primer Bank |
| | Reverse | GAGTACAGCCGCTGGATGAT | | |
| hERG1 | Forward | ATGGGGAAGGTGAAGGTCG | 118 | Primer3 |
| | Reverse | GGGGTCATTGATGGCAACAATA | | |
| MYH11 | Forward | CAACGCCAAAACAGTGAAGA | 118 | Primer3 |
| | Reverse | GCCCGTGATTTTTCTAGCAG | | |
| VEGFA | Forward | CGAAACCATGAACTTTCTGC | 302 | Simpson, 2000 |
| | Reverse | CCTCAGTGGGCACACACTCC | | |

**Table 1.** Primers sequences of potassium voltage-gated channel gene (hERG1), glyceraldehyde-3-phosphate dehydrogenase gene (GAPDH), myosin, heavy chain 11, smooth muscle (MYH11) and vascular endothelial growth factor A (VEGFA).

## RESULTS

### Evaluation of hERG1 gene expression in CRC samples.

In order to verify whether FFPE specimens (Tab. 2) could be used to perform hERG1 expression analysis, we compared the amount of the hERG1 transcript (by quantitative PCR, Q-PCR) in the same specimens, either cryopreserved (CRYO) or formalin-fixed for 24 hours and paraffin-embedded (FFPE 24h), or formalin-fixed for longer times (average time of fixation = 21.15 days ) and paraffin-embedded (FFPE 21d). Raw data, expressed as Ct values, are reported in table 3. All measures were expressed as log fold of the original value, in order to normalize the data (see Materials and Methods). Agreement between the measures obtained on the FFPE and CRYO samples was evaluated according to the Blan-Altman method. It emerged that the 95% limits of agreement ranged from –1.32 to +1.05 (FFPE 24h vs CRYO) and from -2.10 to +1.77 (FFPE 21d vs CRYO), most of the differences lying between these limits. It is worth noting that the precision of the measures performed on FFPE 24h samples was higher (SD of differences = ±0.59) than in the FFPE21d group (SD of differences= ±0.97). This was mainly due to the higher number of outliers in the latter group. Thus, the second method introduces a relevant error, unacceptable from a diagnostic point of view (Fig. 1). On the whole, these data suggest that CRYO and FFPE 24h methods provide similar Q-PCR measurements, whereas the FFPE 21d method does not. We then applied the RNA extraction and cDNA synthesis procedures reported above to determine, by Q-PCR, the expression levels of both hERG1 and VEGF-A genes in the whole set of 40 CRC samples. Our aim was to confirm, at the RNA level, previously reported immunohistochemistry (IHC) data (Lastraioli, 2012), as well as to have a quantitative estimate of the levels of the two transcripts in colon carcinoma cells. Either transcript turned out to be expressed in primary tumors specimens (see the raw data in table 4, as expected. However, at difference from what occurs for the levels of the two proteins as emerged from IHC analysis

(Lastraioli, 2012), the expression of the two genes did not correlate in the tumor samples processed *in toto* (Tab. 5).

TABLE 2. Clinicopathological data of FFPE samples

| specimens | TNM | grade | colloid | IHC |
|---|---|---|---|---|
| cr 62 | 4 | 1 | 0 | 1 |
| cr 70 | 4 | 2 | 0 | 0 |
| cr 74 | 5 | 1 | 1 | 0 |
| cr 76 | 1 | 2 | 0 | 1 |
| cr 79 | 2 | 2 | 0 | 0 |
| cr 94 | 2 | 2 | 0 | 1 |
| cr 96 | ND | ND | 0 | 1 |
| cr 100 | 1 | 2 | 0 | 1 |
| cr 102 | ND | ND | 0 | 0 |
| cr 103 | 2 | 2 | 0 | 1 |
| cr 117 | 2 | 2 | 0 | 0 |
| cr 132 | 1 | 3 | 0 | 1 |
| cr 133 | 2 | 2 | 0 | 0 |
| cr 139 | 4 | ND | 0 | 1 |
| cr 140 | 1 | 2 | 0 | 1 |
| cr 145 | 5 | ND | 1 | 0 |
| cr 154 | 2 | ND | 1 | 0 |
| cr 155 | 2 | 2 | 1 | 0 |
| cr 156 | ND | ND | 0 | 0 |
| cr 157 | 6 | 2 | 0 | 1 |

**Table 2.** Clinicopathological data: TNM (Tumor, Node, Metastasis) staging system for colorectal cancer; grade=cancer grading; colloid = colloid histology, IHC = immunoistochemistry anti-HERG1.

TABLE 3. hERG1 gene expression in cryopreserved and FFPE samples

| | cryopreserved | | | FFPE 24h | | | FFPE | | |
|---|---|---|---|---|---|---|---|---|---|
| samples | GAPDH Ct | hERG1 Ct | hERG1 log fold | GAPDH Ct | hERG1 Ct | hERG1 log fold | GAPDH Ct | hERG1 Ct | hERG1 log fold |
| cr 62 | 16.74 | 25.86 | 0.20 | 28.71 | 30.01 | 0.08 | 25.13 | 32.85 | 0.09 |
| cr 70 | 16.27 | 22.63 | 1.06 | 24.03 | 30.90 | 0.25 | 29.42 | 35.39 | 0.63 |
| cr 74 | 14.90 | 23.73 | 0.29 | 18.52 | 26.27 | -0.07 | 27.57 | 34.99 | 0.18 |
| cr 76 | 16.05 | 24.08 | 0.54 | 19.59 | 26.93 | 0.07 | 28.81 | 35.82 | 0.31 |
| cr 79 | 17.27 | 26.73 | 0.09 | 19.32 | 25.95 | 0.29 | 24.26 | 33.35 | -0.35 |
| cr 94 | 17.13 | 25.01 | 0.59 | 31.40 | 31.49 | -0.07 | 24.20 | 33.38 | -0.37 |
| cr 96 | 18.00 | 27.11 | 0.20 | 26.45 | 35.96 | 0.70 | 25.00 | 33.55 | -0.17 |
| cr 100 | 16.21 | 20.98 | 1.56 | 19.57 | 24.14 | 0.94 | 33.66 | 31.49 | 3.19 |
| cr 102 | 16.94 | 25.81 | 0.28 | 22.08 | 28.77 | 0.10 | 22.29 | 30.47 | -0.06 |
| cr 103 | 15.83 | 24.40 | 0.37 | 23.06 | 29.59 | 0.34 | 32.39 | 33.21 | 2.25 |
| cr 117 | 17.11 | 23.87 | 0.94 | 22.42 | 28.98 | 0.33 | 26.53 | 35.06 | -0.17 |
| cr 132 | 16.51 | 29.17 | -0.91 | 23.03 | 33.31 | 0.28 | 24.54 | 35.21 | -0.84 |
| cr 133 | 17.98 | 22.10 | 1.77 | 36.35 | 31.88 | 0.98 | 24.32 | 35.53 | -1.01 |
| cr 139 | 15.81 | 27.86 | -0.72 | 29.98 | 37.06 | -0.04 | 23.44 | 34.68 | -1.02 |
| cr 140 | 18.04 | 24.67 | 0.98 | 26.76 | 34.38 | 0.03 | 34.47 | 35.91 | 2.05 |
| cr 145 | 17.02 | 26.84 | -0.02 | 31.05 | 35.28 | -0.19 | 22.16 | 30.08 | 0.02 |
| cr 154 | 16.86 | 25.38 | 0.39 | 26.81 | 33.46 | 0.92 | 27.16 | 33.76 | 0.43 |
| cr 155 | 15.92 | 24.85 | 0.26 | 24.53 | 32.63 | 0.63 | 20.44 | 28.76 | -0.10 |
| cr 156 | 15.85 | 26.64 | -0.32 | 27.06 | 33.16 | 0.03 | 26.67 | 35.91 | -0.39 |
| cr 157 | 16.22 | 24.89 | 0.34 | 20.87 | 34.05 | -0.41 | 26.21 | 34.44 | -0.07 |

**Table 3.** hERG1 expression values (log fold) in colorectal cancer specimens. Ct=raw data. Each specimens was divided into three parts: FFPE 24h=fixed in formalin for 24 hours, FFPE=fixed for 21.9 days (average), cryopreserved= only cryopreserved. Data were normalized to normal colonic mucosa.

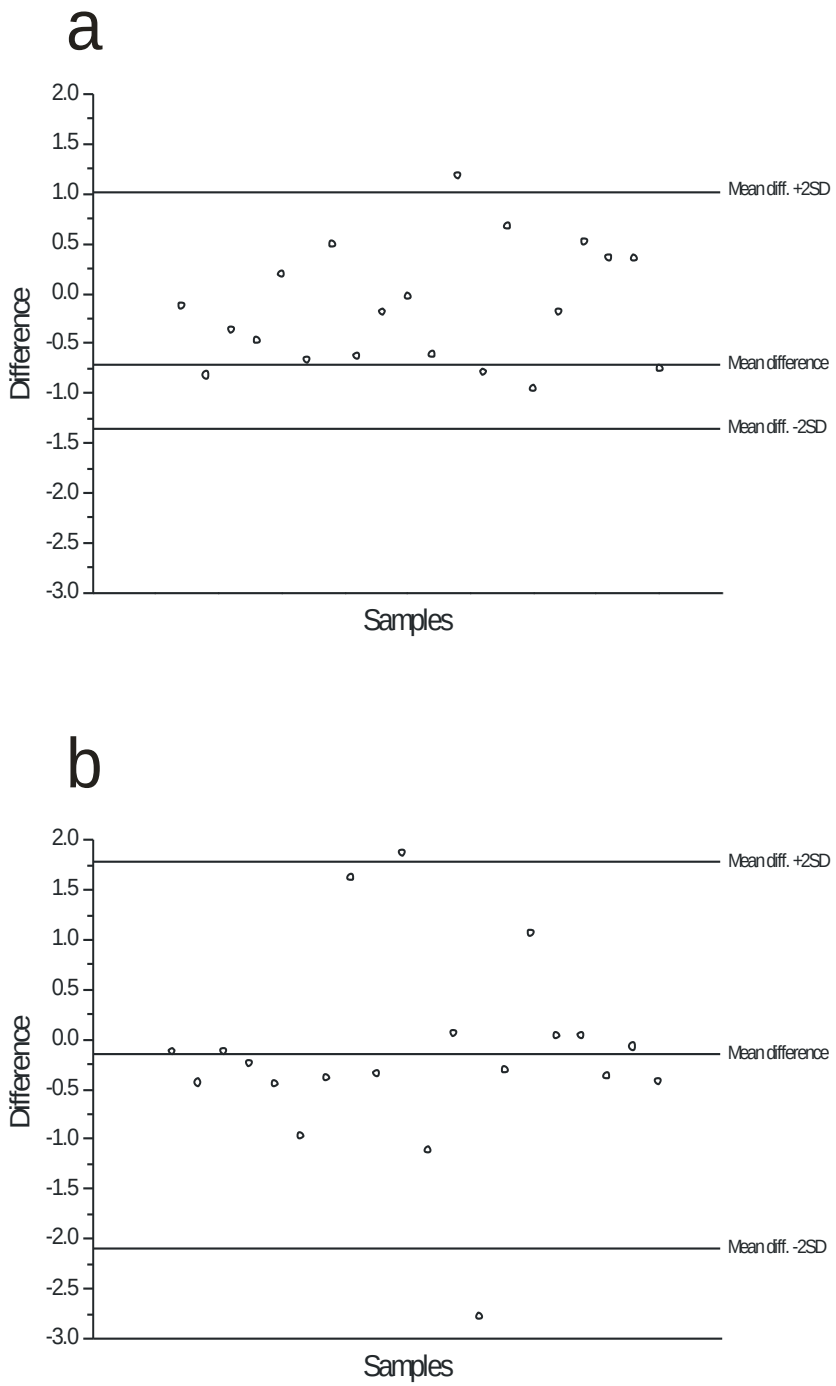


**Figure 1. Comparison of the CRYO and FFPE protocols of gene expression quantification of CRC samples through Bland-Altman analysis.**

The Bland-Altman analysis indicates that the 95% limits of agreement between the two protocols ranged from –1.32 to 1.05 (FFPE 24h) (a) and from -2.10 to 1.77 (FFPE 21d) (b). Most of the differences lie between these limits with both protocols. But, the differences against mean in the fist protocol (FFPE 24h) follow a normal distribution instead in the second protocol (FFPE 21d) the differences are not normally distributed (Shapiro-Wilk test, df=20, W=0.861, p=0.008). This suggest that the FFPE 24h protocol is more reliable than the FFPE 21d protocol.

TABLE 4: Analysis of MYH11, hERG1 and VEGFA expression in colorectal cancer samples

| | GAPDH | MYH11 | MYH11 | GAPDH | hERG1 | hERG1 | GAPDH | VEGFA | VEGFA |
|---|---|---|---|---|---|---|---|---|---|
| | Ct | Ct | fold log | Ct | Ct | fold log | Ct | Ct | fold log |
| cr 5 | 21.14 | 26.27 | 4.00 | 19.93 | 26.53 | 1.10 | 21.14 | 27.20 | -0.28 |
| cr 12 | 18.69 | 26.53 | 3.15 | 18.26 | 27.92 | 0.14 | 18.69 | 25.82 | -0.61 |
| cr 29 | 19.12 | 28.13 | 2.79 | 18.50 | 28.11 | 0.16 | 19.12 | 26.56 | -0.71 |
| cr 62 | 19.22 | 27.10 | 3.14 | 16.74 | 25.86 | 0.31 | 19.22 | 25.09 | -0.21 |
| cr 65 | 18.35 | 28.16 | 2.54 | 16.36 | 26.10 | 0.12 | 18.35 | 25.13 | -0.49 |
| cr 70 | 19.00 | 27.96 | 2.80 | 16.27 | 22.63 | 1.17 | 19.00 | 25.61 | -0.44 |
| cr 73 | 17.58 | 26.53 | 2.80 | 15.29 | 25.15 | 0.08 | 17.58 | 24.01 | -0.37 |
| cr 74 | 17.49 | 27.49 | 2.48 | 14.90 | 23.73 | 0.40 | 17.49 | 23.86 | -0.35 |
| cr 76 | 19.02 | 28.51 | 2.64 | 16.05 | 24.08 | 0.65 | 19.02 | 25.45 | -0.38 |
| cr 77 | 20.03 | 29.96 | 2.50 | 17.18 | 26.82 | 0.15 | 20.03 | 27.34 | -0.68 |
| cr 78 | 19.43 | 28.35 | 2.82 | 16.46 | 23.90 | 0.84 | 19.43 | 25.08 | -0.14 |
| cr 79 | 18.69 | 25.17 | 3.57 | 17.27 | 26.73 | 0.20 | 18.69 | 24.42 | -0.16 |
| cr 89 | 21.33 | 29.42 | 3.08 | 18.43 | 23.75 | 1.50 | 21.33 | 28.68 | -0.70 |
| cr 94 | 19.33 | 27.77 | 2.97 | 17.13 | 25.01 | 0.70 | 19.33 | 25.31 | -0.24 |
| cr 96 | 19.97 | 26.29 | 3.63 | 18.00 | 27.11 | 0.31 | 19.97 | 24.47 | 0.23 |
| cr 100 | 19.17 | 26.89 | 3.19 | 16.21 | 20.98 | 1.67 | 19.17 | 24.62 | -0.07 |
| cr 101 | 17.10 | 26.48 | 2.67 | 14.66 | 25.40 | -0.20 | 17.10 | 23.76 | -0.44 |
| cr 103 | 18.42 | 26.54 | 3.07 | 15.83 | 24.40 | 0.48 | 18.42 | 24.39 | -0.23 |
| cr 104 | 19.95 | 28.00 | 3.09 | 16.07 | 26.10 | 0.03 | 19.95 | 25.14 | 0.01 |
| cr 106 | 21.43 | 28.82 | 3.30 | 18.15 | 27.45 | 0.25 | 21.43 | 27.54 | -0.30 |
| cr 107 | 18.37 | 29.60 | 2.10 | 15.44 | 24.89 | 0.21 | 18.37 | 26.13 | -0.81 |
| cr 110 | 18.00 | 28.08 | 2.45 | 15.44 | 26.30 | -0.24 | 18.00 | 23.82 | -0.18 |
| cr 117 | 19.09 | 28.49 | 2.67 | 17.11 | 23.87 | 1.05 | 19.09 | 24.90 | -0.19 |
| cr 123 | 18.73 | 27.62 | 2.82 | 17.42 | 27.45 | 0.03 | 18.73 | 24.95 | -0.31 |
| cr 132 | 18.79 | 28.86 | 2.46 | 16.51 | 29.17 | -0.80 | 18.79 | 25.12 | -0.35 |
| cr 133 | 20.34 | 19.70 | 5.79 | 17.98 | 22.10 | 1.88 | 20.34 | 26.76 | -0.39 |
| cr 138 | 17.27 | 27.07 | 2.54 | 15.98 | 27.03 | -0.29 | 17.27 | 23.40 | -0.27 |
| cr 139 | 17.13 | 26.94 | 2.53 | 15.81 | 27.86 | -0.61 | 17.13 | 23.07 | -0.21 |
| cr 140 | 19.24 | 29.08 | 2.53 | 18.04 | 24.67 | 1.09 | 19.24 | 26.00 | -0.49 |
| cr 145 | 20.48 | 30.34 | 2.53 | 17.02 | 26.84 | 0.09 | 20.48 | 28.22 | -0.82 |
| cr 150 | 20.01 | 29.53 | 2.63 | 17.21 | 28.97 | -0.52 | 20.01 | 27.34 | -0.68 |
| cr 154 | 17.91 | 26.19 | 3.01 | 16.86 | 25.38 | 0.50 | 17.91 | 24.74 | -0.50 |
| cr 155 | 17.25 | 27.54 | 2.39 | 15.92 | 24.85 | 0.37 | 17.25 | 24.03 | -0.48 |
| cr 157 | 18.44 | 25.92 | 3.26 | 16.22 | 24.89 | 0.45 | 18.44 | 24.89 | -0.38 |
| cr158 | 19.15 | 27.32 | 3.05 | 18.46 | 28.46 | 0.03 | 19.15 | 25.15 | -0.25 |
| cr159 | 17.59 | 27.60 | 2.47 | 16.59 | 25.82 | 0.28 | 17.59 | 25.31 | -0.79 |
| cr170 | 20.98 | 27.04 | 3.71 | 19.27 | 26.71 | 0.84 | 20.98 | 26.78 | -0.20 |
| cr171 | 21.21 | 26.02 | 4.10 | 19.93 | 27.80 | 0.70 | 21.21 | 26.67 | -0.09 |
| cr172 | 20.15 | 26.44 | 3.64 | 18.99 | 28.22 | 0.28 | 20.15 | 26.61 | -0.41 |
| cr176 | 18.16 | 26.06 | 3.13 | 17.36 | 26.48 | 0.31 | 18.16 | 24.46 | -0.34 |

**Table 4.** MYH11, hERG1 and VEGFA expression values (log fold) in colorectal cancer specimens. Ct=raw data. Data were normalized to HT29 cell line.

TABLE 5. Statistical analysis of MYH11, hERG1 and VEGFA gene expression

| | | MYH11 | hERG1 | VEGF/MYH11 |
|---|---|---|---|---|
| **hERG1** | Pearson corr. value | 0.526 | | |
| | Sig. | **p=0.0001** | | |
| | n | 40 | | |
| **VEGFA** | Pearson corr. value | 0.349 | 0.093 | |
| | Sig. | **p=0.027** | **p=0.569** | |
| | | 40 | 40 | |
| **hERG1/MYH11** | Pearson corr. value | | | 0.494 |
| | Sig. | | | **p=0.001** |
| | n | | | 40 |

**Table 5.** Pearson correlation between the gene expression of MYH11, VEGFA and normalized by the expression of MYH11 (hERG1/MYH11 and VEGFA/MYH11). n=number of specimens; Sig.=test of significance value (2-tailed).

**Stromal myofibroblasts express MHY11, hERG1 and VEGF-A.**

Such discrepancy could be due to the fact that, while the evaluation of the IHC staining in the tumor samples reported in Lastraioli *et al*., 2013, took into account only the expression of hERG1 and VEGF-A in the adenocarcinoma (epithelial) component of the tumor sample, the Q-PCR was performed on RNA extracted from the whole tumor tissue. Hence, we hypothesized that some cellular phenotype, in the stromal component of the tumor, could contribute to the expression of either genes.

hERG1 is expressed in muscle cells (Schwarz, 2004), including smooth muscle cells underlying the intestinal mucosa (Shoeb, 2013). Hence, we hypothesized that stromal myofibroblasts, whose features resemble the contractile phenotype of smooth muscle cells (Tomasek, 2002), inside the tumor microenvironment, could contribute to hERG1 expression. We first demonstrated that myofibroblasts (as evidenced by $\alpha$-smooth muscle actin ($\alpha$-SMA) positivity) are present at low levels in the human colonic mucosa (Fig. 2a), and their number increases in colon adenomas (Fig. 2b) and even more in adenocarcinomas (Fig. 2c,d).

Then we tested whether myofibroblasts express the smooth muscle myosin heavy chain 11 (MYH11) gene, to be further used as a molecular marker for myofibroblasts. To this purpose we first analyzed a human colon-derived fibroblast cell line (CCD-18Co), which was described as myofibroblast, according to its molecular profile (Yoo, 2011). For comparison, CRC cell lines were analyzed. CCD-18Co cells indeed expressed the MYH11 gene at high levels, whereas CRC cells did not (Fig. 3a).

Moreover, CCD-18Co cells expressed the hERG1 gene at levels comparable to those detected in CRC cells (Crociani, personal communication) (Fig. 3b). Interestingly, CCD-18Co cells expressed the VEGF-A gene (Fig. 2c) and secreted VEGF-A into the medium (Fig. 3d), similarly to CRC cells. Moreover, IHC analysis confirmed that myofibroblasts simultaneously express the $\alpha$-SMA, hERG1 and VEGF-A proteins (Fig. 2 d-f) in CRC samples.

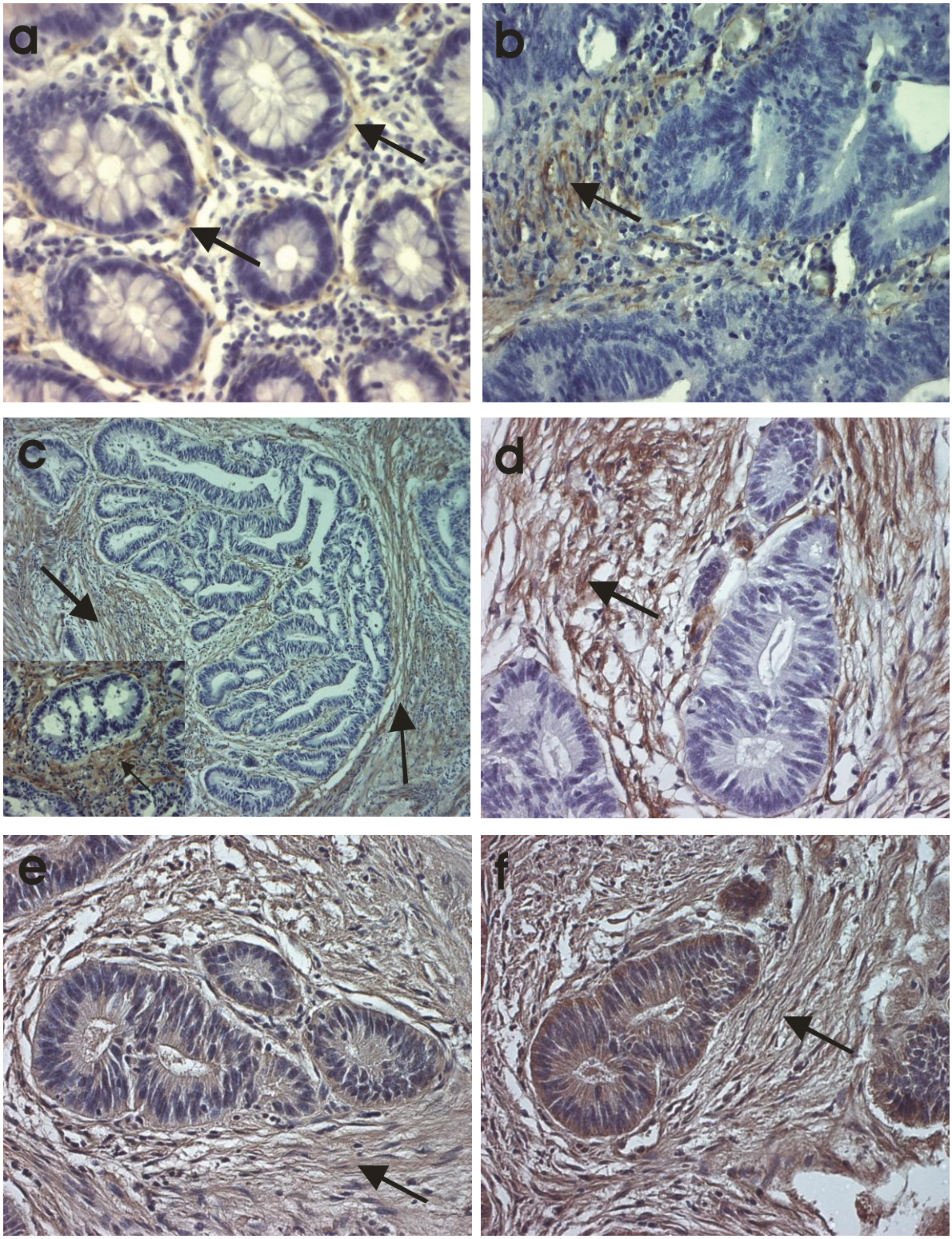


**Figure 2. Immunohistochemical staining of myofibroblasts in colorectal cancer specimens.**
Immunohistochemical staining with anti-α smooth muscle actin has shown that myofibroblasts (brownish stained) are present in a limited number in normal colonic mucosa (arrows) (a) but are already over-represented in the adenomatous polyps specimens. Myofibroblasts are the main component of the stroma in colorectal cancer specimens (arrows) (c-f). The insert in the c image is a magnification (40x) of epithelial cancer cells surrounded by myofibroblasts. Subsequent section of the same tumoral samples are immunohistochemicaly stained (brownish) with anti-α smooth muscle actin (d), anti-ERG1(e) and anti-VEGFA (f). Anti-α smooth muscle actin stains the stroma but does not stains the epithelial cells while hERG1and VEGFA antibodies exhibit immunoreactivity with both stroma and epithelial cancer cells. Arrows indicate myofibroblasts. Magnifications: a, b, d, f=40x; c=10x

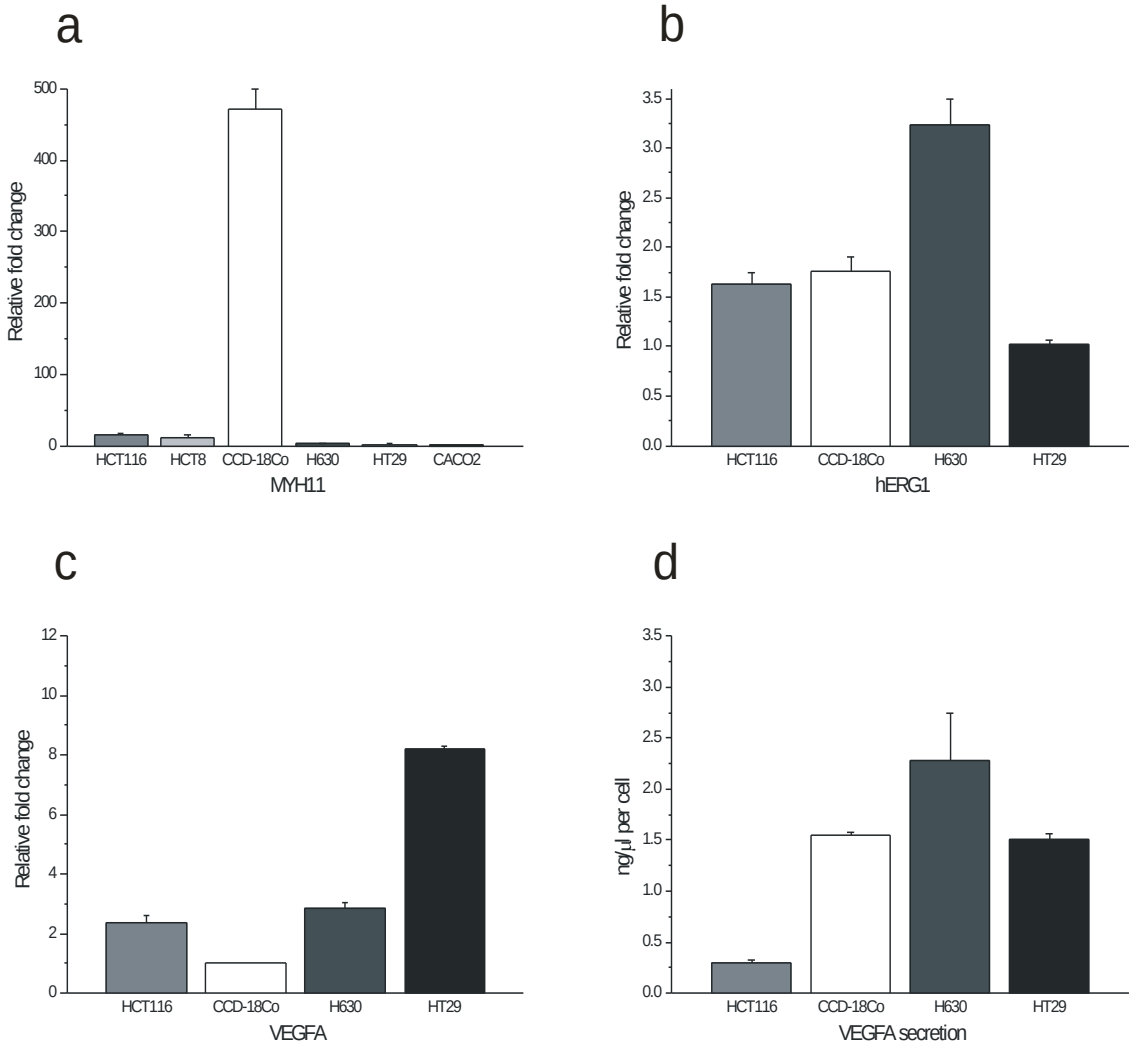


**Figure 3. Gene expression and VEGFA secretion analysis of myofibroblasts and colorectal cell lines.**
*MYH11* is expressed mainly in myofibroblasts (CCD-18Co) and is only expressed at very low level in colorectal cell lines (a). hERG1 and VEGFA genes are expressed in all the colorectal cancer and CCD-18Co cell lines but at different levels (b,c). All the cell lines tested, included myofibroblasts, secreted VEGFA into the media as indicted by ELISA assay (d). Histogram represent the fold-mean ± s.e.m (error bars).

**Evaluation of hERG1 and VEGF-A expression in the epithelial component of CRC samples.**

Based on the above results, we quantified hERG1 expression in the epithelial component present in the CRC samples we collected, by normalizing hERG1 gene expression over MYH11 expression (norm-hERG1). Raw data are reported in table 3. From such analysis it emerged that norm-hERG1 had a mean of 0.12 (relative fold change) and a median of 0.10 (relative fold change), and was expressed above the mean in 57.5% of cases, whereas was expressed below the mean in 42.5% of cases, respectively (Fig. 4). When the same procedure was applied to the VEGF-A gene (see raw data in table 4), a statistical correlation ($p=0.001$) emerged in the expression of the two genes (Tab. 5). Moreover, a preliminary survival analysis, performed on a small cohort of patients (16), showed an increased risk of death in patients with high hERG1 gene expression.

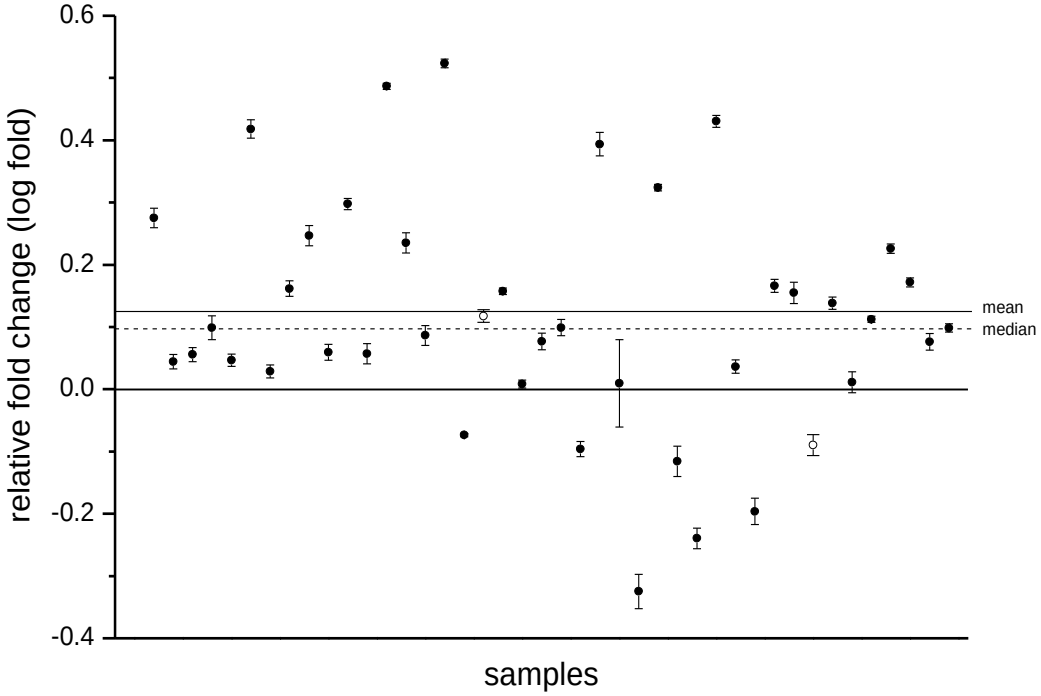


**Figure 4. hERG1 gene expression in colorectal cancer patients.**
hERG1 gene was expressed in the 57.5% above the mean and in the 42.5% below the mean of 40 different colorectal cancer patients (solid circle). Relative expression values for hERG1 gene were expressed as a ratio of hERG1 gene expression level to GAPDH expression value in the same specimen and normalized for the value of expression of HT29 cell line. Then, hERG1 gene expression levels were normalized to MYH11 gene expression. Mean=mean of hERG1 expression; median=median of hERG1 expression. Open circle=non-cancerous adenomatous polyps.

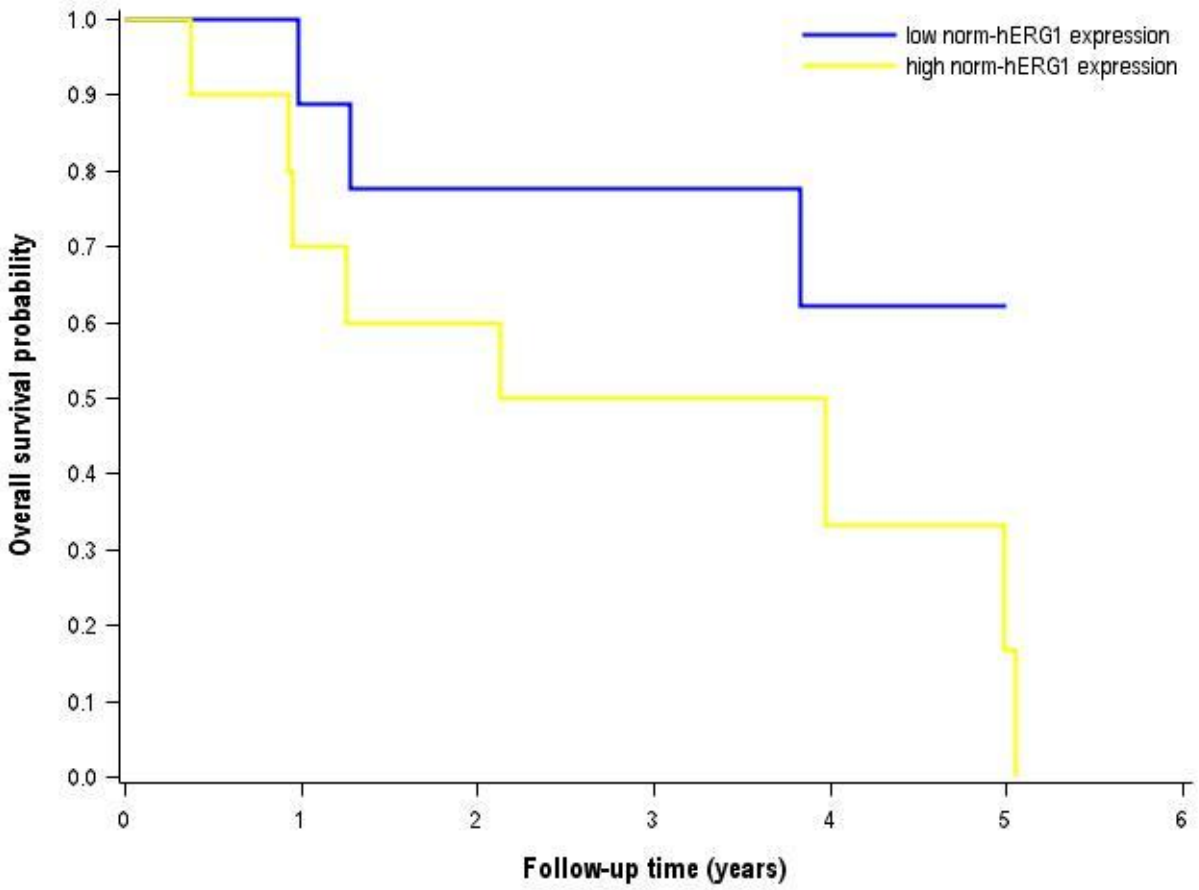


**Figure 5. Kaplan-Meier curves of overall survival analysis.**
Kaplan-Meier analysis shows a relationship between overall survival of patients (n=16) and hERG1 gene expression. Patients with normalized hERG1 (norm-hERG1) values higher than 0.0593 displayed worse survival experience compared with patients with lower values (Hazard ratio equal to 2.62, adjusted p=0.253)

## DISCUSSION

The heterogeneous molecular profile of individual tumors and the variability of patients response to therapy is forcing the implementation of the molecular screening of patients, to be exploited for the design of personalized therapeutic protocols. Hence, the implementation cost-effective and time-saving protocols to facilitate the application of molecular diagnosis in standard pathological departments is strongly encouraged.

We exploited the expression of hERG1, a $K^+$ channel encoding gene commonly expressed in CRC, to develop an analytical procedure to be applied to either cryopreserved or FFPE samples, without need of microdissection.

First, we evaluated the possibility to use FFBE blocks made ready for standard histopatological analysis to study the expression of hERG1 in CRC. We verified that FFBE samples fixed in formalin for 24 hours could be used for genetic analysis. Samples fixed for longer periods, although giving rise to good amounts of RNA, displayed a deteriorated RNA, no longer suitable for diagnostic molecular analyses.

The objective of the present work was that of obtaining a method for the quantitative detection of the expression of genes, as those encoding ion channels and transporters, with a complex expression profile in tumor solid samples. In fact, solid cancers are constituted by both cancer (epithelial) and stromal cells the latter contributing to disease aggressiveness and progression (Joyce, 2009; Donjacour, 1991). Ion channels, are acquiring an increasing relevance in human cancers (Erkkilä, 2010), and their expression is being exploited for diagnostic purposes (Arcangeli, 2009). However, being expressed in both cancer and stromal cells (Arcangeli, 2011), ion channels are difficult to analyze quantitatively at the gene expression level in complex cancers without substantial bias. One possibility to overcome such hindrances is to develop short term cultures, which only contain tumor cells (Masselli, 2012).

In the present paper, we adopted a different approach developing a protocol to estimate the hERG1 expression in epithelial cancer cells without the need of microdissection. In fact,

microdissection techniques, besides allowing to improve the purity of the sample processed for molecular analysis, allow to extract only small amounts of RNA, which could not be efficiently and linearly retrotranscribed to cDNA (Erkkilä, 2010; Otsuka, 2007; Sooriakumaran, 2009). Moreover, the subsequent high number of cycles during PCR amplification steps could additionally increase the error in the gene expression estimation. Finally, the error of the pathologists to select correctly the cells is estimated about ± 10% (Roepman, 2009), that additionally reduce part of the benefit of microdissection techniques.

The method we adopted relies on the discovery, reported in this paper for the first time, that hERG1 is expressed in myofibroblasts, which represent a very abundant component of the stroma in CRC (Desmoulière, 2004; Kunz-Schughart, 2002) (see also Fig. 2). Moreover, we showed a very low expression of the MYH11 gene, which characterizes myofibroblasts (Tomasek, 2009), in CRC cells. Hence, it was possible to obtain a quantitative but selective estimate of hERG1 expression in CRC cells inside the whole tumor sample, by normalizing hERG1 expression on the MYH11 expression. This method can be particularly useful in those CRC samples where a high stromal contamination occurs, although it does not allow an exact, mathematical estimate of epithelial CRC cells present in the sample.

As preliminary validation of this method, we confirmed previous IHC results (Lastraioli, 2012) by analyzing the relationships between hERG1 and VEGFA expression in the cohort of CRC samples under study. Both i*n vitro* experiments and IHC analysis on tumor samples showed that myofibroblasts express also VEGF-A transcript and proteins. Hence, we applied the normalization procedure onto the MYH11 gene, to obtain a quantitative estimate of VEGF-A in CRC cells. A statistically significant correlation between hERG1 and VEGF-A emerged, strengthening the validity of the analytical method we developed.

Moreover, a preliminary survival analysis, performed on a small cohort of patients, suggested the presence of an increased risk of death in patients with high norm-hERG1 values (Fig. 5).

These results, although requiring further validation, encourage to use the analytical method here described for the quantification of hERG1 and the evaluation of its prognostic role.

On the whole, we believe that our method is rather robust, introducing only a marginal effect in the gene expression estimation due to the little expression of MYH11 gene in colorectal cancer cells. In addition, the method can be easily implemented in diagnostic laboratories because it does not require microdissection instruments and we provide the optimized protocol of quantitative gene expression analysis, Moreover, this method can be applied to different tumor types and different genes because myofibroblasts are an important component of stroma of different solid tumors (Desmoulière, 2004; Kunz-Schughart; 2002a, 2002b), provided the gene under study has a significant expression in myofibroblasts, the latter being the main cellular component in the stroma of the tumor under study.

## REFERENCES


Arcangeli A, Crociani O, Lastraioli E, et al.Targeting ion channels in cancer: a novel frontier in antineoplastic therapy. Curr Med Chem. 2009;16:66-93.

Arcangeli A. Ion channels and transporters in cancer. 3. Ion channels in thetumor cell-microenvironment cross talk. Am J Physiol Cell Physiol. 2011;301(4):C762-71

Desmoulière A, Guyot C, Gabbiani G. The stroma reaction myofibroblast: a key player in the control of tumor cell behavior. Int J Dev Biol. 2004;48:509-17.

Donjacour AA, Cunha GR. Stromal regulation of epithelial function. Cancer Treat Res. 1991;53:335-64.

Erkkilä T, Lehmusvaara S, Ruusuvuori P, et al. Probabilistic analysis of gene expression measurements from heterogeneous tissues. Bioinformatics.2010;26:2571-7.

Farragher SM, Tanney A, Kennedy RD, et al. RNA expression analysis from formalin fixed paraffin embedded tissues. Histochem Cell Biol. 2008;130:435-45.

Ferrara N, Gerber HP, LeCouter J. The biology of VEGF and its receptors. Nat Med. 2003;9:669-76.

Huijsmans CJ, Damen J, van der Linden JC, et al. Comparative analysis of four methods to extract DNA from paraffin-embedded tissues: effect on downstream molecular applications. BMC Res Notes. 2010;3:239.

Joyce JA, Pollard JW. Microenvironmental regulation of metastasis. Nat Rev Cancer. 2009;9:239-52.

Kunz-Schughart LA, Knuechel R. Tumor-associated fibroblasts (part I): Active stromal participants in tumor development and progression? Histol Histopathol. 2002;17:599-621.

Kunz-Schughart LA, Knuechel R. Tumor-associated fibroblasts (part II): Functional impact on tumor tissue. Histol Histopathol. 2002;17:623-37.

Lastraioli E., Bencini L., Bianchini E., et al. hERG1 Channels and Glut-1 as Independent Prognostic Indicators of Worse Outcome in Stage I and II Colorectal Cancer: A Pilot Study. Translational Oncology. 2012;868645.

Masi A, Becchetti A, Restano-Cassulini R, et al. hERG1 channels are overexpressed in glioblastoma multiforme and modulate VEGF secretion in glioblastoma cell lines. Br J Cancer. 2005;93:781-92.

Masselli M, Laise P, Tonini G, et al. Deregulation of ion channel and transporter encoding genes in pediatric gliomas. Front Oncol. 2012;2:53.

Otsuka Y, Ichikawa Y, Kunisaki C, et al. Correlating purity by microdissection with gene expression in gastric cancer tissue. Scand J Clin Lab Invest. 2007;67:367-79.

Pfaffl, M.W. A new mathematical model for relative quantification in real-time RT-PCR. Nucleic Acids Research. 2001;29:2002-2007.

Pillozzi S, Brizzi MF, Bernabei PA, et al. VEGFR-1 (FLT-1), beta1 integrin, and hERG K+ channel for a macromolecular signaling complex in acute myeloid leukemia: role in cell migration and clinical outcome. Blood. 2007;110:1238-50.

Roepman P, Schuurman A, Delahaye LJ, et al. A gene expression profile for detection of sufficient tumour cells in breast tumour tissue: microarray diagnosis eligibility. BMC Med Genomics. 2009;2:52.

Sawyers CL. The cancer biomarker problem. Nature. 2008;452:548-52.

Schwarz JR, Bauer CK. Functions of erg K+ channels in excitable cells. J Cell Mol Med. 2004;8(1):22-30.

Shoeb F, Malykhina AP, Akbarali HI. Cloning and functional characterization of the smooth muscle ether-a-go-go-related gene K+ channel. Potential role of a conserved amino acid substitution in the S4 region. J Biol Chem. 2003;278(4):2503-14.

Simpson DA, Feeney S, Boyle C, et al. Retinal VEGF mRNA measured by SYBR green I fluorescence: a versatile approach to quantitative PCR. Mol Vis. 2000; 6:178–183.

Sooriakumaran P, Henderson A, Denham P et al. A novel method of obtaining prostate tissue for gene expression profiling. Int. J. Surg. Pathol. 2009;17: 238–243.

Tomasek JJ, Gabbiani G, Hinz B, et al. Myofibroblasts and mechano-regulation of connective tissue remodelling. Nat Rev Mol Cell Biol. 2002;3:349-63.

van't Veer LJ, Bernards R. Enabling personalized cancer medicine through analysis of gene-expression patterns. Nature. 2008;452:564-70.

Yoo J, Rodriguez Perez CE, Nie W, et al. Protein kinase D1 mediates synergistic MMP-3 expression induced by TNF-α and bradykinin in humancolonic myofibroblasts. Biochem Biophys Res Commun. 2011;413:30-5.

# Chapter 3

## Synergic effect of riluzole and cisplatin on chemoresistant colorectal cancer cells

**ABSTRACT**

Cisplatin is a drug widely used in cancer chemotherapy but the resistance of cancer cells to cisplatin can limit its use as chemotherapeutic agent. The development of new protocols capable of treating tumors irresponsive to cisplatin has a great clinical significance. We found that riluzole, a modulator of ion channels, can augment the effect of cisplatin in HCT116 cisplatin-resistant colorectal cancer cells. Riluzole and cisplatin have a synergic effect on HCT116 cisplatin-resistant cells, suggesting that riluzole may be used in combination with cisplatin to improve the efficacy of chemotherapeutic treatments in colorectal cancer. Since both drugs are approved for the use in humans these findings set a stage for a rapid translational application in clinical practice.

# INTRODUCTION

Cancer has been recognized to be an evolutionary-driven process (Nowell, 1976; Heppner, 1998; Crespi, 2005; Merlo, 2006; Greaves, 2012; Gillies, 2012). Most tumors contain an heterogeneous population of cancer cells. The genetically and epigenetically heterogeneous cells are responsible for the resurgence of cancer following chemotherapy because cancer cells with different genotypes can respond differently to pharmacological treatments, developing resistance to pharmacological agents. Accordingly, to enforce adequate strategies to limit the adaptive capacity of cancer cells we need to develop new drugs capable to target different biological process or to use combinations of existing drugs to exploit eventual additive or synergic effect.

Cisplatin is a drug largely used in chemotherapy and is used to treat different type of cancers. Cisplatin bind to DNA to form adducts triggering cell cycle arrest and apoptosis. But cisplatin often is facing the emergence of resistant cancer cells limiting its use in therapy (Kartalou , 2001; Siddik, 2003; Wang, 2005). The development of therapeutic protocols capable of reducing the capacity of cancer cells to develop resistance to cisplatin will be of great importance in clinical oncology.

Ion channels are an important therapeutic target because they have a critical role in controlling a wide number of physiological process (Hille, 2001). Emerging evidence implicates the involvement of ion channels in cancer growth and progression (Arcangeli, 2010), and pharmacoresistance.

Ion channels have been described to regulate the response of cancer cells to cisplatin (Sharp, 1994; Yarbrough, 1999; Marklund, 2001, 2004; Siddik, 2003; Liang, 2005; Liang, 2005; Ise, 2005; Shimizu, 2008). Activators of the KCa3.1 channel enhance the chemotherapeutic activity of platinum-based agents in human epidermoid cancer cells (Lee, 2008). This finding suggests that ion channel modulators could also augment chemotherapy regimens currently used in colorectal cancer.

Colorectal cancer is one of the leading causes of cancer-related deaths in the world. The discovery of new drugs or novel combination of existing drugs could lead to the development of new protocols for the treatments of colorectal cancer (Gellad, 2010). We tested the hypothesis that riluzole, a modulators of ion channels approved for human use, can modulate cisplatin resistance in colorectal cancer. Riluzole activated KCa1.1, KCa2.3, KCa3.1, $K_{2p}2.1$ and blocked KV1, KV3, KV4, Nav1.2, Nav1.4, Nav1.5, Cav1.2, HERG1 ion channels (Sankaranarayanan, 2009). In this study we demonstrated a synergy between riluzole and cisplatin drugs reducing the cisplatin resistance on HCT116-resistant colorectal cancer cells. This result is suggesting that riluzole may be used, in combination with cisplatin, to improve the efficacy of chemiotherapic treatments.

## MATERIALS AND METHODS

### Cell culture

The human colorectal cancer HCT116, H630, HCT8 and HT29 cell lines were purchased from the American Type Culture Collection (ATCC) (Rockville, MD). HCT116, H630 and HCT8 cells were grown in RPMI-1640 (EuroClone) medium and HT29 in McCoy's medium (EuroClone), supplemented with 2% L-Glut, 10% fetal bovine serum (FBS) (Hyclone) and 1% penicillin/streptomycin. Cells were incubated at 37°C, 5% $CO_2$ atmosphere and 90% humidity.

### RNA isolation, reverse transcription and real time PCR analysis

We collected 45 colorectal cancer specimens immediately after surgical resection of tumors from different patients. The tumor samples were stored at -80° C. Cryopreseved specimens and cells lines were homogenised in TRIzol® Reagent (Invitrogen™) to isolate total RNA. The RNA integrity was assessed on the Agilent 2100 Bioanalyzer. One microgram of RNA of each specimens was retrotranscribed (RT) using random primers and reverse transcriptase (SuperScript™ II Reverse Transcriptase, Invitrogen™) according to manufacturer's protocol. cDNA, diluted 1:3, was used as template for real time PCR analysis. SYBR green fluorescent dye (Power SYBR® Green, PCR master mix, Applied Biosystems) was used to monitor the DNA synthesis. Relative expression values for each target gene is expressed as a ratio of target gene expression level to control gene (GAPDH) expression value in the same specimen and normalized for the value of expression of the mean of two adenomas specimens, using the method of Pfaffl, for quantification (Pfaffl, 2001). The sequence of primers and amplicons size of the target and housekeeping genes are reported in Table 1.

| Table 1. Primer sequences | | | | |
|---|---|---|---|---|
| **Gene** | | **Sequence** | **Amplificon Size** | **Source** |
| GAPDH | Forward | ACGTCTCTCCCAACACCAAC | 108 | Primer Bank |
| | Reverse | GAGTACAGCCGCTGGATGAT | | |
| hERG1 | Forward | ATGGGGAAGGTGAAGGTCG | 118 | Primer3 |
| | Reverse | GGGGTCATTGATGGCAACAATA | | |
| KCa1.1 | Forward | AAGCGGAGAAGCACGTTCATA | 182 | Primer Bank |
| | Reverse | CTGGTGGATAGCTTGGAGGAA | | |
| KCa2.3 | Forward | TCTTTGCTCTCAGCATCGGTG | 146 | Primer Bank |
| | Reverse | CCGCAAGCCGAAGTAGAGAAG | | |
| KCa3.1 | Forward | GCCTGTGCACTGGAGTCAT | 93 | Primer3 |
| | Reverse | CGTGCTTCTCTGCCTTGTTA | | |

**Table 1. Primer sequences**
Primers sequences of potassium voltage-gated channel gene (hERG1), glyceraldehyde-3-phosphate dehydrogenase gene (GAPDH), potassium intermediate/small conductance calcium-activated channel (KCa3.1), potassium large conductance calcium-activated channel, subfamily M, alpha member 1 (KCa1.1) and potassium intermediate/small conductance calcium-activated channel, subfamily N, member 3 (KCa2.3).

## Chemicals

We dissolved riluzole (Sigma-Aldrich) in DMSO at the concentration of 5 mM and cisplatin (Sigma-Aldrich) in bidistilled water, at the concentration of 8.3 mM. Stock solution of riluzole and cisplatin were stored at -20°C; immediately before the use, the drugs were diluted to the required concentrations.

## Flow cytometry analysis

We investigated the sensitivity to cisplatin of 4 colorectal cancer cell lines: HCT116, HCT8, H630 and HT29 by flow cytometry. $1.5x10^5$ cells were seeded in 6-well plates (Costar, Corning). After 24 hours the cells were treated with 3 different concentrations of cisplatin (50, 100 and 150 µM) for 24h. Thus, we detected apoptotic, necrotic, dead and living cells by FACSCanto flow cytometry (Becton Dickinson), using a Annexin-V-FLUOS staining kit (Roche).

In order to study the effect of cisplatin in combination with riluzole, $1.5x10^5$ cells were seeded with 500 µL of growth medium into a 24-well plate (Costar, Corning) and treated with constant amount of cisplatin (175µM) determined by the first round of experiments and an increasing concentration of riluzole or DMSO (1µM, 5µM, 10µM, 15µM, 20µM and 25µM). At the end of the treatment (24 or 48 hours), cells of each sample were harvested and resuspended in 500 µL phosphate buffered saline and stained with propidium iodide (PI) (P4170, Sigma-Aldrich). A total of 1x104 cells for each sample were analyzed by FACSCanto flow cytometry (Becton Dickinson), aggregates and debris were excluded. The percentage of PI positive cells were recorded. All experiments were performed at least twice.

**Cell viability assay**

Cell viability in response to drug treatments were measured using WST-1(Roche) reagent. $10^4$ cells were seeded into a 96-well plates (Costar, Corning) with 200µL of growth medium. Thus, medium was replaced with drug-containing medium or drug-free medium (control). 24 hours after treatment, medium was replaced with 100µL per well of fresh medium, containing 10% WST-1. Cells were incubated for 20 minutes and the absorbance of each sample was measured using a microplate reader (ELx 800) at a wavelength of 450nm every 20 minutes.

To evaluate the IC50 of each drug, cells were exposed to an increasing concentrations of ciplatin, riluzole or DMSO (1µM, 12,5µM, 25µM, 55µM, 85µM, 115µM, 175µM). All experiments were performed at least in triplicate. The IC50s were calculated by using Origin software.

Finally we investigate whether the combination of cisplatin and riluzole have a synergic, additive or antagonistic effect by Calcusyn software (version 2, Biosoft). This analysis is based on the method of the combination index (CI) described by Chou and Talahay (2006). CI=1, indicates an additive effect, CI<1, indicates a synergistic effect and CI>1, indicates an antagonistic effect. Experiments were conducted following the diagonal constant ratio

combination design, proposed by Chou and Talalay (2006). We treated cells with the mixture of two drugs at their IC50 concentrations with a 2-fold serial dilution (1/2, 1/4, 1/8, 1/16, 1/32, 1/64) of the IC50s. All experiments were repeated at least in triplicate.

**Patch-clamp experiments.**

Membranes currents were recorded with patch-clamp technique in the whole-cell configuration, at room temperature (25°C). Electrodes were pulled from borosilicate glass capillaries (i.d 0.86 mm, o.d. 1.5 mm; Harvard Apparatus, Holliston, MA, USA), using a PC-10 pipette puller (Narishige, Tokio, Japan). Electrodes typically had a resistance of 4-7 MΩ. Series resistance was always compensated up to 80%. Currents were amplified and filtered using a Axopatch-1D (Molecular Devices, Sunnyvale, CA) equipped with pClamp hardware and software (pClamp 10.3). Currents were low-pass filtered at 5 kHz and digitized online at 10 kHz with pClamp (Axon Instruments) hardware and software. Data were subsequently analyzed with pClamp and Origin (Microcal Inc., Northhampton, MA, USA) software.

For the hERG1 currents recording pipettes contained (in mM): $K^+$ aspartate 130, NaCl 10, $MgCl_2$ 2, $CaCl_2$ 2, Hepes-KOH 10, EGTA-KOH 10, pH 7.3. The extracellular solution contained (in mM): NaCl 95, KCl 40, $CaCl_2$ 2, $MgCl_2$ 2, Hepes-NaOH 10, Glucose 5, pH 7.4. High extracellular [$K^+$] allows to increase the amplitude of inward hERG1 currents, thus avoiding the necessity of applying excessively negative test potentials. The $K^+$ equilibrium potential was -30mV.

For measurements of KCa channels (KCa 3.1 and KCa 1.1) currents, we used an internal pipette solution containing (in mM): $K^+$ aspartate 145, $MgCl_2$ 2, HEPES 10, $K_2$EGTA 10, and $CaCl_2$ 5.96 (250 nM free $Ca^{2+}$) or 8.55 (1μM free $Ca^{2+}$), pH 7.2. $Na^+$ aspartate Ringer was used as an external solution: 160 mM $Na^+$ aspartate, 4.5 mM KCl, 2 mM $CaCl_2$, 1 mM $MgCl_2$, and 5 mM HEPES, pH 7.4 (as reported in Sankaranarayanan A *et al.* 2009).

KCa 3.1 currents (250 nM ree $Ca^{2+}$) were elicited by 200-ms voltage ramps from -120 to +40 mV applied every 10 s, and the fold increase of slope conductance by drug was taken as a indication of channel activation. KCa 1.1 currents were elicited by 200-ms voltage steps from -80 to +60 mV applied every 10 s (1μM free $Ca^{2+}$), and channel activation was measured as the increase in mean current amplitude (as reported in Sankaranarayanan A *et al.*, 2009). hERG1 currents were elicited by a two step protocol, pre-conditioning the cell for 8 s at membrane potentials of 0 mV and -70 mV and then testing the tail current at -120 mV (for 450 ms). The effect of riluzole was determined on maximal hERG1 tail currents (i.e. after conditioning at 0 mV).

## RESULTS

### Colorectal HCT116 cancer cell line is resistant to cisplatin treatment.

We investigated the response of 4 colorectal cancer cell lines, HCT116, HCT8, HT29 and H630, to cisplatin treatment by flow cytometry using the Annexin-V-FLUOS staining kit. In order to identify the drug concentration suitable for the experiments we performed a dose-finding experiment with 3 different concentrations (50, 100 and 150μM) of cisplatin (Fig. 1A). Then, we selected the 100μM concentration of cisplatin to carried out the subsequent experiments (Fig. 1B). We observed a different effect in terms of number of apoptotic and necrotic cells in the 4 cell lines after cisplatin treatment suggesting a different sensitivity to cisplatin between the different cell lines (Fig. 1). Among the cell lines tested, HCT116 and H630 cells are quite resistant to cisplatin instead HCT8 and HT29 cells are sensitive to cisplatin (Fig. 1).

### KCa1.1, KCa2.3, KCa3.1 and hERG1 genes expression in colorectal cancer cell lines.

We investigated the calcium-activated potassium channels (KCa1.1, KCa2.3, KCa3.1 ) and hERG1 gene expression in the above described colorectal cancer cell lines. The expression of these genes vary among the cell lines tested (Fig.2). Between the calcium activated potassium channels the KCa3.1 is expressed at highest level (average Ct values: KCa1.1=33.11, KCa2.3=30.50, KCa3.1=22.17) with a log fold ratio of: KCa3.1/KCa1.1=3.53, KCa3.1/KCa2.3=2.68). The expression of KCa3.1 is greatly the most expressed calcium-activated potassium channels between the KCa channels tested. Both HCT116 and H630 cell lines expressed KCa3.1 and hERG1 genes at higher level compared to HCT8 and HT29. In particular, the expression of KCa3.1 gene is much more higher (about 6.3 fold) in HCT116 and H630 cell lines compared to HCT8 and HT29 cell lines (Fig. 2D).

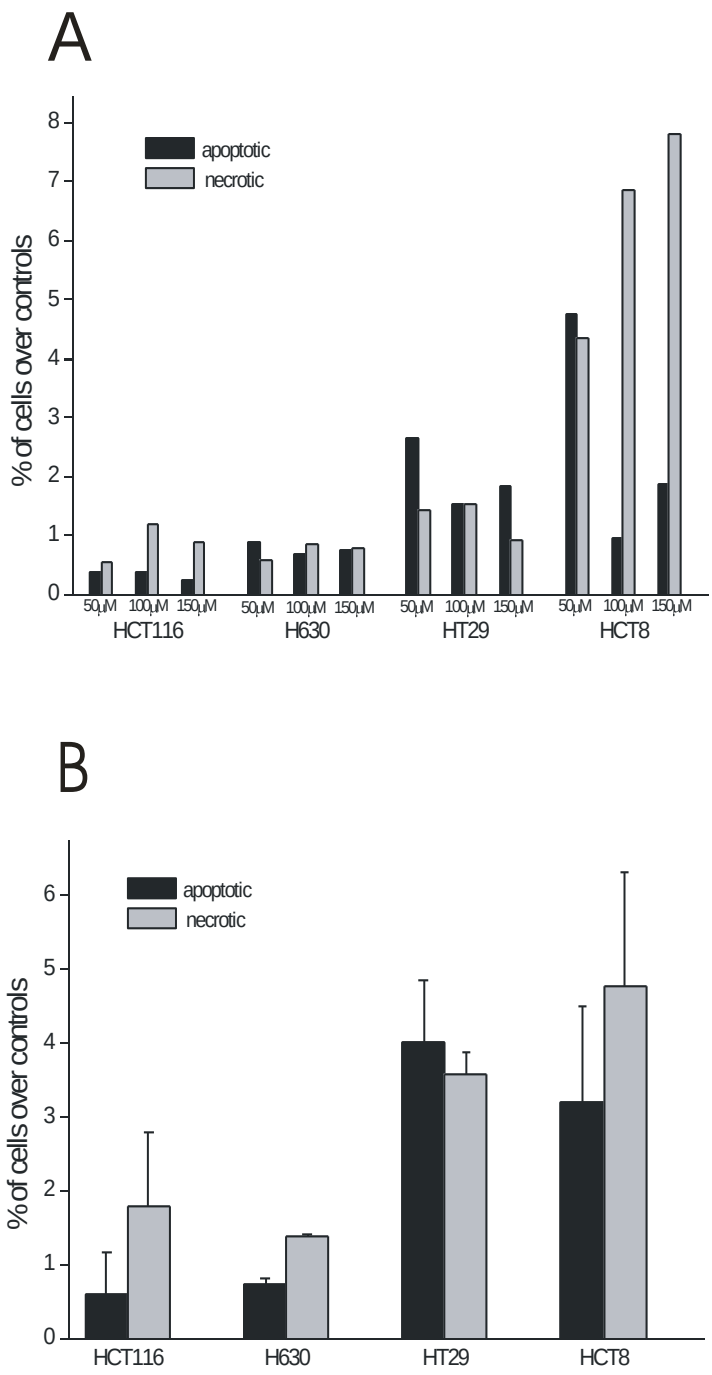


**Figure 1. Apoptotic and necrotic effect on colorectal cancer cell lines induced by cisplatin treatment.**
Colorectal cancer cell lines, HCT116, HCT8, HT29 and H630 have different level of sensitivity to cisplatin. (A) Dose-finding experiment with 3 different concentrations of cisplatin: 50, 100 and 150 µM. (B) HCT116 and H630 cell lines are resistant to cisplatin (100 µM concentration), instead HCT8 and HT29 cells shown an increasing induction of apoptosis. Apoptosis was measured by Annexin-V staining following 24 hours treatment over untreated control. Error bars represent SEM; data was acquired by flow cytometric analysis.

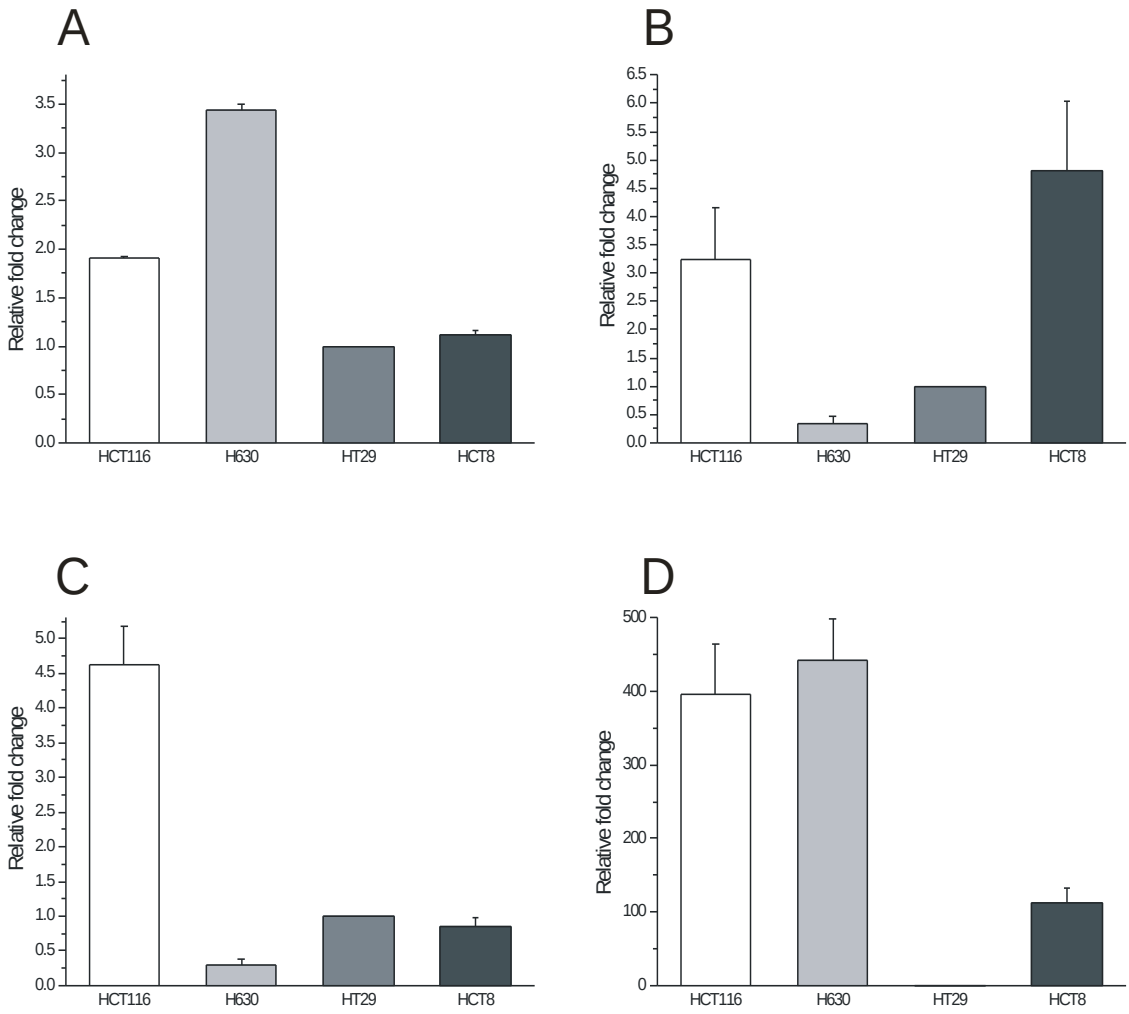


**Figure 2. hERG1, KCa1.1, KCa2.3 and KCa3.1genes expression in colorectal cancer cell lines.**
(a) hERG1, (b) KCa1.1, (c) KCa2.3, (d) KCa3.1. genes expression in colorectal cancer cell lines. Both HCT116 and H630 cell lines expressed hERG1and KCa3.1 genes at higher level compared to HCT8 and HT29 but the expression of KCa3.1 gene is much more higher in HCT116 and H630 cell lines compared to HCT8 and HT29 cell lines. Relative expression values of the genes are normalized for the values of HT29 cell line expression. Histograms represent the relative fold-mean ± s.e.m (error bars).

**Patch-clamp measurements.**

Membranes currents were recorded with patch-clamp technique in the HCT116 cells. In comparison with controls, 45 μM riluzole (i.e. the $IC_{50}$) significantly increased KCa3.1 currents (paired t-test, p=0.017) and KCa1.1 currents (Wilcoxon matched-pairs signed-ranks test, p=0.002), elicited with free $Ca^{2+}$. Instead riluzole (45 μM) inhibits HERG1 currents (paired t-test, p<0.0001). These data confirmed previously reported data on transformed HEK293 cells (Sankaranarayanan, 2009) (Fig. 3, tab. 2).

**KCa3.1 gene expression in colorectal cancer specimens.**

In consideration that KCa3.1 channels have the highest level of expression (between the calcium activated potassium genes tested) in colorectal cancer cell lines, we investigated its expression in bioptic cancer samples. Gene expression analysis of 45 colorectal cancer specimens has shown that KCa3.1 gene is expressed in all the specimens (KCa3.1, Ct=23.56±1.61 SD; GAPDH, Ct=17.79 ±1.50 SD). The expression level of KCa3.1 varies in different patients but, the 71% of specimens over express KCa3.1, compared to adenomas control specimens, suggesting a role in the tumor progression of KCa3.1 (Fig. 4).

**Riluzole drug has a synergic effect in combination with cisplatin on HCT116 cells.**

In order to investigate whether the treatment with riluzole, a drug that interfere with ion channels activity, is able to potentiate the effect of cisplatin in HCT116-resistent cells we treated the HCT116 cells with cisplatin and riluzole in combination. First, we treated HCT116 cells for 24 and 48 hours with a constant concentration of cisplatin and an increasing concentration of riluzole (Fig. 5). We found that the riluzole do not have a significant effect on cell vitality but the riluzole in combination with cisplatin increases the mortality of cells both at

24 and 48 hours compared to controls. In the experiments in which the cells were exposed to 48 hours treatment we observed an increase effect of the cisplatin efficacy in combination with

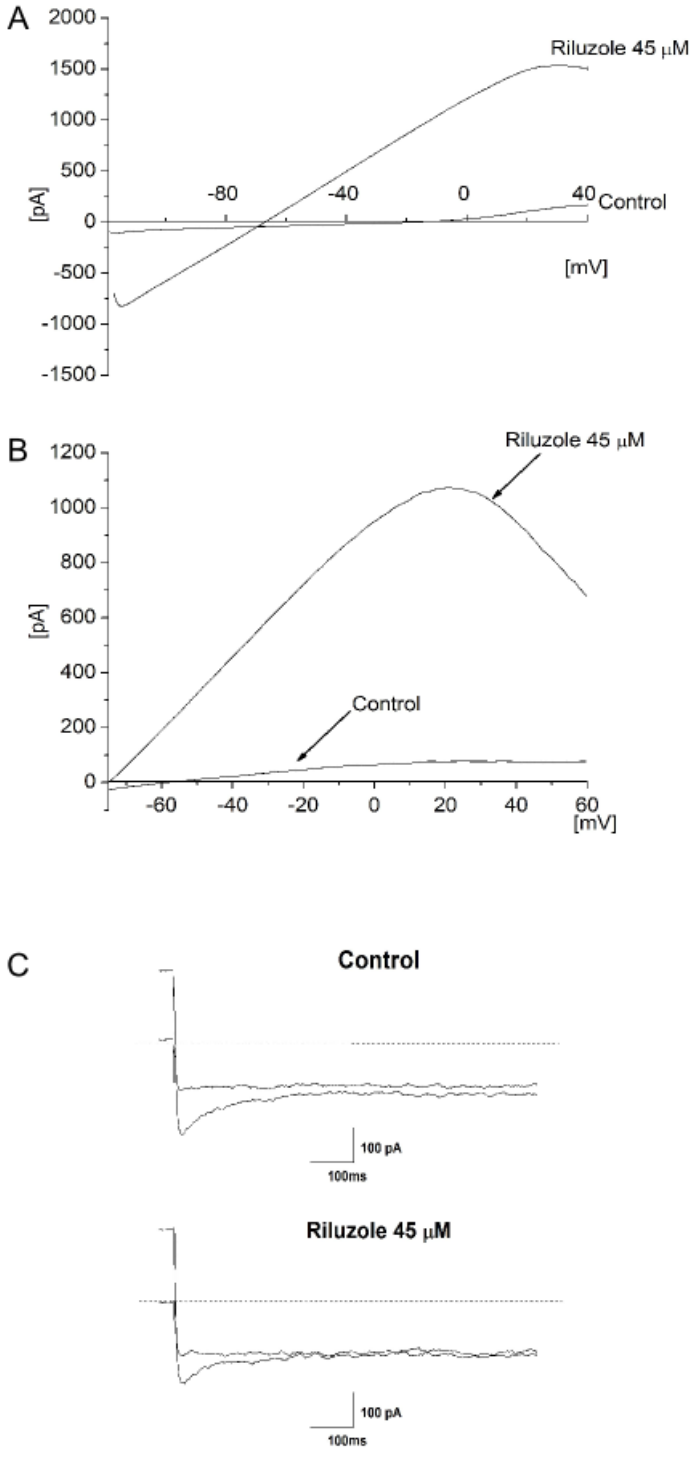


**Figure 3. Effects of Riluzole on KCa3.1, KCa1.1 and hERG1 currents.** (A): As expected 45 μM Riluzole (i.e. the $IC_{50}$) significantly increased KCa3.1 current, elicited with 250 nM concentration of free $Ca^{2+}$ from HCT116 cell lines. The channel activation is clearly highlighted by the ten fold increase in the slope conductance between control and riluzole-treated curves; (B): the same concentration of Riluzole (45 μM) also induced an activation of Kca1.1 channels, thus producing a strong increase in the outward current; (C): Representative current of hERG channels in HCT116 cells and the effect of Riluzole. It emerged that Riluzole (45 μM) inhibits hERG1 currents of about 43.8 ±7% (n=6), in line with the previously reported $IC_{50}$ of 50 ± 4 μM (Sankaranarayanan A *et al*., 2009).

**Table 2. Patch-clamp**

| n. cells | **KCa1.1** Control | **KCa1.1** Riluzole [45μM] | **KCa3.1** Control | **KCa3.1** Riluzole [45μM] | **HERG1** Control | **HERG1** Riluzole [45μM] |
|---|---|---|---|---|---|---|
| 1 | 138 | 895 | 5.8 | 14 | -20 | -5 |
| 2 | 64 | 467 | 1.85 | 4.84 | -34 | -17 |
| 3 | 345 | 400 | 8.5 | 12.6 | -57 | -41 |
| 4 | 24 | 806 | 6.14 | 10.15 | -25 | -15 |
| 5 | 76 | 1046 | 1.45 | 17.6 | -43 | -30 |
| 6 | 42 | 616 | 0.8 | 16.15 | -42 | -25 |
| 7 | 544 | 1461 | | | | |
| 8 | 108 | 568 | | | | |
| 9 | 245 | 750 | | | | |
| 10 | 91 | 478 | | | | |

**Table2. Patch-clamp measurements.**
Values of patch-clamp measurements carry out on the HCT116 cells of KCa1.1, KCa3.1 and HERG1 ion channels currents. n. cells: number of cells tested; Control: current values of untreated cell; Riluzole [45μM]: current values after riluzole treatment.

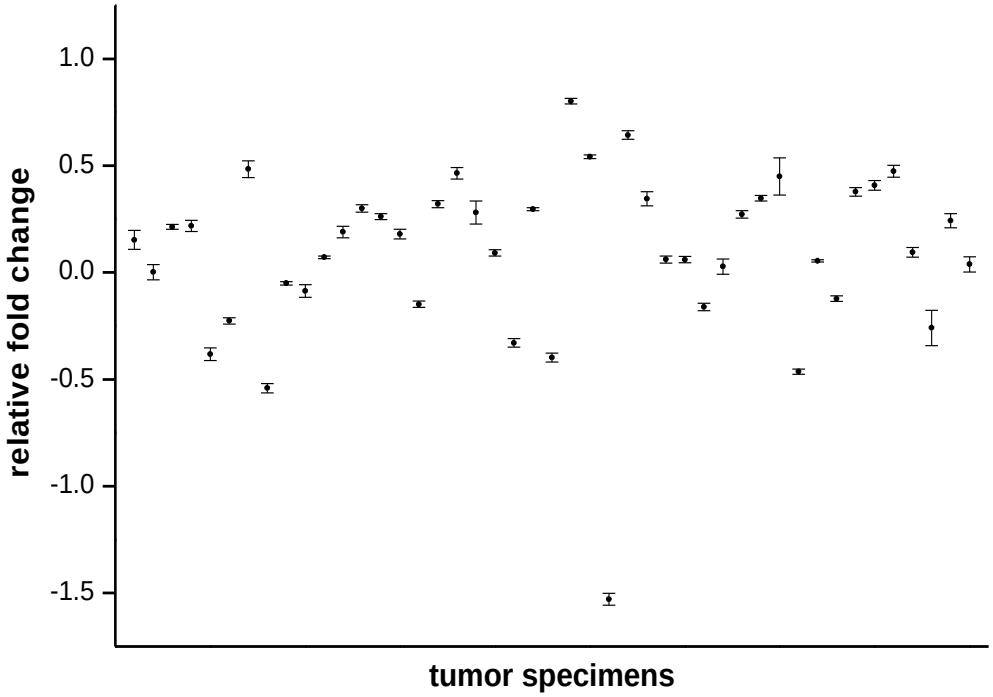


**Figure 4. KCa3.1 gene expression in colorectal cancer specimens.**
Gene expression analysis of 45 colorectal cancer specimens has shown that KCa3.1 gene is expressed in all the specimens. The 71% of patients specimens over express KCa3.1 compared to adenomas. Histogram represent the fold-mean ± s.e.m (error bars).

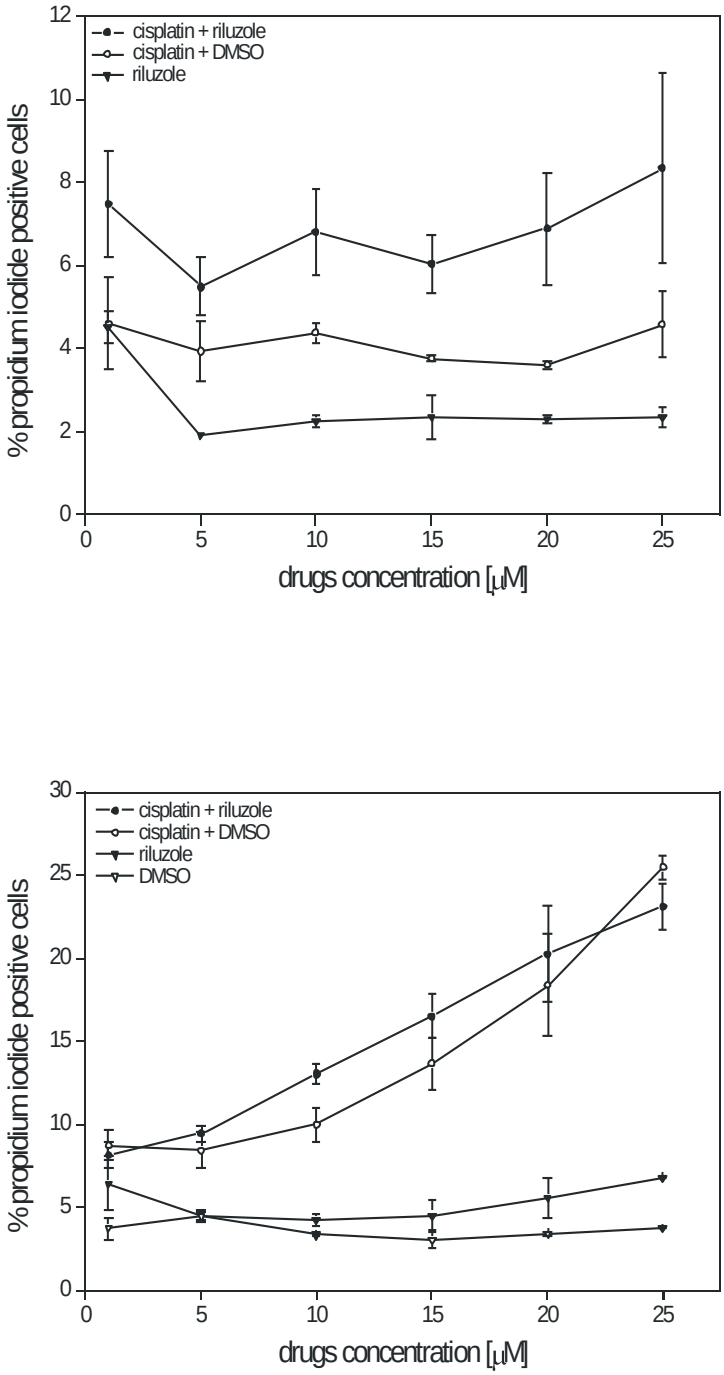


**Figure 5. Cisplatin and riluzole effect on HCT116 cells.**
HCT116-resistent cells were treated with cisplatin and riluzole in combination for 24 (A) and 48 (B) hours with a constant concentration of cisplatin and an increasing concentration of riluzole. Riluzole and DMSO (solvent) do not have a significant effect on cell vitality but the riluzole in combination with cisplatin increase the mortality of cells both at 24 and 48 hours compared to controls. Cells were stained with propidium iodide. Data was acquired by flow cytometric analysis. Error bars represent s.e.m.

DMSO. Interestingly, DMSO do not have a significant toxic effect on the cells at these concentrations (Fig. 5) suggesting that the DMSO increase cells uptake of cisplatin probably by increasing membrane permeability (Gurtovenko, 2007).

Subsequently we validated the results of these first experiments by a different assay. We determined the IC50s of the drugs used by WST-1 assay (Fig.6) and in order to study whether the riluzole enhanced the toxic effect of cisplatin we exposed the cells to an increasing concentration of cisplatin (1μM, 12,5μM, 25 μM, 55 μM, 85 μM, 115 μM), in combination with constant amount of riluzole (10μM; 25μM; 45μM; 65μM) including the IC50 value (45 μM) of riluzole. We found that the toxicity of the drugs mixture increase along with the concentration of riluzole (Fig. 6,7).

Moreover, we performed a third round of experiments to determine whether cisplatin and riluzole have a synergic, additive or antagonistic effect by cells viability assay (WST-1) and Calcusyn data analysis software. For these experiments, we treated the HCT116 cells with a mixture of cisplatin and riluzole at different concentration but a constant a ratio of the two drugs with a 2-fold serial dilution of their IC50s (1/2, 1/4, 1/8, 1/16, 1/32, 1/64). We found that two drugs in combination have a synergic or additive effect at low concentration (Tab. 3, Fig. 8).

**hERG1 gene silencing increase HCT116 colorectal cancer cells sensitivity to cisplatin**

We investigated whether the expression of hERG1 gene could has a role in the apoptotic resistance of HCT116 cells. Hence, we investigated whether the silencing of hERG1 reduce the capacity of cells to oppose apoptosis. We treated the control (pLKO.1) and silenced cell lines (sh4 and sh7) with three different concentration of cisplatin (124.5 μM, 174.3 μM, 224.1 μM). We found that the silenced cells (derived from HCT116 cells) became more sensitive to cisplatin, suggesting a role of hERG1 gene in cisplatin resistance (Fig. 9).

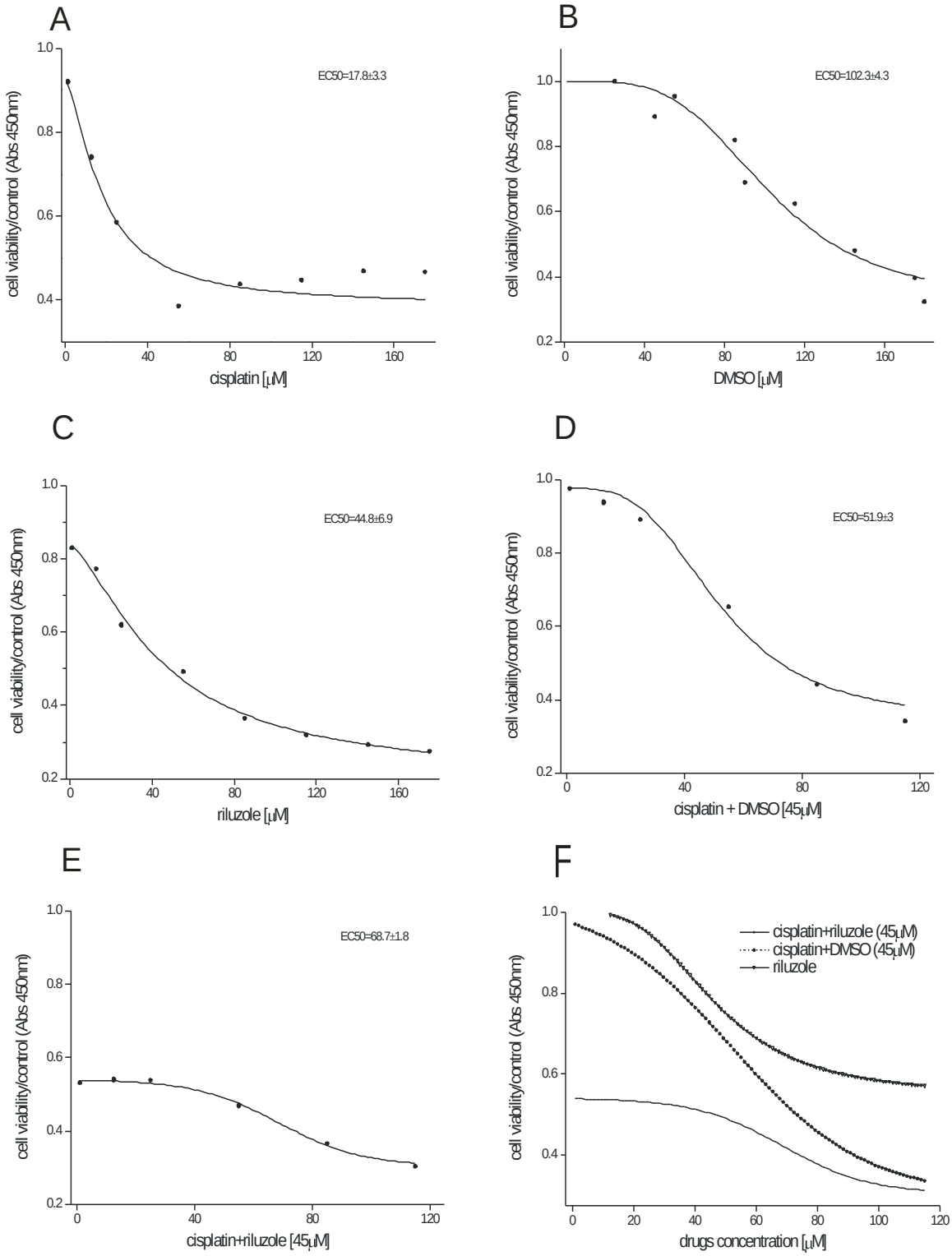


**Figure 6. Measurement of the IC50.**
Cells were treated with an increasing concentration of cisplatin (A), DMSO (B), riluzole (C), cisplatin + DMSO (D), cisplatin + Riluzole (E) to determine the IC50 of each drugs and their mixture. Absorbance of each sample was measured using a microplate reader (ELx 800) at a wave length of 450nm every 20 minutes.

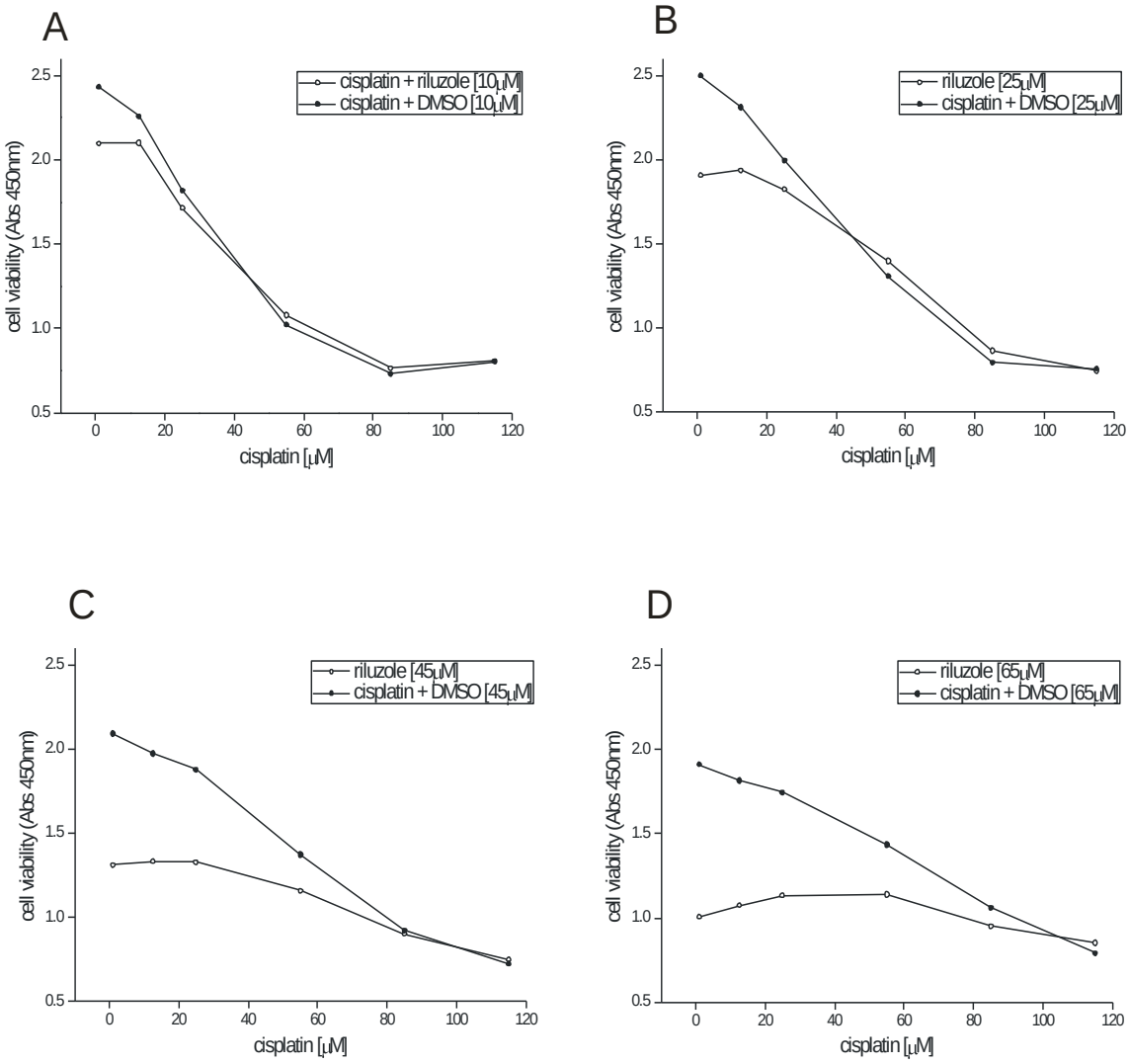


**Figure 7. Toxicity of cisplatin and riluzole mixture**
The toxicity of the drugs mixture cisplatin + riluzole increase along with the concentration of riluzole. Riluzole concentration: 10µM (A); 25µM (B); 45µM (C); 65µM (D).

| Table 3. | | |
|---|---|---|
| **cisplatin [µM]** | **riluzole [µM]** | **Combination Index (CI)** |
| 0.781 | 0.703 | 0.63 |
| 1.563 | 1.406 | 0.40 |
| 3.125 | 2.813 | 0.50 |
| 6.250 | 5.625 | 1.04 |
| 12.500 | 11.250 | 1.13 |
| 25.000 | 22.500 | 2.39 |

**Table 3. Riluzole has a synergic effect in combination with cisplatin on HCT116 cells.**
Cisplatin and riluzole have a synergic, additive or antagonistic effect when used in combination, determined by cell viability assay (WST-1) and Calcusyn data analysis software. HCT116 cells were treated with a mixture of cisplatin and riluzole at different concentration but a constant a ratio of the two drugs with a 2-fold serial dilution of their IC50 (1/2, 1/4, 1/8, 1/16, 1/32, 1/64). In the table are reported the concentration of cisplatin and riluzole drugs and the combination index. CI=1, indicates an additive effect, CI<1, indicates a synergistic effect and CI>1, indicates an antagonistic effect.

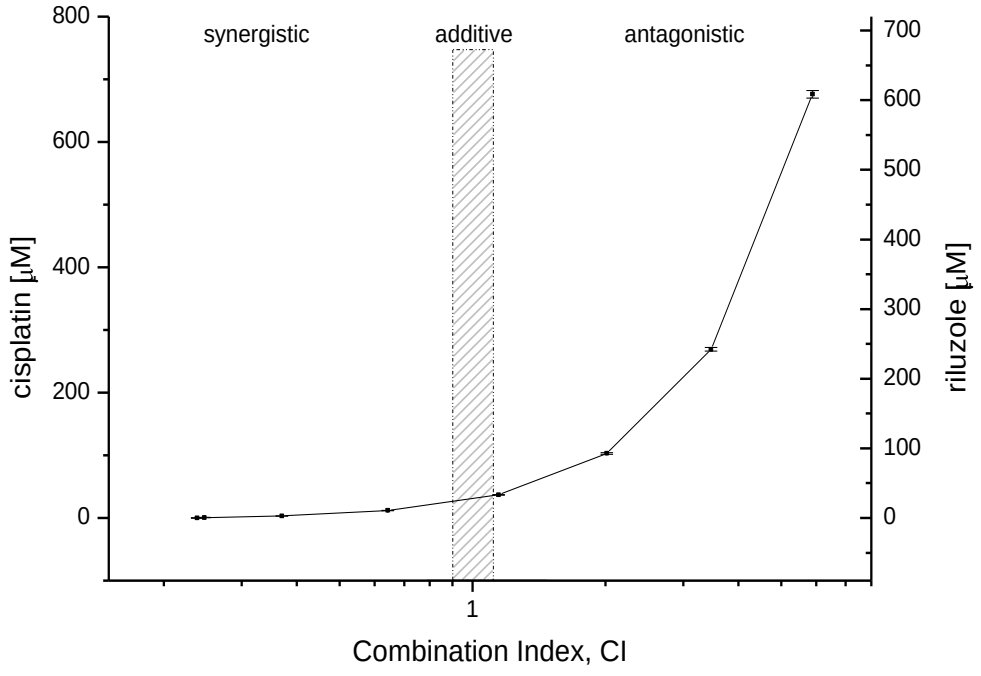


**Figure 8. CI simulation of cisplatin and riluzole mixture.**
CI simulation of cisplatin and riluzole mixture determined by Calcusyn data analysis software.

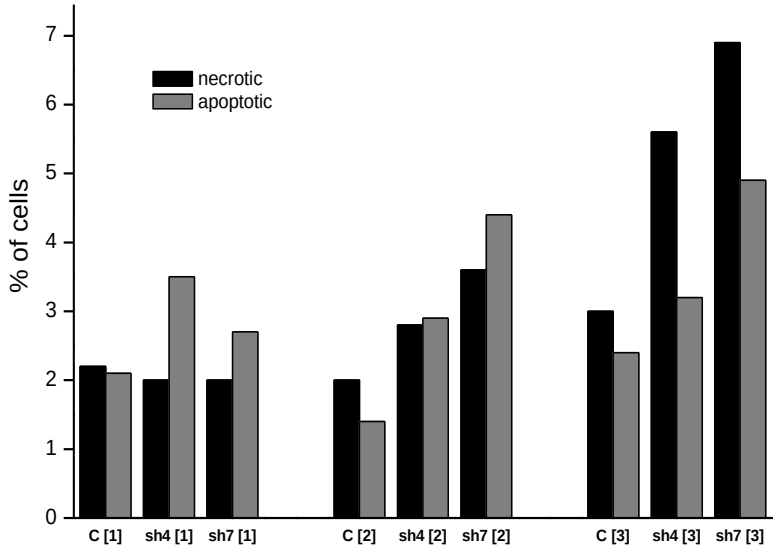


**Figure 9. Apoptotic and necrotic effect on control and hERG1-silenced HCT116 cell lines induced by cisplatin treatment.**
hERG1-silenced cell lines (sh4, sh7) show a higher sensitivity to cisplatin at 3 different progressive concentrations compared to control cells (pLKO.1). Apoptosis and necrosis were measured by Annexin-V staining kit following 24 hours treatment. Cisplatin concentrations: [1]=124.5µM, [2]=174.3µM, [3]=224.1µM. Histograms represent the percentage of apoptotic and necrotic cells, error bars= ± s.e.m.

# DISCUSSION

Chemoresistance is a major problem in clinical oncology. The development of new protocols capable of treating tumors irresponsive to chemioterapic agents has a great clinical significance. Cisplatin is a drug largely used in cancer chemotherapy and it is used to treat different type of cancers. Nevertheless, cancer cells often develop resistance to cisplatin treatment (Kartalou , 2001; Siddik, 2003; Wang 2005). A possible strategy to develop novel therapeutic protocols consist in using cisplatin in combination with other drugs capable of potentiating the effect of cisplatin on resistant cells. In particular, we focused on riluzole, a drug commercially distributed and therefore already approved for the use in humans to treat neurodegenerative diseases. Riluzole has a combined action on ion channels: activates calcium-activated potassium channels and inhibits the voltage dependent potassium channels. A previous study has shown that the activation of the KCa3.1 channel enhance the chemotherapeutic activity of platinum-based agents in human epidermoid cancer cells (Lee, 2008). The analysis of gene expression and electrophysiological measurements have confirmed that HCT116 cells express these ion channels and these channels are activated or repressed by the action of riluzole. We found that when riluzole was administered together with cisplatin increases the effectiveness of cisplatin on HCT116 cisplatin-resistant colorectal cancer cells. Since the post-transcriptional silencing of hERG1 determines itself a reduction of resistance of HCT116 to cisplatin it seems that the effect of riluzole is achieved through the simultaneous activation of Kca channels and Kv channels inhibition. Not necessarily the modulation of channels has a strict physiological effect in the regulation of ion flux but it could activate or inhibits signaling pathways that could interfere with the capacity of cells to oppose apoptosis. However, given that cisplatin and riluzole are drugs already in use in humans this result sets the stage for a rapid translational application in clinical practice through the development of a

therapeutic protocol that combines the use of these two drugs in order to exploit their synergic effect on cisplatin resistant tumors.

## REFERENCES


Arcangeli A. and Becchetti A. "New trends in cancer therapy: targeting ion channels and transporters." Pharmaceuticals, 3: 1202-1224, 2010.

Chou TC. Theoretical basis, experimental design, and computerized simulation of synergism and antagonism in drug combination studies. Pharmacol Rev. 2006 Sep;58(3):621-81. Erratum in: Pharmacol Rev. 2007 Mar;59(1):124.

Chandy KG, Wulff H., Beeton C, Calabresi PA, Gutman GA, Pennington M The Kv1.3 potassium channel: physiology, pharmacology and therapeutic indications. (2006) In The Chemical Pharmacology of Voltage-gated Ion Channels - "Methods and Principles in Medicinal Chemistry. Ed. Triggle, D., Gopalakrishnan, M, Rampe, D., Zheng, W. I ISBN 3-527-31258-7-Wily-VCH, Weinheim. pp 214-274.

Crespi B, Summers K. Evolutionary biology of cancer. Trends Ecol Evol. 2005Oct;20(10):545-52.

Gellad ZF, Provenzale D. Colorectal cancer: national and international perspective on the burden of disease and public health impact. Gastroenterology. 2010 Jun;138(6):2177-90.
Gillies RJ, Verduzco D, Gatenby RA. Evolutionary dynamics of carcinogenesis and why targeted therapy does not work. Nat Rev Cancer. 2012 Jun 14;12(7):487-93.

Greaves M, Maley CC. Clonal evolution in cancer. Nature. 2012 Jan 18;481(7381):306-13.

Heppner GH, Miller FR. The cellular basis of tumor progression. Int Rev Cytol.1998;177:1-56.

Hille , B. 2001 . Ion Channels of Excitable Membranes. Third edition. Sinauer Associates, Inc., Sunderland, MA . 814 pp.

Ise T, Shimizu T, Lee EL, Inoue H, Kohno K, Okada Y. Roles of volume-sensitive $Cl^-$ channel in cisplatin-induced apoptosis in human epidermoid cancer cells. J Membr Biol 205: 139–145, 2005.

Kartalou M and Essigmann JM: Mechanisms of resistance to cisplatin. Mutat Res 478: 23-43, 2001.

Lee EL, Hasegawa Y, Shimizu T, Okada Y. IK1 channel activity contributes to cisplatin sensitivity of human epidermoid cancer cells. Am J Physiol Cell Physiol. 2008 Jun;294(6):C1398-406.

Liang F, Schulte BA, Qu C, Hu W, Shen Z. Inhibition of the calcium- and voltage-dependent big conductance potassium channel ameliorates cisplatin-induced apoptosis in spiral ligament fibrocytes of the cochlea. Neuroscience 135: 263–271, 2005.

Liang XJ, Taylor B, Cardarelli C, Yin JJ, Annereau JP, Garfield S, Wincovitch S, Szakacs G, Gottesman MM, Aszalos A. Different roles for $K^+$ channels in cisplatin-resistant cell lines argue against a critical role for these channels in cisplatin resistance. Anticancer Res 25: 4113–4122, 2005.

Marklund L, Henriksson R, Grankvist K. Cisplatin-induced apoptosis of mesothelioma cells is affected by potassium ion flux modulator amphotericin B and bumetanide. Int J Cancer 93: 577–583, 2001.

Marklund L, Andersson B, Behnam-Motlagh P, Sandstrom PE, Henriksson R, Grankvist K. Cellular potassium ion deprivation enhances apoptosis induced by cisplatin. Basic Clin Pharmacol Toxicol 94: 245–251, 2004.

Merlo LM, Pepper JW, Reid BJ, Maley CC. Cancer as an evolutionary and ecological process. Nat Rev Cancer. 2006 Dec;6(12):924-35.

Nowell PC. The clonal evolution of tumor cell populations. Science. 1976 Oct 1;194(4260):23-8.

Sankaranarayanan A, Raman G, Busch C, Schultz T, Zimin PI, Hoyer J, Köhler R, Wulff H. Naphtho[1,2-d]thiazol-2-ylamine (SKA-31), a new activator of KCa2 and KCa3.1 potassium channels, potentiates the endothelium-derived hyperpolarizing factor response and lowers blood pressure. Mol Pharmacol. 2009 Feb;75(2):281-95.

Sharp SY, Mistry P, Valenti MR, Bryant AP, Kelland LR. Selective potentiation of platinum drug cytotoxicity in cisplatin-sensitive and -resistant human ovarian carcinoma cell lines by amphotericin B. Cancer Chemother Pharmacol 35: 137–143, 1994.

Siddik ZH: Cisplatin: mode of cytotoxic action and molecular basis of resistance. Oncogene 22: 7265-7279, 2003.

Shimizu T, Lee EL, Ise T, Okada Y. Volume-sensitive Cl(-) channel as a regulator of acquired cisplatin resistance. Anticancer Res. 2008 Jan-Feb;28(1A):75-83.

Wang D and Lippard SJ: Cellular processing of platinum anticancer drugs. Nat Rev Drug Discov 4: 307-320, 2005.

Yarbrough JW, Merryman JI, Barnhill MA, Hahn KA. Inhibitors of intracellular chloride regulation induce cisplatin resistance in canine osteosarcoma cells. In Vivo 13: 375–383, 1999.

# Chapter 4

## Deregulation of LH/hCG receptor and KCNA7 potassium channel is associated with poor prognosis in endometrial cancer

## ABSTRACT

The endometrial adenocarcinoma is the most spread gynecologic malignancy in women and its incidence is rising. According to histopathologic criteria, the endometrial adenocarcinoma patients are allocated in two groups: type I and type II. However, the prognostic value of this distinction, is limited because about 20% of tumors of type I develop recurrence while half of the tumors of type II do not undergo recrudescence of the disease. This diagnostic uncertainty is especially critical for patients belonging to the type I group because their effective risk of recurrence can be underestimated. For these reasons clinicians need novel prognostic protocols capable of integrating histopathological and molecular analyses in order to implement effective therapeutic strategies. In this study we found that a sub-set of potassium channels and the LH/hCG receptors are deregulated in endometrial cancer. Moreover, there is a statistical association between ion channels and LHCGR expression and between different ion channels as well. Most importantly, the high expression of LHCGR and low expression of KCNA7 have a negative effect on overall survival of endometrial cancer patients. Interestingly, the expression of LHCGR and KCNA7 genes has an opposite effect on patient survival; the concurrent high expression of LHCGR and low expression of KCNA7 increases sharply the risk of death due to endometrial cancer.

# INTRODUCTION

The endometrial adenocarcinoma is the most common gynecologic malignancy in women and its incidence is rising (Amant, 2005). Currently, the endometrial adenocarcinomas are classified in two groups: type I and type II. Type I is characterized by an endometrioid histology, a low stage and grade, mutations in K-RAS, PTEN, PIK3CA and β-catenin genes, microsatellite instability and a good prognosis; the type II instead has a non-endometrioid histology, a high stage and grade, molecular alterations of CDKN2A, TP53, ERBB2, STK15, p16 and E-cadherin genes, loss of heterozygosity, and poor prognosis (Rose, 1996; Salvesen, 1999, 2009; Lax, 2004; Amant, 2005; Yeramian, 2013). However, the prognostic value of this distinction, based on histopathological criteria, is restricted because approximately 20% of tumors of type I develop recurrence while half of the tumors of type II do not undergo recrudescence of the disease (Rose, 1996). Moreover, the type II is composed of a high-heterogeneous grouping of different histological types (Amant, 2005) suggesting an insufficient characterization of patients belonging to this group. In addiction, there are tumors with mixed or overlapping characteristics difficult to be classified by morphological features (Yeramian, 2013). Microarray-based analysis revealed that gene expression analysis can be used to distinguish two subgroups of patients with different possibility to undergoing recurrence of the disease (Salvesen, 2009). But, according to this study, the molecular-based prognosis do not overlap well with the histopathological-based prognosis, suggesting that clinically high-risk patients are missed by routine histopathology evaluation. This is particularly critical for patients belonging to the type I group because their effective risk of recurrence can be underestimated. These data strongly suggest that clinicians need new prognostic protocols capable to integrate histopathological and molecular analyses in order to implement effective therapeutic strategies. Previous studies on endometrial cancer emphasized that the expression of the luteinizing hormone/human chorionic gonadotropin receptor (LHCGR) gene could be an important factor

in the development and progression of endometrial adenocarcinoma (Lin, 1994; Mandai, 1997; Pike, 1997; Davis, 2000; Noci, 2000; Dabizzi, 2003; Noci, 2008). Moreover, in vivo experiments suggested a role of this receptor in metastatic seeding (Pillozzi, submitted). The activation of LH/hCG receptors can trigger a complex signaling cascades involving key signaling pathways with diverse functions. For instance, the LH hormone activates both cAMP/PKA and PLC/inositide tris-phosphate pathways (Stepien, 2002). In particular a subgroup of patients may be sensitive to high levels of luteinizing hormone/human chorionic gonadotropin (LH/hCG), which occur during the post-menopausal phase. Therefore, the high level of LH/hCG hormone and the simultaneous high level of expression of its receptor (LHCGR) in endometrial cells, may promote the development and progression of endometrial adenocarcinoma. Hence, the expression of LHCGR gene could represent a prognostic marker for endometrial adenocarcinoma.

Ion channels are a class of genes of which has been demonstrated to be involved in tumor progression of several types of cancer including endometrial cancer. Ion channels are an attractive target for therapeutic treatments because there are available numerous compounds capable of interacting with these channels by blocking or activating their function. Thus, the identification of ion channels involved in endometrial cancer could be uncover novel diagnostic and therapeutic targets. Thus far, it has been shown that the hERG1 (other aliases: KCNH2, Kv11.1) potassium channels are over expressed in endometrial cancer (Cherubini, 2000).

In this study we found that a sub-set of potassium channels and the LHCGR gene are deregulated in endometrial cancer. In addition, we detected an association between the ion channels studied and between ion channels and LHCGR gene expression. Most importantly, we found that the levels of expression of LHCGR and KCNA7 genes have a profound impact on the overall survival of endometrial cancer patients.

## MATIRIALS AND METHODS

### Statistical analysis of microarray

Data analysis was performed using R software version 2.15.0 (http://www.r-project.org). To perform differential expression analysis, between recurrence-free patients and patients that developed tumor recurrence, a t-test was applied to the log-ratios and a *p*-value was calculated for each gene. To select the differentially express genes we considered a threshold of 0.01 *p*-value then we selected the most up-regulated and down-regulated ion channels genes. The data were obtained from the Gene Expression Omnibus (GEO) database, www.ncbi.nlm.gov/projects/geo (accession no. GSE14860).

### Gene expression analysis: real time PCR

TRIzol® Reagent (Invitrogen™) was used for the isolation of total RNA according to manufactorer's protocol. The RNA integrity was assessed on the Agilent 2100 Bioanalyzer. After excluding genomic DNA contamination, 1µg of total RNA of each specimen was retrotranscribed using random primers and SuperScript™ II Reverse Transcriptase (Invitrogen™) according to manufacturer's protocol. SYBR green fluorescent dye (Power SYBR® Green, PCR master mix, Applied Biosystems) was used for monitoring product synthesis. Specific primer pairs were designed using the software Primer3 (http://frodo.wi.mit.edu/) or selected from previously published articles (Tab.1). All primer pairs span intron/exon boundaries. A 10-fold serial dilution of endometrial cancer cDNA was used to generated a linear regression equation for the target and control genes. In order to select the best control gene among a set of reference genes (GAPDH, GUSB, ACTB, OTUB1, RPL13, B2M and CANX) the NormFinder algorithm was implemented (Anderson, 2004). GAPDH was identified as the most stable gene by NormFinder analysis. Thus, the expression

levels of LHCGR, HERG1, KCNH6, KCNA7 were normalized to the levels of GAPDH reference gene using the method of Pfaffl, for quantification (Pfaffl, 2001).

**Table 1. Primer sequences**

| Gene | | Sequence | Amplificon Size | Source |
|---|---|---|---|---|
| GAPDH | Forward | GCTCTCTGCTCCTCCTGTTC | 115 | Primer3 |
| | Reverse | ACGACCAAATCCGTTGACTC | | |
| GUSB | Forward | AAACGATTGCAGGGTTTCAC | 146 | Primer3 |
| | Reverse | GAAATCGGCAAAATTCCAAA | | |
| ACTB | Forward | AAATCTGGCACCACACCTTC | 139 | Yu, 2006 |
| | Reverse | GGGGTGTTGAAGGTCTCAAA | | |
| OTUB1 | Forward | ATTGCTGTGCAGAACCCTCT | 135 | Primer3 |
| | Reverse | GGTCTTGCGGATGTACGAGT | | |
| RPL13 | Forward | CGAGGTTGGCTGGAAGTACC | 121 | PrimerBank |
| | Reverse | CTTCTCGGCCTGTTTCCGTAG | | |
| B2M | Forward | GTGCTCGCGCTACTCTCTCT | 143 | Primer3 |
| | Reverse | TCAATGTCGGATGGATGAAA | | |
| CANX | Forward | GATGGTGGCACTGTCAGTCA | 93 | Primer3 |
| | Reverse | TGGCTTTCTGTTTCTTGGTGA | | |
| LHCGR | Forward | TGCCTACCTCCCTGTCAAAG | 129 | Primer3 |
| | Reverse | TTGAGGAGGTTGTCAAAGG | | |
| KCNA7 | Forward | GTCATCCTCGTCTCCATCGT | 149 | Primer3 |
| | Reverse | GGTGGATTTCCAGGCATTT | | |
| HERG1 | Forward | ATGGGGAAGGTGAAGGTCG | 118 | Primer3 |
| | Reverse | GGGGTCATTGATGGCAACAATA | | |
| KCNH6 | Forward | GTCGCTCCCCAAAACACTTA | 80 | Primer3 |
| | Reverse | GCATTGGCAATCAGGAACTT | | |

**Table 1. Primer sequences**
Primers sequences of glyceraldehyde-3-phosphate dehydrogenase gene (GAPDH), luteinizing hormone/choriogonadotropin receptor (LHCGR), potassium voltage-gated channel, shaker-related subfamily, member 7 (KCNA7), potassium voltage-gated channel gene (HERG1), potassium voltage-gated channel, subfamily H (eag-related), member 6 (KCNH6), beta glucuronidase (GUSB), beta-actin (ACTB), OTU domain, ubiquitin aldehyde binding 1 (OTUB1), ribosomal protein L13 (RPL13), beta-2-microglobulin (B2M) and calnexin (CANX)

**Statistical analysis**

KCNA7, LHCGR, KCNH6, HERG1 genes were categorized as 0/1 respect to their level of expression. In the association analysis variables were categorized in two groups as fallows: age= ≤65 years vs >65 years, histology= endometrioid vs non endometrioid, differentiation= low vs medium/high, FIGO= I-II vs III-IV, lymph nodes= negative vs positive, ploidy= aneuploid vs diploid. The association between demographic, clinical, and biologic parameters was assess by Fisher exact tests. For retrospective analysis the overall surviving of patients was defined as the interval between the intervention and the death for the disease. Univariate analyses of overall surviving were calculated according to the Kaplan-Meier method. Comparisons between survival curves were performed using the log rank test. Cox proportional hazards models were used to estimate the hazard ratios and appropriate 95% confidence intervals (CI).

A multivariate Cox regression model was implemented to evaluate the independent prognostic effect of each variable including age, histology, FIGO, KCNA7, LHCGR, KCNH6, HERG1 on overall survival. Starting from a full model with all variables, progressively non-significant terms were deleted according to a backward stepwise procedure based on the likelihood ratio test. A probability of 0.10 was used to exclude the factors that did not significantly improve the model. The Cox model was then used to convert the total risk score that is directly related to the probability of death of patients. All statistical analyses were performed using the statistical software SAS (SAS Corporation, Cary, NC).

## RESULTS

### Clinical description of patients and relationship between clinical parameters.

Besides the data obtained from GEO database, we collected bioptic specimens from 115 endometrial cancer patients. For each patient it was available the clinical characterization and the follow up data. According to previous studies, the analysis of mortality rate showing that the FIGO III-IV stages, non-endometrioid histology, low differentiation level and lymph nodes positive detection increase the probability of patients death (Tab. 2,3, supplementary data pag.121).

### Identification of ion channels involved in endometrial cancer

In order to identify the ion channels involved in tumor progression in endometrial cancer, we conducted whole-genome expression analysis on a gene expression data set obtained from microarray experiments (GEO database, see methods). We identified a number of ion channels with an expression profile that may suggest their involvement in this disease. Among these genes we focused on HERG1, KCNH6 (up-regulated) and KCNA7 (down-regulated) genes because they seem to be among the most deregulated ion channel genes. HERG1 gene was already described to be over expressed in endometrial cancer (Cherubini, 2000). We validated the effective gene expression level of these genes in 115 samples of endometrial cancer by real time PCR. We found that all the selected genes were deregulated in endometrial cancer (Fig. 1).

### LHCGR gene expression

We investigated also the level of expression of the LHCGR gene in the same specimens, and we found that LHCGR gene has a deregulated expression in endometrial cancer (Fig. 1A). Then, we studied whether LHCGR gene expression, ion channel genes expression and other clinical-pathological parameters are associated. Indeed, we found that the expression of

| Table 2. Overall survival | | | | |
|---|---|---|---|---|
| | | 3-year survival | Long-rank test | hazard ratio |
| **variable** | **n** | **%** | **p-value** | **95% CI** |
| **age** | | | **0.099** | |
| ≤ 65 | 50 | 0.82 | | 1 (ref.) |
| >65 | 51 | 0.69 | | **2.37** (0.82-6.83) |
| **histology** | | | **<0.001** | |
| endometroid | 83 | 0.87 | | 1 (ref.) |
| non-endometroid | 18 | 0.17 | | **13.43** (4.65-38.76) |
| **differentiation** | | | **<0.001** | |
| low | 40 | 0.46 | | 1 (ref.) |
| medium/high | 61 | 0.94 | | **0.13** (0.04-0.44) |
| **FIGO** | | | **<0.001** | |
| I-II | 81 | 0.91 | | 1 (ref.) |
| III-IV | 20 | 0.19 | | **18.27** (5.77-57.8) |
| **nodes** | | | **<0.001** | |
| negative | 80 | 0.85 | | 1 (ref.) |
| positive | 12 | | | **15.01** (5.12-44.05) |
| **ploidy** | | | **0.04** | |
| aneuploid | 26 | 0.56 | | 1 (ref.) |
| diploid | 57 | 0.84 | | **0.34** (0.11-1.0) |
| **KCNA7** | | | **0.005** | |
| high expressed | 80 | 0.82 | | 1 (ref.) |
| low expressed | 21 | 0.48 | | **3.81** (1.41-10.30) |
| **LHCGR** | | | **0.047** | |
| high expressed | 56 | 0.65 | | 1 (ref.) |
| low expressed | 45 | 0.87 | | **0.34** (0.11-1.04) |
| **KCNH6** | | | **0.603** | |
| high expressed | 73 | 0.72 | | 1 (ref.) |
| low expressed | 28 | 0.80 | | **0.74** (0.24-2.31) |
| **hERG1** | | | **0.351** | |
| high expressed | 91 | 0.78 | | 1 (ref.) |
| low expressed | 10 | 0.60 | | **1.80** (0.51-6.35) |

**Table 2. Overall survival analysis**
Overall survival with clinical and biological risk factors

| Table 3. Disease-free survival | | | | |
|---|---|---|---|---|
| | | 3-year survival | Long-rank test | hazard ratio |
| **variable** | **n** | **%** | **p-value** | **95% CI** |
| **age** | | | **0.212** | |
| ≤ 65 | 47 | 0.72 | | 1 (ref.) |
| >65 | 48 | 0.65 | | **1.74** (0.72-4.20) |
| **histology** | | | **<0.001** | |
| endometroid | 80 | 0.76 | | 1 (ref.) |
| non-endometroid | 15 | 0.32 | | **6.88** (2.82-16.82) |
| **differentiation** | | | **<0.001** | |
| low | 35 | 0.27 | | 1 (ref.) |
| medium/high | 60 | 0.89 | | **0.13** (0.05-0.37) |
| **FIGO** | | | **<0.001** | |
| I-II | 81 | 0.80 | | 1 (ref.) |
| III-IV | 14 | | | **9.19** (3.85-21.90) |
| **nodes** | | | **<0.001** | |
| negative | 77 | 0.77 | | 1 (ref.) |
| positive | 11 | | | **7.71** (2.97-19.96) |
| **ploidy** | | | **0.049** | |
| aneuploid | 24 | 0.47 | | 1 (ref.) |
| diploid | 55 | 0.72 | | **0.42** (0.17-1.03) |
| **KCNA7** | | | **0.016** | |
| high expressed | 75 | 0.75 | | 1 (ref.) |
| low expressed | 20 | 0.42 | | **2.83** (1.17-6.87) |
| **LHCGR** | | | **0.507** | |
| high expressed | 51 | 0.70 | | 1 (ref.) |
| low expressed | 44 | 0.68 | | **0.75** (0.31-1.78) |
| **KCNH6** | | | **0.16** | |
| high expressed | 68 | 0.65 | | 1 (ref.) |
| low expressed | 27 | 0.78 | | **0.46** (0.16-1.39) |
| **hERG1** | | | **0.852** | |
| high expressed | 86 | 0.68 | | 1 (ref.) |
| low expressed | 9 | 0.71 | | **0.87** (0.20-3.75) |

**Table 3:Disease-free survival.**
Disease-free survival with clinical and biological risk factors

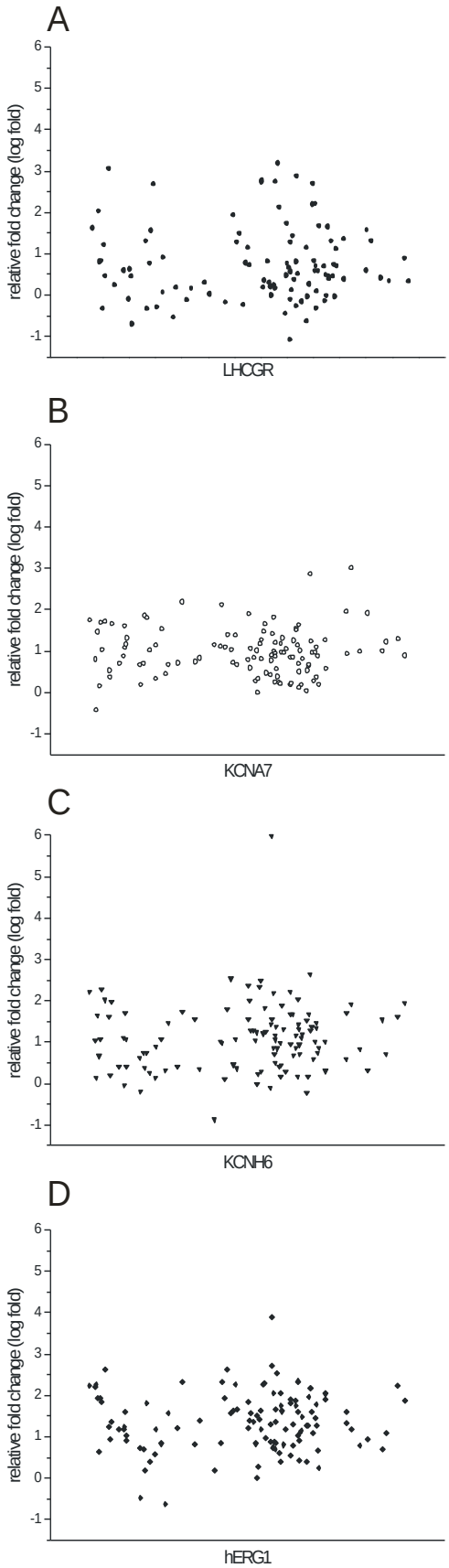


**Figure 1. Gene expression analysis by real time PCR.**
Relative expression values (log fold) of LHCGR, hERG1, KCNH6 and KCNA7 gene were reported as a ratio of the gene of interest expression level to GAPDH expression value in the same sample and normalized for the value of expression of a low expressing sample.

LHCGR is associated with KCNA7 and KCNH6 expression (Fig. 2, Tab. 4, supplementary data pag.121). Also the expression of KCNA7, HERG1, and KCNH6 ion channels is statistically associated (Tab. 4).

**Association between genes expression and surviving rate**

Univariate analysis showed a relationship between patient survival and the KCNA7 gene expression. Interestingly the KCNA7 low-expression determines a substantial increasing of the probability of patients death (Kaplan-Meier, Long rank test, p=0.005). Univariate analysis also highlighted a relationship between LHCGR gene expression and patient survival: the higher LHCGR expression increases the probability of patients death (Kaplan-Meier, Long rank test, p=0.047) (Tab. 2, 3 and Fig. 3). Multivariate overall survival analysis identified the following independent prognostic factors: histology, FIGO and KCNA7 (Tab. 2). Interestingly, the expression of LHCGR and KCNA7 genes has an opposite effect on patient overall survival. In particular, the expression of LHCGR and KCNA7 have a strong effect in survival when the expression of LHCGR is high and concurrently the level of expression of KCNA7 is low (Long rank test $p<0.001$), increasingly the hazard risk of this sub-group of patients (Tab. 5, supplementary data pag.121).

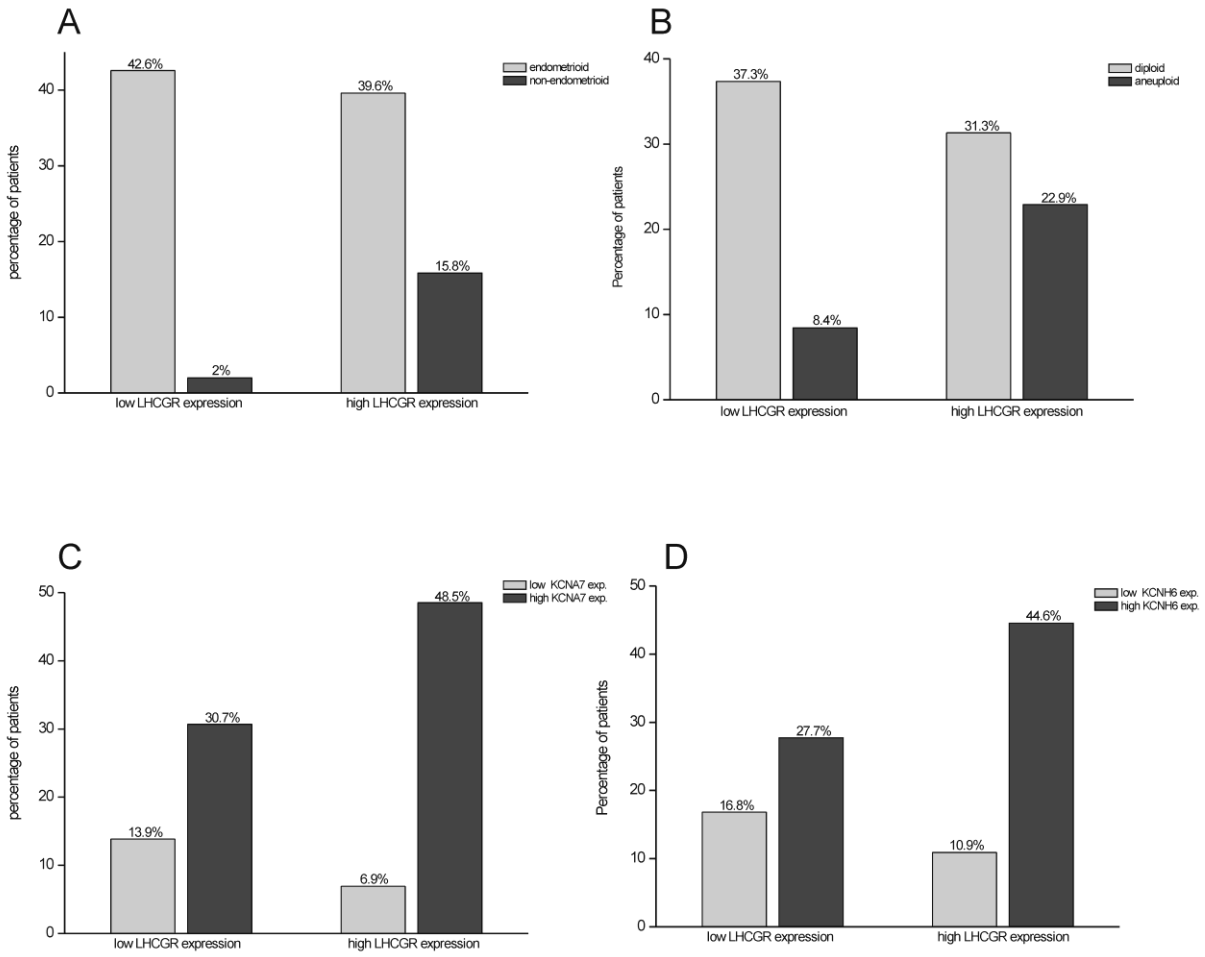


**Figure 2. Association between LHCGR gene expression and other factors.**
The expression level of the LHCGR gene is associated to the histological type (A) Fisher exact test, p=0.0016; with the chromosomal ploidy (B) Fisher exact test, p=0. 0198; with the expression of KCNA7 gene (C) Fisher exact test, p=0.0220; and with HCNH6 (D) Fisher exact test, p=0.0430

| Table 4. Association between gene expression | | | | | | | | | | |
|---|---|---|---|---|---|---|---|---|---|---|
| | | KCNA7 low exp. | KCNA7 high exp. | | KCNH6 low exp. | KCNH6 high exp. | | HERG1 low exp. | HERG1 high exp. | |
| **gene** | **level exp.** | **%** | **%** | **p-value** | **%** | **%** | **p-value** | **%** | **%** | **p-value** |
| **LHCGR** | low | 13.9 | 6.9 | **0.022** | 16.8 | 10.9 | **0.043** | 5.9 | 4.0 | **0.3005** |
| | high | 30.7 | 48.5 | | 27.7 | 44.6 | | 38.6 | 51.5 | |
| **KCNA7** | low | | | | 7.9 | 19.8 | **0.2328** | 6.9 | 3.0 | **<0.0001** |
| | high | | | | 12.9 | 59.4 | | 13.9 | 76.2 | |
| **KCNH6** | low | | | | | | | 5.9 | 4.0 | **0.0163** |
| | high | | | | | | | 21.8 | 68.3 | |

**Table 4. Association between, LHCGR, HERG1, KCNH6 and KCNA7 genes expression.**
Association between LHCGR, HERG1, KCNH6 and KCNA7 genes expression levels, Fisher exact tests.
exp.= expression

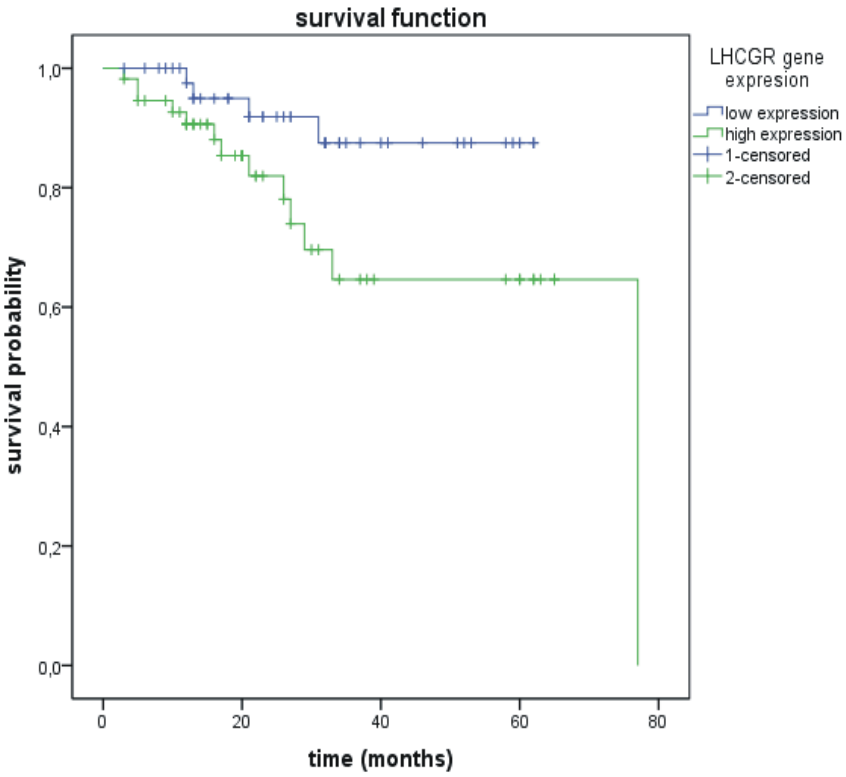


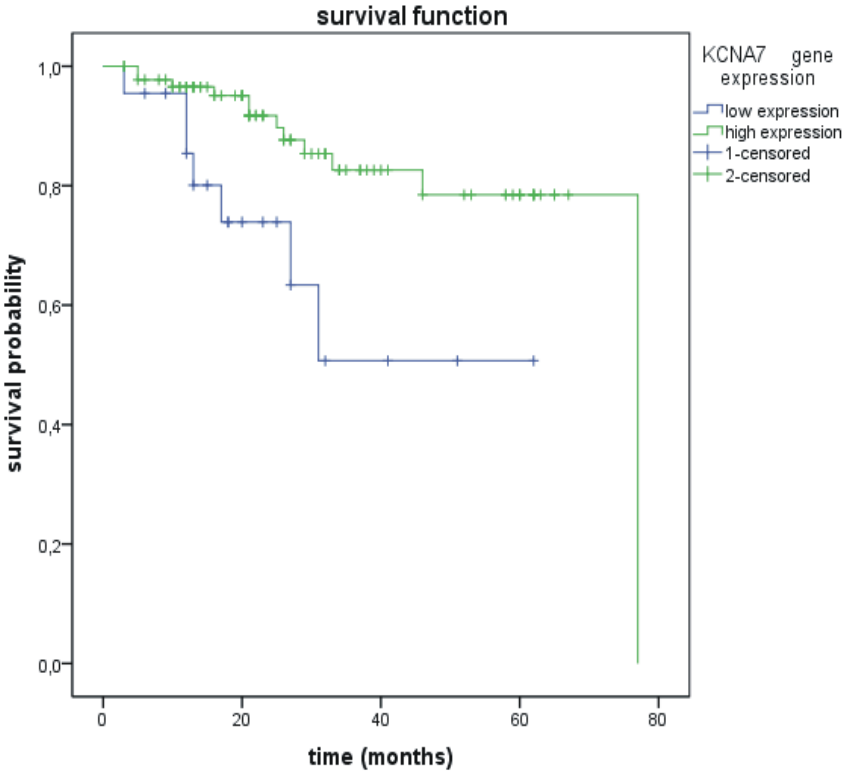


**Figure 3. Kaplan-Meier curves of overall survival analysis**
Kaplan-Meier analysis shows a relationship between overall survival of patients and LHCGR gene expression, Long rank test, p=0.047 (A) and KCNA7 gene expression, Long rank test, p=0.005 (B). Time= months of follow up.

| Table 5. Combinatorial effects | | | | |
|---|---|---|---|---|
| **LHCGR / KCNA7** | | **3-years survival** | **Long rank test** | **hazard ratio** |
| | **n** | **%** | **p-value** | **(95% CI)** |
| - / - | 14 | 0.6713 | <0.001 | 1 (ref.) |
| + / - | 7 | 0 | | 5.58 (1.19-26.13) |
| - / + | 31 | 0.9565 | | 0.12 (0.01-1.15) |
| + / + | 49 | 0.7219 | | 0.77 (0.20-2.89) |

**Table 5. Analysis of combinatorial effects of LHCGR and KCNA7 gene expression.**
Analysis of combinatorial effects of LHCGR and KCNA7 genes expression (LHCGR/KCNA7). (+)=high gene expression; (-)=low gene expression

## DISCUSSION

The endometrial adenocarcinoma is currently classified in two sub-groups: type I and type II, according to histopathological criteria but, the prognostic value of this distinction is uncertain because approximately 20% of tumors of type I develop recurrence while about 50% of the tumors of type II do not manifest recurrence (Rose, 1996; Amant, 2005; Arcangeli, 2010;Yeramian, 2013). Moreover, there are tumors with mixed or overlapping characteristics that can not be assigned to either group by morphological features (Amant, 2005; Yeramian, 2013). In addition, the type II group itself is composed of a high-heterogeneous batching of histological types suggesting the need of a molecular screening to better classify the endometrial cancer. The current lacking of molecular markers is particularly critical for patients belonging to type I group because their effective risk of recurrence can be dramatically underestimated in the 20% of the cases. In consideration that 90% of endometrial cancer belonging to type 1 group, about 50% of the total recidives appertain to this group, underlining the importance of a better characterization of type1-patients. Microarray-based analysis has proved that gene expression could be an invaluable resource to better stratify the patient risk (Salvesen, 2009).

The expression of LHCGR gene in endometrial cancer could be an important factor in the development and progression of endometrial adenocarcinoma (Lin, 1994; Mandai, 1997; Pike, 1997; Davis, 2000; Noci, 2000; Dabizzi, 2003; Noci, 2008). Therefore, we investigated the level of expression of the LHCGR gene in 115 patients affected by endometrial cancer by real time PCR. We found that LHCGR gene is over expressed in the 55% of patients (Fig. 1). Then, we investigated whether LHCGR and clinical-pathological parameters are associated. Indeed, we found that the expression level of the LHCGR gene is associated to the histological type and with the chromosomal ploidy (Fig. 2). Most importantly, we found that Kaplan-Meier overall survival analysis highlighted a relationship between LHCGR gene expression and

patient survival: the higher LHCGR expression increases the probability of death for patients (Fig. 3). In order to identify additional biomarkers that could integrate LHCGR expression data analysis, we focused on ion channel genes because ion channels are involved in tumor progression of several different type of cancer. In particular, HERG1 potassium channel was described to be up regulated in endometrial cancer (Cherubini, 2000). Thus, we conducted whole-genome expression analysis using microarrays data available in the GEO database and we identified a number of ion channels, including HERG1, with an expression profiles that may suggest their involvement in endometrial cancer. Among these genes we focused on HERG1, KCNH6 and KCNA7 genes because they seem to be the most deregulated ion channel genes. We validated their effective gene expression level by real time PCR confirming the microarray analysis. Statistical analysis of the gene expression data showed that the expression of LHCGR correlate with the expression of KCNH6 and KCNA7. Moreover, our data underlined a correlation between ion channel genes expression.

Univariate overall survival analysis showed a relationship between patient survival and the KCNA7 gene expression: the KCNA7 low-expression determines a substantial increase of the probability of death for patients. Interestingly, the expression of LHCGR and KCNA7 genes has an opposite effect on patient survival. In particular, the expression of LHCGR and KCNA7 have a strong effect in survival when, concurrently, the expression of LHCGR is high and the level of expression of KCNA7 is low. Multivariate overall survival analysis retained the following independent prognostic factors: histology, FIGO and KCNA7 (Tab. 2).

These results identified new biomarkers for molecular diagnostic purposes. These biomarkers could be used for screening bioptic samples of patients to evaluate their effective risk of recurrence of the disease independently to the histopathological classification. Moreover, in consideration that LHCGR over-expression is linked to patient survival probability, there is the possibility to develop a novel therapeutic protocol employing Gn-RH analogues (Noci, 2000, 2001; Arcangeli, 2010). In fact, the use of analogues of Gn-RH reduces the secretion of

LH/hCG hormone with consequent impairment of LHCGR and a reduction of signaling pathways triggered by LHCGR. Hence, patients that display a high LHCGR level of expression can benefit by treatments employing Gn-RH analogues. Remains to clarify the molecular mechanisms that link ion channels and LHCGR expression. In this regard it is worth mentioning that the activation of LHCGR induces the activation of G proteins that in turn trigger signal transduction cascades. The activation of signalling pathways can, indirectly, affect ion channels expression and function because ion channels contribute to regulate many different physiological cell functions. However, we could also speculate a more direct action of LHCGR on ion channels mediated by G proteins (Boland, 1993; Ford, 2003; Bellono, 2013). Indeed, several ion channels are G-protein-gated (Jelacic, 1999). Moreover, hormones can modulate ion channels (Boland, 1993; Ford, 2003). For instance, the erg $K^+$ channels are modulated by GnRH in mouse gonadotropes (Hirdes, 2010). Thus, a molecular relationship between ion channels and LHCGR may be not incidental and could characterize at least a sub-set of endometrial cancers.

## REFERENCES


Amant F, Moerman P, Neven P, Timmerman D, Van Limbergen E, Vergote I. Endometrial cancer. Lancet. 2005 Aug 6-12;366(9484):491-505.

Arcangeli A, Noci I, Fortunato A, Scarselli GF. The LH/hCG Axis in Endometrial Cancer: A New Target in the Treatment of Recurrent or Metastatic Disease. Obstet Gynecol Int. 2010;2010. doi:pii: 486164.

Bellono NW, Kammel LG, Zimmerman AL, Oancea E. UV light phototransduction activates transient receptor potential A1 ion channels in human melanocytes. Proc Natl Acad Sci U S A. 2013 Jan 23.

Boland LM, Bean BP. Modulation of N-type calcium channels in bullfrog sympathetic neurons by luteinizing hormone-releasing hormone: kinetics and voltage dependence. J Neurosci. 1993 Feb;13(2):516-33.

Cherubini A, Taddei GL, Crociani O, Paglierani M, Buccoliero AM, Fontana L, Noci I, Borri P, Borrani E, Giachi M, Becchetti A, Rosati B, Wanke E, Olivotto M, Arcangeli A. HERG potassium channels are more frequently expressed in human endometrial cancer as compared to non-cancerous endometrium. Br J Cancer. 2000 Dec;83(12):1722-9.

Dabizzi S, Noci I, Borri P, Borrani E, Giachi M, Balzi M, Taddei GL, Marchionni M, Scarselli GF, Arcangeli A. Luteinizing hormone increases human endometrial cancer cells invasiveness through activation of protein kinase A. Cancer Res. 2003 Jul 15;63(14):4281-6.

Davies S, C. M. R. Bax, E. Chatzaki, T. Chard, and R.K. Iles, "Regulation of endometrial cancer cell growth by luteinizing hormone (LH) and follicle stimulating hormone (FSH)," British Journal of Cancer, vol. 83, no. 12, pp. 1730–1734, 2000.

Ford CP, Dryden WF, Smith PA. Neurotrophic regulation of calcium channels by the peptide neurotransmitter luteinizing hormone releasing hormone. J Neurosci. 2003 Aug 6;23(18):7169-75.

Jelacic TM, Sims SM, Clapham DE. Functional expression and characterization of G-protein-gated inwardly rectifying K+ channels containing GIRK3. J Membr Biol. 1999 May 15;169(2):123-9.

Lax, SF "Molecular genetic pathways in various types of endometrial carcinoma: from a phenotypical to a molecularbased classification," Virchows Archiv, vol. 444, no. 3, pp. 213–223, 2004.

Lin J, Z. M. Lei, S. Lojun, C. V. Rao, P. G. Satyaswaroop, and T.G. Day, "Increased expression of luteinizing hormone/human chorionic gonadotropin receptor gene in human endometrial carcinomas," Journal of Clinical Endocrinology andMetabolism, vol. 79, no. 5, pp. 1483–1491, 1994.

Mandai M, I. Konishi, H. Kuroda et al., "Messenger ribonucleic acid expression of LH/hCG receptor gene in human ovarian carcinomas," European Journal of Cancer Part A, vol. 33, no. 9, pp. 1501–1507, 1997.

Noci I, Coronnello M, Borri P, Borrani E, Giachi M, Chieffi O, Marchionni M, Paglierani M, Buccoliero AM, Cherubini A, Arcangeli A, Mini E, Taddei G. Inhibitory effect of luteinising hormone-releasing hormone analogues on human endometrial cancer in vitro. Cancer Lett. 2000 Mar 13;150(1):71-8.

Noci I, Borri P, Bonfirraro G, Chieffi O, Arcangeli A, Cherubini A, Dabizzi S,Buccoliero AM, Paglierani M, Taddei GL. Longstanding survival without cancer progression in a patient affected by endometrial carcinoma treated primarily with leuprolide. Br J Cancer. 2001 Aug 3;85(3):333-6.

Noci I, Pillozzi S, Lastraioli E, Dabizzi S, Giachi M, Borrani E, Wimalasena J, Taddei GL, Scarselli G, Arcangeli A. hLH/hCG-receptor expression correlates with in vitro invasiveness in human primary endometrial cancer. Gynecol Oncol. 2008 Dec;111(3):496-501.

Pfaffl, M.W. A new mathematical model for relative quantification in real-time RT-PCR. Nucleic Acids Research. 2001;29:2002-2007.

Pike MC, R. K. Peters, W. Cozen et al., "Estrogen-progestin replacement therapy and endometrial cancer," Journal of the National Cancer Institute, vol. 89, no. 15, pp. 1110–1116, 1997.

Rose, PG "Endometrial carcinoma," New England Journal of Medicine, vol. 335, no. 9, pp. 640–649, 1996.

Salvesen HB, O. E. Iversen, and L. A. Akslen, "Prognostic significance of angiogenesis and ki-67, p53, and p21 expression: a population-based endometrial carcinoma study," Journal of Clinical Oncology, vol. 17, no. 5, pp. 1382–1390, 1999.

Salvesen HB, Carter SL, Mannelqvist M, Dutt A, Getz G, Stefansson IM, Raeder MB, Sos ML, Engelsen IB, Trovik J, Wik E, Greulich H, Bø TH, Jonassen I, Thomas RK, Zander T, Garraway LA, Oyan AM, Sellers WR, Kalland KH, Meyerson M, Akslen LA, Beroukhim R. Integrated genomic profiling of endometrial carcinoma associates aggressive tumors with indicators of PI3 kinase activation. Proc Natl Acad Sci U S A. 2009 Mar 24;106(12):4834-9.

Stepien A. and A. J. Ziecik, "Second messenger systems in the action of LH and oxytocin on porcine endometrial cells in vitro," Theriogenology, vol. 57, no. 9, pp. 2217–2227, 2002.

Yeramian A, Moreno-Bueno G, Dolcet X, Catasus L, Abal M, Colas E, Reventos J, Palacios J, Prat J, Matias-Guiu X. Endometrial carcinoma: molecular alterations involved in tumor development and progression. Oncogene. 2013 Jan 24;32(4):403-13.

Yu J, Ohuchida K, Mizumoto K, Ishikawa N, Ogura Y, Yamada D, Egami T, Fujita H, Ohashi S, Nagai E, Tanaka M. Overexpression of c-met in the early stage of pancreatic carcinogenesis; altered expression is not sufficient for progression from chronic pancreatitis to pancreatic cancer. World J Gastroenterol. 2006 Jun 28;12(24):3878-82.

# Supplementary statistical analysis
# Of endometrial cancer gene expression

Statistical Report

**TABLES OF CONTENTS**

**TABLE 1.1: Comparison of clinical and biological characteristics by type of cohort**

| Variable | Type of cohort included (N=101) | | excluded (N=13) | | P-value |
|---|---|---|---|---|---|
| ageyr, median (min, max) | 66.0 | (42.0, 93.0) | 63.0 | (50.0, 79.0) | 0.4691 |
| b_ageyr, no. (%) | | | | | 0.3733 |
| . <=65 yrs | 50 | (87.7%) | 7 | (12.3%) | |
| . >65 yrs | 51 | (92.7%) | 4 | (7.3%) | |
| histo, no. (%) | | | | | 0.4638 |
| . endometroid | 83 | (89.2%) | 10 | (10.8%) | |
| . non endometroid | 18 | (94.7%) | 1 | (5.3%) | |
| diff, no. (%) | | | | | 0.0643 |
| . medium-high | 61 | (87.1%) | 9 | (12.9%) | |
| . low | 40 | (97.6%) | 1 | (2.4%) | |
| b_FIGO, no. (%) | | | | | 0.8978 |
| . I-II | 81 | (90.0%) | 9 | (10.0%) | |
| . III-IV | 20 | (90.9%) | 2 | (9.1%) | |
| FIGO, no. (%) | | | | | 0.2264 |
| . I | 67 | (93.1%) | 5 | (6.9%) | |
| . II | 14 | (77.8%) | 4 | (22.2%) | |
| . III | 15 | (93.8%) | 1 | (6.3%) | |
| . IV | 5 | (83.3%) | 1 | (16.7%) | |
| node, no. (%) | | | | | 0.7840 |
| . negative | 80 | (89.9%) | 9 | (10.1%) | |
| . positive | 12 | (92.3%) | 1 | (7.7%) | |
| ploidy, no. (%) | | | | | 0.0474 |
| . diploid | 57 | (86.4%) | 9 | (13.6%) | |
| . aneuploid | 26 | (100%) | 0 | (0.0%) | |
| b_KCNA7, no. (%) | | | | | 0.2599 |
| . normal | 21 | (95.5%) | 1 | (4.5%) | |
| . hyperexpressed | 80 | (87.0%) | 12 | (13.0%) | |
| b_LHCGR, no. (%) | | | | | 0.6998 |
| . normal | 45 | (97.8%) | 1 | (2.2%) | |
| . hyperexpressed | 56 | (96.6%) | 2 | (3.4%) | |
| combination, no. (%) | | | | | 0.8432 |

NOTE: patients with missing data were excluded from the analyses

combination represents the combination of LHCGR and KCNA7, respectively

**TABLE 1.1: Comparison of clinical and biological characteristics by type of cohort**

| Variable | Type of cohort included (N=101) | | excluded (N=13) | | P-value |
|---|---|---|---|---|---|
| . - / - | 14 | (100%) | 0 | (0.0%) | |
| . + / - | 7 | (100%) | 0 | (0.0%) | |
| . - / + | 31 | (96.9%) | 1 | (3.1%) | |
| . + / + | 49 | (96.1%) | 2 | (3.9%) | |
| b_kcnh6, no. (%) | | | | | 0.1186 |
| . normal | 28 | (96.6%) | 1 | (3.4%) | |
| . hyperexpressed | 73 | (85.9%) | 12 | (14.1%) | |
| b_HERG1, no. (%) | | | | | 0.7996 |
| . normal | 10 | (90.9%) | 1 | (9.1%) | |
| . hyperexpressed | 91 | (88.3%) | 12 | (11.7%) | |

NOTE: patients with missing data were excluded from the analyses

combi represents the combination of LHCGR and KCNA7, respectively

**TABLE 1.2: Association between histology and other factors**

| Variable | Histology: endometroid (N=83) | non endometroid (N=18) | P-value |
|---|---|---|---|
| b_ageyr, no. (%) | | | 0.0107 |
| . <=65 yrs | 46 (92.0%) | 4 (8.0%) | |
| . >65 yrs | 37 (72.5%) | 14 (27.5%) | |
| diff, no. (%) | | | <.0001 |
| . medium-high | 61 (100%) | 0 (0.0%) | |
| . low | 22 (55.0%) | 18 (45.0%) | |
| b_FIGO, no. (%) | | | 0.0004 |
| . I-II | 72 (88.9%) | 9 (11.1%) | |
| . III-IV | 11 (55.0%) | 9 (45.0%) | |
| FIGO, no. (%) | | | 0.0049 |
| . I | 59 (88.1%) | 8 (11.9%) | |
| . II | 13 (92.9%) | 1 (7.1%) | |
| . III | 8 (53.3%) | 7 (46.7%) | |
| . IV | 3 (60.0%) | 2 (40.0%) | |
| node, no. (%) | | | 0.0026 |
| . negative | 69 (86.3%) | 11 (13.8%) | |
| . positive | 6 (50.0%) | 6 (50.0%) | |
| ploidy, no. (%) | | | 0.0028 |
| . diploid | 51 (89.5%) | 6 (10.5%) | |
| . aneuploid | 16 (61.5%) | 10 (38.5%) | |
| b_KCNA7, no. (%) | | | 0.1481 |
| . normal | 15 (71.4%) | 6 (28.6%) | |
| . hyperexpressed | 68 (85.0%) | 12 (15.0%) | |
| b_LHCGR, no. (%) | | | 0.0016 |
| . normal | 43 (95.6%) | 2 (4.4%) | |
| . hyperexpressed | 40 (71.4%) | 16 (28.6%) | |
| b_KCNH6, no. (%) | | | 0.2477 |
| . normal | 25 (89.3%) | 3 (10.7%) | |
| . hyperexpressed | 58 (79.5%) | 15 (20.5%) | |
| b_HERG1, no. (%) | | | 0.2891 |
| . normal | 7 (70.0%) | 3 (30.0%) | |
| . hyperexpressed | 76 (83.5%) | 15 (16.5%) | |

**TABLE 1.3: Association between differentiation and other factors**

| Variable | Differentiation: medium-high (N=61) | | low (N=40) | | P-value |
|---|---|---|---|---|---|
| b_ageyr, no. (%) | | | | | 0.0182 |
| . <=65 yrs | 36 | (72.0%) | 14 | (28.0%) | |
| . >65 yrs | 25 | (49.0%) | 26 | (51.0%) | |
| histo, no. (%) | | | | | <.0001 |
| . endometroid | 61 | (73.5%) | 22 | (26.5%) | |
| . non endometroid | 0 | (0.0%) | 18 | (100%) | |
| b_FIGO, no. (%) | | | | | <.0001 |
| . I-II | 57 | (70.4%) | 24 | (29.6%) | |
| . III-IV | 4 | (20.0%) | 16 | (80.0%) | |
| FIGO, no. (%) | | | | | 0.0006 |
| . I | 46 | (68.7%) | 21 | (31.3%) | |
| . II | 11 | (78.6%) | 3 | (21.4%) | |
| . III | 3 | (20.0%) | 12 | (80.0%) | |
| . IV | 1 | (20.0%) | 4 | (80.0%) | |
| node, no. (%) | | | | | 0.0084 |
| . negative | 52 | (65.0%) | 28 | (35.0%) | |
| . positive | 3 | (25.0%) | 9 | (75.0%) | |
| ploidy, no. (%) | | | | | 0.0038 |
| . diploid | 39 | (68.4%) | 18 | (31.6%) | |
| . aneuploid | 9 | (34.6%) | 17 | (65.4%) | |
| b_KCNA7, no. (%) | | | | | 0.1786 |
| . normal | 10 | (47.6%) | 11 | (52.4%) | |
| . hyperexpressed | 51 | (63.8%) | 29 | (36.3%) | |
| b_LHCGR, no. (%) | | | | | 0.1177 |
| . normal | 31 | (68.9%) | 14 | (31.1%) | |
| . hyperexpressed | 30 | (53.6%) | 26 | (46.4%) | |
| b_KCNH6, no. (%) | | | | | 0.9677 |
| . normal | 17 | (60.7%) | 11 | (39.3%) | |
| . hyperexpressed | 44 | (60.3%) | 29 | (39.7%) | |
| b_HERG1, no. (%) | | | | | 0.4788 |
| . normal | 5 | (50.0%) | 5 | (50.0%) | |
| . hyperexpressed | 56 | (61.5%) | 35 | (38.5%) | |

**TABLE 1.4: Association between FIGO and other factors**

| Variable | FIGO I-II (N=81) | | FIGO III-IV (N=20) | | P-value |
|---|---|---|---|---|---|
| b_ageyr, no. (%) | | | | | 0.1474 |
| . <=65 yrs | 43 | (86.0%) | 7 | (14.0%) | |
| . >65 yrs | 38 | (74.5%) | 13 | (25.5%) | |
| histo, no. (%) | | | | | 0.0004 |
| . endometroid | 72 | (86.7%) | 11 | (13.3%) | |
| . non endometroid | 9 | (50.0%) | 9 | (50.0%) | |
| diff, no. (%) | | | | | <.0001 |
| . medium-high | 57 | (93.4%) | 4 | (6.6%) | |
| . low | 24 | (60.0%) | 16 | (40.0%) | |
| node, no. (%) | | | | | <.0001 |
| . negative | 75 | (93.8%) | 5 | (6.3%) | |
| . positive | 0 | (0.0%) | 12 | (100%) | |
| ploidy, no. (%) | | | | | 0.3261 |
| . diploid | 47 | (82.5%) | 10 | (17.5%) | |
| . aneuploid | 19 | (73.1%) | 7 | (26.9%) | |
| b_KCNA7, no. (%) | | | | | 0.0804 |
| . normal | 14 | (66.7%) | 7 | (33.3%) | |
| . hyperexpressed | 67 | (83.8%) | 13 | (16.3%) | |
| b_LHCGR, no. (%) | | | | | 0.6472 |
| . normal | 37 | (82.2%) | 8 | (17.8%) | |
| . hyperexpressed | 44 | (78.6%) | 12 | (21.4%) | |
| b_KCNH6, no. (%) | | | | | 0.4169 |
| . normal | 21 | (75.0%) | 7 | (25.0%) | |
| . hyperexpressed | 60 | (82.2%) | 13 | (17.8%) | |
| b_HERG1, no. (%) | | | | | 0.0913 |
| . normal | 6 | (60.0%) | 4 | (40.0%) | |
| . hyperexpressed | 75 | (82.4%) | 16 | (17.6%) | |

**TABLE 1.5: Association between nodes and other factors**

| Variable | Nodes negative (N=80) | positive (N=12) | P-value |
|---|---|---|---|
| b_ageyr, no. (%) | | | 0.2469 |
| . <=65 yrs | 41 (91.1%) | 4 (8.9%) | |
| . >65 yrs | 39 (83.0%) | 8 (17.0%) | |
| histo, no. (%) | | | 0.0026 |
| . endometroid | 69 (92.0%) | 6 (8.0%) | |
| . non endometroid | 11 (64.7%) | 6 (35.3%) | |
| diff, no. (%) | | | 0.0084 |
| . medium-high | 52 (94.5%) | 3 (5.5%) | |
| . low | 28 (75.7%) | 9 (24.3%) | |
| b_FIGO, no. (%) | | | <.0001 |
| . I-II | 75 (100%) | 0 (0.0%) | |
| . III-IV | 5 (29.4%) | 12 (70.6%) | |
| FIGO, no. (%) | | | <.0001 |
| . I | 63 (100%) | 0 (0.0%) | |
| . II | 12 (100%) | 0 (0.0%) | |
| . III | 2 (14.3%) | 12 (85.7%) | |
| . IV | 3 (100%) | 0 (0.0%) | |
| ploidy, no. (%) | | | 0.5387 |
| . diploid | 46 (88.5%) | 6 (11.5%) | |
| . aneuploid | 20 (83.3%) | 4 (16.7%) | |
| b_KCNA7, no. (%) | | | 0.0954 |
| . normal | 16 (76.2%) | 5 (23.8%) | |
| . hyperexpressed | 64 (90.1%) | 7 (9.9%) | |
| b_LHCGR, no. (%) | | | 0.8920 |
| . normal | 35 (87.5%) | 5 (12.5%) | |
| . hyperexpressed | 45 (86.5%) | 7 (13.5%) | |
| b_KCNH6, no. (%) | | | 0.0729 |
| . normal | 20 (76.9%) | 6 (23.1%) | |
| . hyperexpressed | 60 (90.9%) | 6 (9.1%) | |
| b_HERG1, no. (%) | | | 0.0571 |
| . normal | 6 (66.7%) | 3 (33.3%) | |
| . hyperexpressed | 74 (89.2%) | 9 (10.8%) | |

**TABLE 1.6: Association between ploidy and other factors**

| | Ploidy | | |
|---|---|---|---|
| Variable | diploid (N=57) | aneuploid (N=26) | P-value |
| b_ageyr, no. (%) | | | 0.0010 |
| . <=65 yrs | 33 (86.8%) | 5 (13.2%) | |
| . >65 yrs | 24 (53.3%) | 21 (46.7%) | |
| histo, no. (%) | | | 0.0028 |
| . endometroid | 51 (76.1%) | 16 (23.9%) | |
| . non endometroid | 6 (37.5%) | 10 (62.5%) | |
| diff, no. (%) | | | 0.0038 |
| . medium-high | 39 (81.3%) | 9 (18.8%) | |
| . low | 18 (51.4%) | 17 (48.6%) | |
| b_FIGO, no. (%) | | | 0.3261 |
| . I-II | 47 (71.2%) | 19 (28.8%) | |
| . III-IV | 10 (58.8%) | 7 (41.2%) | |
| FIGO, no. (%) | | | 0.6708 |
| . I | 38 (73.1%) | 14 (26.9%) | |
| . II | 9 (64.3%) | 5 (35.7%) | |
| . III | 8 (61.5%) | 5 (38.5%) | |
| . IV | 2 (50.0%) | 2 (50.0%) | |
| node, no. (%) | | | 0.5387 |
| . negative | 46 (69.7%) | 20 (30.3%) | |
| . positive | 6 (60.0%) | 4 (40.0%) | |
| b_KCNA7, no. (%) | | | 0.4839 |
| . normal | 15 (75.0%) | 5 (25.0%) | |
| . hyperexpressed | 42 (66.7%) | 21 (33.3%) | |
| b_LHCGR, no. (%) | | | 0.0198 |
| . normal | 31 (81.6%) | 7 (18.4%) | |
| . hyperexpressed | 26 (57.8%) | 19 (42.2%) | |
| b_KCNH6, no. (%) | | | 0.0481 |
| . normal | 21 (84.0%) | 4 (16.0%) | |
| . hyperexpressed | 36 (62.1%) | 22 (37.9%) | |
| b_HERG1, no. (%) | | | 0.1211 |
| . normal | 9 (90.0%) | 1 (10.0%) | |
| . hyperexpressed | 48 (65.8%) | 25 (34.2%) | |

**TABLE 1.7: Association between KCNA7 and other factors**

| Variable | KCNA7 normal (N=21) | KCNA7 hyperexpressed (N=80) | P-value |
|---|---|---|---|
| b_ageyr, no. (%) | | | 0.4315 |
| . <=65 yrs | 12 (24.0%) | 38 (76.0%) | |
| . >65 yrs | 9 (17.6%) | 42 (82.4%) | |
| histo, no. (%) | | | 0.1481 |
| . endometroid | 15 (18.1%) | 68 (81.9%) | |
| . non endometroid | 6 (33.3%) | 12 (66.7%) | |
| diff, no. (%) | | | 0.1786 |
| . medium-high | 10 (16.4%) | 51 (83.6%) | |
| . low | 11 (27.5%) | 29 (72.5%) | |
| b_FIGO, no. (%) | | | 0.0804 |
| . I-II | 14 (17.3%) | 67 (82.7%) | |
| . III-IV | 7 (35.0%) | 13 (65.0%) | |
| FIGO, no. (%) | | | 0.1526 |
| . I | 10 (14.9%) | 57 (85.1%) | |
| . II | 4 (28.6%) | 10 (71.4%) | |
| . III | 6 (40.0%) | 9 (60.0%) | |
| . IV | 1 (20.0%) | 4 (80.0%) | |
| node, no. (%) | | | 0.0954 |
| . negative | 16 (20.0%) | 64 (80.0%) | |
| . positive | 5 (41.7%) | 7 (58.3%) | |
| ploidy, no. (%) | | | 0.4839 |
| . diploid | 15 (26.3%) | 42 (73.7%) | |
| . aneuploid | 5 (19.2%) | 21 (80.8%) | |
| b_LHCGR, no. (%) | | | 0.0220 |
| . normal | 14 (31.1%) | 31 (68.9%) | |
| . hyperexpressed | 7 (12.5%) | 49 (87.5%) | |
| b_KCNH6, no. (%) | | | 0.2328 |
| . normal | 8 (28.6%) | 20 (71.4%) | |
| . hyperexpressed | 13 (17.8%) | 60 (82.2%) | |
| b_HERG1, no. (%) | | | <.0001 |
| . normal | 7 (70.0%) | 3 (30.0%) | |
| . hyperexpressed | 14 (15.4%) | 77 (84.6%) | |

**TABLE 1.8: Association between LHCGR and other factors**

| | LHCGR | | |
|---|---|---|---|
| Variable | normal (N=45) | hyperexpressed (N=56) | P-value |
| b_ageyr, no. (%) | | | 0.2756 |
| . <=65 yrs | 25 (50.0%) | 25 (50.0%) | |
| . >65 yrs | 20 (39.2%) | 31 (60.8%) | |
| histo, no. (%) | | | 0.0016 |
| . endometroid | 43 (51.8%) | 40 (48.2%) | |
| . non endometroid | 2 (11.1%) | 16 (88.9%) | |
| diff, no. (%) | | | 0.1177 |
| . medium-high | 31 (50.8%) | 30 (49.2%) | |
| . low | 14 (35.0%) | 26 (65.0%) | |
| b_FIGO, no. (%) | | | 0.6472 |
| . I-II | 37 (45.7%) | 44 (54.3%) | |
| . III-IV | 8 (40.0%) | 12 (60.0%) | |
| FIGO, no. (%) | | | 0.3005 |
| . I | 28 (41.8%) | 39 (58.2%) | |
| . II | 9 (64.3%) | 5 (35.7%) | |
| . III | 7 (46.7%) | 8 (53.3%) | |
| . IV | 1 (20.0%) | 4 (80.0%) | |
| node, no. (%) | | | 0.8920 |
| . negative | 35 (43.8%) | 45 (56.3%) | |
| . positive | 5 (41.7%) | 7 (58.3%) | |
| ploidy, no. (%) | | | 0.0198 |
| . diploid | 31 (54.4%) | 26 (45.6%) | |
| . aneuploid | 7 (26.9%) | 19 (73.1%) | |
| b_KCNA7, no. (%) | | | 0.0220 |
| . normal | 14 (66.7%) | 7 (33.3%) | |
| . hyperexpressed | 31 (38.8%) | 49 (61.3%) | |
| b_KCNH6, no. (%) | | | 0.0430 |
| . normal | 17 (60.7%) | 11 (39.3%) | |
| . hyperexpressed | 28 (38.4%) | 45 (61.6%) | |
| b_HERG1, no. (%) | | | 0.3005 |
| . normal | 6 (60.0%) | 4 (40.0%) | |
| . hyperexpressed | 39 (42.9%) | 52 (57.1%) | |

**TABLE 1.9: Association between kcnh6 and other factors**

| Variable | KCNH6 normal (N=28) | | KCNH6 hyperexpressed (N=73) | | P-value |
|---|---|---|---|---|---|
| b_ageyr, no. (%) | | | | | 0.7017 |
| . <=65 yrs | 13 | (26.0%) | 37 | (74.0%) | |
| . >65 yrs | 15 | (29.4%) | 36 | (70.6%) | |
| histo, no. (%) | | | | | 0.2477 |
| . endometroid | 25 | (30.1%) | 58 | (69.9%) | |
| . non endometroid | 3 | (16.7%) | 15 | (83.3%) | |
| diff, no. (%) | | | | | 0.9677 |
| . medium-high | 17 | (27.9%) | 44 | (72.1%) | |
| . low | 11 | (27.5%) | 29 | (72.5%) | |
| b_FIGO, no. (%) | | | | | 0.4169 |
| . I-II | 21 | (25.9%) | 60 | (74.1%) | |
| . III-IV | 7 | (35.0%) | 13 | (65.0%) | |
| FIGO, no. (%) | | | | | 0.1875 |
| . I | 17 | (25.4%) | 50 | (74.6%) | |
| . II | 4 | (28.6%) | 10 | (71.4%) | |
| . III | 7 | (46.7%) | 8 | (53.3%) | |
| . IV | 0 | (0.0%) | 5 | (100%) | |
| node, no. (%) | | | | | 0.0729 |
| . negative | 20 | (25.0%) | 60 | (75.0%) | |
| . positive | 6 | (50.0%) | 6 | (50.0%) | |
| ploidy, no. (%) | | | | | 0.0481 |
| . diploid | 21 | (36.8%) | 36 | (63.2%) | |
| . aneuploid | 4 | (15.4%) | 22 | (84.6%) | |
| b_KCNA7, no. (%) | | | | | 0.2328 |
| . normal | 8 | (38.1%) | 13 | (61.9%) | |
| . hyperexpressed | 20 | (25.0%) | 60 | (75.0%) | |
| b_LHCGR, no. (%) | | | | | 0.0430 |
| . normal | 17 | (37.8%) | 28 | (62.2%) | |
| . hyperexpressed | 11 | (19.6%) | 45 | (80.4%) | |
| b_HERG1, no. (%) | | | | | 0.0163 |
| . normal | 6 | (60.0%) | 4 | (40.0%) | |
| . hyperexpressed | 22 | (24.2%) | 69 | (75.8%) | |

**TABLE 1.10: Association between HERG1 and other factors**

| Variable | HERG1 normal (N=10) | | HERG1 hyperexpressed (N=91) | | P-value |
|---|---|---|---|---|---|
| b_ageyr, no. (%) | | | | | 0.4844 |
| . <=65 yrs | 6 | (12.0%) | 44 | (88.0%) | |
| . >65 yrs | 4 | (7.8%) | 47 | (92.2%) | |
| histo, no. (%) | | | | | 0.2891 |
| . endometroid | 7 | (8.4%) | 76 | (91.6%) | |
| . non endometroid | 3 | (16.7%) | 15 | (83.3%) | |
| diff, no. (%) | | | | | 0.4788 |
| . medium-high | 5 | (8.2%) | 56 | (91.8%) | |
| . low | 5 | (12.5%) | 35 | (87.5%) | |
| b_FIGO, no. (%) | | | | | 0.0913 |
| . I-II | 6 | (7.4%) | 75 | (92.6%) | |
| . III-IV | 4 | (20.0%) | 16 | (80.0%) | |
| FIGO, no. (%) | | | | | 0.4149 |
| . I | 5 | (7.5%) | 62 | (92.5%) | |
| . II | 1 | (7.1%) | 13 | (92.9%) | |
| . III | 3 | (20.0%) | 12 | (80.0%) | |
| . IV | 1 | (20.0%) | 4 | (80.0%) | |
| node, no. (%) | | | | | 0.0571 |
| . negative | 6 | (7.5%) | 74 | (92.5%) | |
| . positive | 3 | (25.0%) | 9 | (75.0%) | |
| ploidy, no. (%) | | | | | 0.1211 |
| . diploid | 9 | (15.8%) | 48 | (84.2%) | |
| . aneuploid | 1 | (3.8%) | 25 | (96.2%) | |
| b_KCNA7, no. (%) | | | | | <.0001 |
| . normal | 7 | (33.3%) | 14 | (66.7%) | |
| . hyperexpressed | 3 | (3.8%) | 77 | (96.3%) | |
| b_LHCGR, no. (%) | | | | | 0.3005 |
| . normal | 6 | (13.3%) | 39 | (86.7%) | |
| . hyperexpressed | 4 | (7.1%) | 52 | (92.9%) | |
| b_KCNH6, no. (%) | | | | | 0.0163 |
| . normal | 6 | (21.4%) | 22 | (78.6%) | |
| . hyperexpressed | 4 | (5.5%) | 69 | (94.5%) | |

**FOLLOW-UP INFORMATION**

TABLE 2.1: Percentiles of the distribution of follow-up time

| Median of follow-up time (yrs) | IQR of follow-up time (yrs) |
|---|---|
| 2.2 | (1.3 - 3.4) |

NOTE: IQR = interquartile range.

DISEASE-FREE SURVIVAL ANALYSIS

**TABLE 3.1: Disease-free survival by type of cohort**

| Variable | N | Number failed | 3-yr survival | Log-rank test p-value | Hazard ratio (95% CI) |
|---|---|---|---|---|---|
| Cohort | . | . | . | | |
| excluded | 10 | 2 | 0.9000 | 0.564 | 1 (ref.) |
| included | 95 | 21 | 0.6826 | | 1.53 (0.36-6.55) |

NOTE: three and six patients have missing information about disease-free interval in the excluded and included cohorts, respectively

**TABLE 3.2: Disease-free survival of included cohort by clinical and biological characteristics**

| Variable | N | Number failed | 3-yr survival | Log-rank test p-value | Hazard ratio (95% CI) |
|---|---|---|---|---|---|
| Age | . | . | . | | |
| <=65 yrs | 47 | 8 | 0.7171 | 0.212 | 1 (ref.) |
| >65 yrs | 48 | 13 | 0.6547 | | 1.74 (0.72-4.20) |
| Histology | . | . | . | | |
| endometroid | 80 | 12 | 0.7561 | <0.001 | 1 (ref.) |
| non endometroid | 15 | 9 | 0.3160 | | 6.88 (2.82-16.82) |
| Differentiation | . | . | . | | |
| low | 35 | 16 | 0.2669 | <0.001 | 1 (ref.) |
| medium-high | 60 | 5 | 0.8948 | | 0.13 (0.05-0.37) |
| FIGO | . | . | . | | |
| I-II | 81 | 11 | 0.8000 | <0.001 | 1 (ref.) |
| III-IV | 14 | 10 | 0 | | 9.19 (3.85-21.90) |
| FIGO | . | . | . | | |
| I | 67 | 9 | 0.8192 | <0.001 | 1 (ref.) |
| II | 14 | 2 | 0.6154 | | 1.39 (0.30-6.47) |
| III | 14 | 10 | 0 | | 9.70 (3.89-24.19) |
| Nodes | . | . | . | | |
| negative | 77 | 12 | 0.7689 | <0.001 | 1 (ref.) |
| positive | 11 | 7 | . | | 7.71 (2.97-19.96) |
| Ploidy | . | . | . | | |
| aneuploid | 24 | 9 | 0.4691 | 0.049 | 1 (ref.) |
| diploid | 55 | 10 | 0.7190 | | 0.42 (0.17-1.03) |
| b_KCNA7 | . | . | . | | |
| hyperexpressed | 75 | 13 | 0.7496 | 0.016 | 1 (ref.) |
| normal | 20 | 8 | 0.4204 | | 2.83 (1.17-6.87) |
| b_LHCGR | . | . | . | | |
| hyperexpressed | 51 | 12 | 0.7015 | 0.507 | 1 (ref.) |
| normal | 44 | 9 | 0.6751 | | 0.75 (0.31-1.78) |
| LHCGR / KCNA7 | . | . | . | | |
| - / - | 14 | 5 | 0.4911 | 0.024 | 1 (ref.) |
| + / - | 6 | 3 | . | | 2.38 (0.55-10.31) |
| - / + | 30 | 4 | 0.7552 | | 0.31 (0.08-1.16) |
| + / + | 45 | 9 | 0.7456 | | 0.55 (0.19-1.65) |
| b_KCNH6 | . | . | . | | |

combi represents the combination of LHCGR and KCNA7, respectively

**TABLE 3.2: Disease-free survival of included cohort by clinical and biological characteristics**

| Variable | N | Number failed | 3-yr survival | Log-rank test p-value | Hazard ratio (95% CI) |
|---|---|---|---|---|---|
| hyperexpressed | 68 | 17 | 0.6519 | 0.160 | 1 (ref.) |
| normal | 27 | 4 | 0.7775 | | 0.46 (0.16-1.39) |
| b_HERG1 | . | . | . | | |
| hyperexpressed | 86 | 19 | 0.6760 | 0.852 | 1 (ref.) |
| normal | 9 | 2 | 0.7111 | | 0.87 (0.20-3.75) |

**TABLE 3.3: Disease-free survival analysis: interaction between LHCGR and KCNA7**

The PHREG Procedure

Model Information

| | |
|---|---|
| Data Set | WORK.ENDOM |
| Dependent Variable | mdfs |
| Censoring Variable | ldfs |
| Censoring Value(s) | 0 |
| Ties Handling | BRESLOW |

| | |
|---|---|
| Number of Observations Read | 101 |
| Number of Observations Used | 95 |

Class Level Information

| Class | Value | Design Variables |
|---|---|---|
| b_KCNA7 | hyperexpressed | 0 |
| | normal | 1 |
| b_LHCGR | hyperexpressed | 0 |
| | normal | 1 |

Summary of the Number of Event and Censored Values

| Total | Event | Censored | Percent Censored |
|---|---|---|---|
| 95 | 21 | 74 | 77.89 |

Convergence Status

Convergence criterion (GCONV=1E-8) satisfied.

Model Fit Statistics

| Criterion | Without Covariates | With Covariates |
|---|---|---|
| -2 LOG L | 173.827 | 166.897 |
| AIC | 173.827 | 172.897 |
| SBC | 173.827 | 176.030 |

Testing Global Null Hypothesis: BETA=0

| Test | Chi-Square | DF | Pr > ChiSq |
|---|---|---|---|
| Likelihood Ratio | 6.9306 | 3 | 0.0741 |
| Score | 9.3325 | 3 | 0.0252 |
| Wald | 7.8375 | 3 | 0.0495 |

Type 3 Tests

| Effect | DF | Wald Chi-Square | Pr > ChiSq |
|---|---|---|---|
| b_KCNA7 | 1 | 4.5630 | 0.0327 |
| b_LHCGR | 1 | 0.9224 | 0.3368 |
| b_KCNA7*b_LHCGR | 1 | 0.0923 | 0.7613 |

**TABLE 3.3: Disease-free survival analysis: interaction between LHCGR and kcnh7**

The PHREG Procedure

Analysis of Maximum Likelihood Estimates

| Parameter | | | DF | Parameter Estimate | Standard Error | Chi-Square | Pr > ChiSq |
|---|---|---|---|---|---|---|---|
| b_KCNA7 | normal | | 1 | 1.46028 | 0.68362 | 4.5630 | 0.0327 |
| b_LHCGR | normal | | 1 | -0.57930 | 0.60318 | 0.9224 | 0.3368 |
| b_KCNA7*b_LHCGR | normal | normal | 1 | -0.28933 | 0.95241 | 0.0923 | 0.7613 |

Analysis of Maximum Likelihood Estimates

| Parameter | | | Hazard Ratio | 95% Hazard Ratio Confidence Limits | | Label |
|---|---|---|---|---|---|---|
| b_KCNA7 | normal | | . | . | . | b_KCNA7 normal |
| b_LHCGR | normal | | . | . | . | b_LHCGR normal |
| b_KCNA7*b_LHCGR | normal | normal | . | . | . | b_KCNA7 normal * b_LHCGR normal |

Hazard Ratios for b_LHCGR

| Description | Point Estimate | 95% Wald Confidence Limits | |
|---|---|---|---|
| b_LHCGR normal vs hyperexpressed At b_KCNA7=hyperexpressed | 0.560 | 0.172 | 1.827 |
| b_LHCGR normal vs hyperexpressed At b_KCNA7=normal | 0.420 | 0.097 | 1.815 |

Hazard Ratios for b_KCNA7

| Description | Point Estimate | 95% Wald Confidence Limits | |
|---|---|---|---|
| b_KCNA7 normal vs hyperexpressed At b_LHCGR=hyperexpressed | 4.307 | 1.128 | 16.447 |
| b_KCNA7 normal vs hyperexpressed At b_LHCGR=normal | 3.225 | 0.863 | 12.046 |

**TABLE 3.4: Multivariate diseae-free survival analysis**

The PHREG Procedure

Model Information

| | |
|---|---|
| Data Set | WORK.ENDOM |
| Dependent Variable | mdfs |
| Censoring Variable | ldfs |
| Censoring Value(s) | 0 |
| Ties Handling | BRESLOW |

| | |
|---|---|
| Number of Observations Read | 101 |
| Number of Observations Used | 95 |

Class Level Information

| Class | Value | Design Variables |
|---|---|---|
| b_ageyr | <=65 yrs | 0 |
| | >65 yrs | 1 |
| histo | endometroid | 0 |
| | non endometroid | 1 |
| diff | low | 0 |
| | medium-high | 1 |
| b_FIGO | I-II | 0 |
| | III-IV | 1 |
| b_KCNA7 | hyperexpressed | 0 |
| | normal | 1 |
| b_LHCGR | hyperexpressed | 0 |
| | normal | 1 |
| b_KCNH6 | hyperexpressed | 0 |
| | normal | 1 |
| b_HERG1 | hyperexpressed | 0 |
| | normal | 1 |

Summary of the Number of Event and Censored Values

| Total | Event | Censored | Percent Censored |
|---|---|---|---|
| 95 | 21 | 74 | 77.89 |

Step 0. The model contains the following effects:

b_ageyr histo diff b_FIGO b_KCNA7 b_LHCGR b_KCNH6 b_HERG1

Convergence Status

Convergence criterion (GCONV=1E-8) satisfied.

Model Fit Statistics

| Criterion | Without Covariates | With Covariates |
|---|---|---|
| -2 LOG L | 173.827 | 134.987 |
| AIC | 173.827 | 150.987 |
| SBC | 173.827 | 159.343 |

**TABLE 3.4: Multivariate diseae-free survival analysis**

The PHREG Procedure

Testing Global Null Hypothesis: BETA=0

| Test | Chi-Square | DF | Pr > ChiSq |
|---|---|---|---|
| Likelihood Ratio | 38.8400 | 8 | <.0001 |
| Score | 57.9950 | 8 | <.0001 |
| Wald | 37.3105 | 8 | <.0001 |

Type 3 Tests

| Effect | DF | Wald Chi-Square | Pr > ChiSq |
|---|---|---|---|
| b_ageyr | 1 | 0.1543 | 0.6945 |
| histo | 1 | 0.2482 | 0.6183 |
| diff | 1 | 3.5397 | 0.0599 |
| b_FIGO | 1 | 11.8433 | 0.0006 |
| b_KCNA7 | 1 | 0.5094 | 0.4754 |
| b_LHCGR | 1 | 0.0645 | 0.7995 |
| b_KCNH6 | 1 | 4.7456 | 0.0294 |
| b_HERG1 | 1 | 0.1248 | 0.7239 |

Analysis of Maximum Likelihood Estimates

| Parameter | | DF | Parameter Estimate | Standard Error | Chi-Square | Pr > ChiSq | Hazard Ratio | 95% Hazard Ratio Confidence Limits | |
|---|---|---|---|---|---|---|---|---|---|
| b_ageyr | >65 yrs | 1 | 0.21930 | 0.55834 | 0.1543 | 0.6945 | 1.245 | 0.417 | 3.720 |
| histo | non endometroid | 1 | 0.32947 | 0.66128 | 0.2482 | 0.6183 | 1.390 | 0.380 | 5.081 |
| diff | medium-high | 1 | -1.22616 | 0.65173 | 3.5397 | 0.0599 | 0.293 | 0.082 | 1.053 |
| b_FIGO | III-IV | 1 | 2.05689 | 0.59769 | 11.8433 | 0.0006 | 7.822 | 2.424 | 25.238 |
| b_KCNA7 | normal | 1 | 0.41521 | 0.58176 | 0.5094 | 0.4754 | 1.515 | 0.484 | 4.737 |
| b_LHCGR | normal | 1 | 0.14878 | 0.58566 | 0.0645 | 0.7995 | 1.160 | 0.368 | 3.657 |
| b_KCNH6 | normal | 1 | -1.68330 | 0.77271 | 4.7456 | 0.0294 | 0.186 | 0.041 | 0.845 |
| b_HERG1 | normal | 1 | -0.30247 | 0.85609 | 0.1248 | 0.7239 | 0.739 | 0.138 | 3.957 |

Analysis of Maximum Likelihood Estimates

| Parameter | | Label |
|---|---|---|
| b_ageyr | >65 yrs | b_ageyr >65 yrs |
| histo | non endometroid | histo non endometroid |
| diff | medium-high | diff medium-high |
| b_FIGO | III-IV | b_FIGO III-IV |
| b_KCNA7 | normal | b_KCNA7 normal |
| b_LHCGR | normal | b_LHCGR normal |
| b_KCNH6 | normal | b_kcnh6 normal |
| b_HERG1 | normal | b_HERG1 normal |

Analysis of Effects Eligible for Removal

| Effect | DF | Wald Chi-Square | Pr > ChiSq |
|---|---|---|---|
| b_ageyr | 1 | 0.1543 | 0.6945 |
| histo | 1 | 0.2482 | 0.6183 |
| diff | 1 | 3.5397 | 0.0599 |
| b_FIGO | 1 | 11.8433 | 0.0006 |
| b_KCNA7 | 1 | 0.5094 | 0.4754 |
| b_LHCGR | 1 | 0.0645 | 0.7995 |
| b_KCNH6 | 1 | 4.7456 | 0.0294 |
| b_HERG1 | 1 | 0.1248 | 0.7239 |

Step 1. Effect b_LHCGR is removed. The model contains the following effects:

b_ageyr histo diff b_FIGO b_KCNA7 b_KCNH6 b_HERG1

**TABLE 3.4: Multivariate diseae-free survival analysis**

The PHREG Procedure

Convergence Status

Convergence criterion (GCONV=1E-8) satisfied.

Model Fit Statistics

| Criterion | Without Covariates | With Covariates |
|---|---|---|
| -2 LOG L | 173.827 | 135.052 |
| AIC | 173.827 | 149.052 |
| SBC | 173.827 | 156.363 |

Testing Global Null Hypothesis: BETA=0

| Test | Chi-Square | DF | Pr > ChiSq |
|---|---|---|---|
| Likelihood Ratio | 38.7754 | 7 | <.0001 |
| Score | 57.8514 | 7 | <.0001 |
| Wald | 37.4442 | 7 | <.0001 |

Type 3 Tests

| Effect | DF | Wald Chi-Square | Pr > ChiSq |
|---|---|---|---|
| b_ageyr | 1 | 0.1128 | 0.7370 |
| histo | 1 | 0.2039 | 0.6516 |
| diff | 1 | 3.5061 | 0.0611 |
| b_FIGO | 1 | 11.8726 | 0.0006 |
| b_KCNA7 | 1 | 0.6814 | 0.4091 |
| b_KCNH6 | 1 | 4.9049 | 0.0268 |
| b_HERG1 | 1 | 0.1095 | 0.7407 |

Analysis of Maximum Likelihood Estimates

| Parameter | | DF | Parameter Estimate | Standard Error | Chi-Square | Pr > ChiSq | Hazard Ratio | 95% Hazard Ratio Confidence Limits | |
|---|---|---|---|---|---|---|---|---|---|
| b_ageyr | >65 yrs | 1 | 0.17974 | 0.53520 | 0.1128 | 0.7370 | 1.197 | 0.419 | 3.417 |
| histo | non endometroid | 1 | 0.29024 | 0.64271 | 0.2039 | 0.6516 | 1.337 | 0.379 | 4.711 |
| diff | medium-high | 1 | -1.20952 | 0.64595 | 3.5061 | 0.0611 | 0.298 | 0.084 | 1.058 |
| b_FIGO | III-IV | 1 | 2.05759 | 0.59715 | 11.8726 | 0.0006 | 7.827 | 2.428 | 25.229 |
| b_KCNA7 | normal | 1 | 0.45826 | 0.55514 | 0.6814 | 0.4091 | 1.581 | 0.533 | 4.694 |
| b_KCNH6 | normal | 1 | -1.63572 | 0.73857 | 4.9049 | 0.0268 | 0.195 | 0.046 | 0.828 |
| b_HERG1 | normal | 1 | -0.28265 | 0.85398 | 0.1095 | 0.7407 | 0.754 | 0.141 | 4.019 |

Analysis of Maximum Likelihood Estimates

| Parameter | | Label |
|---|---|---|
| b_ageyr | >65 yrs | b_ageyr >65 yrs |
| histo | non endometroid | histo non endometroid |
| diff | medium-high | diff medium-high |
| b_FIGO | III-IV | b_FIGO III-IV |
| b_KCNA7 | normal | b_KCNA7 normal |
| b_KCNH6 | normal | b_kcnh6 normal |
| b_HERG1 | normal | b_HERG1 normal |

Analysis of Effects Eligible for Removal

| Effect | DF | Wald Chi-Square | Pr > ChiSq |
|---|---|---|---|
| b_ageyr | 1 | 0.1128 | 0.7370 |
| histo | 1 | 0.2039 | 0.6516 |
| diff | 1 | 3.5061 | 0.0611 |
| b_FIGO | 1 | 11.8726 | 0.0006 |

**TABLE 3.4: Multivariate diseae-free survival analysis**

The PHREG Procedure

Analysis of Effects Eligible for Removal

| Effect | DF | Wald Chi-Square | Pr > ChiSq |
|---|---|---|---|
| b_KCNA7 | 1 | 0.6814 | 0.4091 |
| b_KCNH6 | 1 | 4.9049 | 0.0268 |
| b_HERG1 | 1 | 0.1095 | 0.7407 |

Step 2. Effect b_HERG1 is removed. The model contains the following effects:

b_ageyr histo diff b_FIGO b_KCNA7 b_KCNH6

Convergence Status

Convergence criterion (GCONV=1E-8) satisfied.

Model Fit Statistics

| Criterion | Without Covariates | With Covariates |
|---|---|---|
| -2 LOG L | 173.827 | 135.166 |
| AIC | 173.827 | 147.166 |
| SBC | 173.827 | 153.433 |

Testing Global Null Hypothesis: BETA=0

| Test | Chi-Square | DF | Pr > ChiSq |
|---|---|---|---|
| Likelihood Ratio | 38.6613 | 6 | <.0001 |
| Score | 56.6284 | 6 | <.0001 |
| Wald | 37.0529 | 6 | <.0001 |

Type 3 Tests

| Effect | DF | Wald Chi-Square | Pr > ChiSq |
|---|---|---|---|
| b_ageyr | 1 | 0.1443 | 0.7040 |
| histo | 1 | 0.2076 | 0.6487 |
| diff | 1 | 3.4138 | 0.0647 |
| b_FIGO | 1 | 11.8958 | 0.0006 |
| b_KCNA7 | 1 | 0.5969 | 0.4398 |
| b_KCNH6 | 1 | 6.1780 | 0.0129 |

Analysis of Maximum Likelihood Estimates

| Parameter | | DF | Parameter Estimate | Standard Error | Chi-Square | Pr > ChiSq | Hazard Ratio | 95% Hazard Ratio Confidence Limits | |
|---|---|---|---|---|---|---|---|---|---|
| b_ageyr | >65 yrs | 1 | 0.20174 | 0.53099 | 0.1443 | 0.7040 | 1.224 | 0.432 | 3.464 |
| histo | non endometroid | 1 | 0.29378 | 0.64482 | 0.2076 | 0.6487 | 1.341 | 0.379 | 4.747 |
| diff | medium-high | 1 | -1.20019 | 0.64957 | 3.4138 | 0.0647 | 0.301 | 0.084 | 1.076 |
| b_FIGO | III-IV | 1 | 2.06028 | 0.59735 | 11.8958 | 0.0006 | 7.848 | 2.434 | 25.307 |
| b_KCNA7 | normal | 1 | 0.42552 | 0.55078 | 0.5969 | 0.4398 | 1.530 | 0.520 | 4.504 |
| b_KCNH6 | normal | 1 | -1.73224 | 0.69692 | 6.1780 | 0.0129 | 0.177 | 0.045 | 0.693 |

Analysis of Maximum Likelihood Estimates

| Parameter | | Label |
|---|---|---|
| b_ageyr | >65 yrs | b_ageyr >65 yrs |
| histo | non endometroid | histo non endometroid |
| diff | medium-high | diff medium-high |
| b_FIGO | III-IV | b_FIGO III-IV |
| b_KCNA7 | normal | b_KCNA7 normal |

**TABLE 3.4: Multivariate diseae-free survival analysis**

The PHREG Procedure

Analysis of Maximum Likelihood Estimates

| Parameter | | Label |
|---|---|---|
| b_kcnh6 | normal | b_kcnh6 normal |

Analysis of Effects Eligible for Removal

| Effect | DF | Wald Chi-Square | Pr > ChiSq |
|---|---|---|---|
| b_ageyr | 1 | 0.1443 | 0.7040 |
| histo | 1 | 0.2076 | 0.6487 |
| diff | 1 | 3.4138 | 0.0647 |
| b_FIGO | 1 | 11.8958 | 0.0006 |
| b_KCNA7 | 1 | 0.5969 | 0.4398 |
| b_KCNH6 | 1 | 6.1780 | 0.0129 |

Step 3. Effect b_ageyr is removed. The model contains the following effects:

histo diff b_FIGO b_KCNA7 b_KCNH6

Convergence Status

Convergence criterion (GCONV=1E-8) satisfied.

Model Fit Statistics

| Criterion | Without Covariates | With Covariates |
|---|---|---|
| -2 LOG L | 173.827 | 135.311 |
| AIC | 173.827 | 145.311 |
| SBC | 173.827 | 150.534 |

Testing Global Null Hypothesis: BETA=0

| Test | Chi-Square | DF | Pr > ChiSq |
|---|---|---|---|
| Likelihood Ratio | 38.5162 | 5 | <.0001 |
| Score | 56.6190 | 5 | <.0001 |
| Wald | 36.7170 | 5 | <.0001 |

Type 3 Tests

| Effect | DF | Wald Chi-Square | Pr > ChiSq |
|---|---|---|---|
| histo | 1 | 0.4636 | 0.4959 |
| diff | 1 | 3.3980 | 0.0653 |
| b_FIGO | 1 | 12.2205 | 0.0005 |
| b_KCNA7 | 1 | 0.4638 | 0.4958 |
| b_KCNH6 | 1 | 6.1310 | 0.0133 |

Analysis of Maximum Likelihood Estimates

| Parameter | | DF | Parameter Estimate | Standard Error | Chi-Square | Pr > ChiSq | Hazard Ratio | 95% Hazard Ratio Confidence Limits | |
|---|---|---|---|---|---|---|---|---|---|
| histo | non endometroid | 1 | 0.39631 | 0.58204 | 0.4636 | 0.4959 | 1.486 | 0.475 | 4.651 |
| diff | medium-high | 1 | -1.20123 | 0.65165 | 3.3980 | 0.0653 | 0.301 | 0.084 | 1.079 |
| b_FIGO | III-IV | 1 | 2.07298 | 0.59299 | 12.2205 | 0.0005 | 7.948 | 2.486 | 25.412 |
| b_KCNA7 | normal | 1 | 0.34656 | 0.50886 | 0.4638 | 0.4958 | 1.414 | 0.522 | 3.834 |
| b_KCNH6 | normal | 1 | -1.67754 | 0.67750 | 6.1310 | 0.0133 | 0.187 | 0.050 | 0.705 |

**TABLE 3.4: Multivariate diseae-free survival analysis**

The PHREG Procedure

Analysis of Maximum Likelihood Estimates

| Parameter | | Label |
|---|---|---|
| histo | non endometroid | histo non endometroid |
| diff | medium-high | diff medium-high |
| b_FIGO | III-IV | b_FIGO III-IV |
| b_KCNA7 | normal | b_KCNA7 normal |
| b_KCNH6 | normal | b_kcnh6 normal |

Analysis of Effects Eligible for Removal

| Effect | DF | Wald Chi-Square | Pr > ChiSq |
|---|---|---|---|
| histo | 1 | 0.4636 | 0.4959 |
| diff | 1 | 3.3980 | 0.0653 |
| b_FIGO | 1 | 12.2205 | 0.0005 |
| b_KCNA7 | 1 | 0.4638 | 0.4958 |
| b_KCNH6 | 1 | 6.1310 | 0.0133 |

Step 4. Effect histo is removed. The model contains the following effects:

diff b_FIGO b_KCNA7 b_KCNH6

Convergence Status

Convergence criterion (GCONV=1E-8) satisfied.

Model Fit Statistics

| Criterion | Without Covariates | With Covariates |
|---|---|---|
| -2 LOG L | 173.827 | 135.776 |
| AIC | 173.827 | 143.776 |
| SBC | 173.827 | 147.954 |

Testing Global Null Hypothesis: BETA=0

| Test | Chi-Square | DF | Pr > ChiSq |
|---|---|---|---|
| Likelihood Ratio | 38.0511 | 4 | <.0001 |
| Score | 51.3198 | 4 | <.0001 |
| Wald | 35.7100 | 4 | <.0001 |

Type 3 Tests

| Effect | DF | Wald Chi-Square | Pr > ChiSq |
|---|---|---|---|
| diff | 1 | 5.1449 | 0.0233 |
| b_FIGO | 1 | 13.6991 | 0.0002 |
| b_KCNA7 | 1 | 0.7725 | 0.3795 |
| b_KCNH6 | 1 | 8.1263 | 0.0044 |

**TABLE 3.4: Multivariate diseae-free survival analysis**

The PHREG Procedure

Analysis of Maximum Likelihood Estimates

| Parameter | | DF | Parameter Estimate | Standard Error | Chi-Square | Pr > ChiSq | Hazard Ratio | 95% Hazard Ratio Confidence Limits | |
|---|---|---|---|---|---|---|---|---|---|
| diff | medium-high | 1 | -1.35877 | 0.59904 | 5.1449 | 0.0233 | 0.257 | 0.079 | 0.831 |
| b_FIGO | III-IV | 1 | 2.13704 | 0.57739 | 13.6991 | 0.0002 | 8.474 | 2.733 | 26.277 |
| b_KCNA7 | normal | 1 | 0.42762 | 0.48655 | 0.7725 | 0.3795 | 1.534 | 0.591 | 3.980 |
| b_KCNH6 | normal | 1 | -1.83310 | 0.64304 | 8.1263 | 0.0044 | 0.160 | 0.045 | 0.564 |

Analysis of Maximum Likelihood Estimates

| Parameter | | Label |
|---|---|---|
| diff | medium-high | diff medium-high |
| b_FIGO | III-IV | b_FIGO III-IV |
| b_KCNA7 | normal | b_KCNA7 normal |
| b_kcnh6 | normal | b_kcnh6 normal |

Analysis of Effects Eligible for Removal

| Effect | DF | Wald Chi-Square | Pr > ChiSq |
|---|---|---|---|
| diff | 1 | 5.1449 | 0.0233 |
| b_FIGO | 1 | 13.6991 | 0.0002 |
| b_KCNA7 | 1 | 0.7725 | 0.3795 |
| b_KCNH6 | 1 | 8.1263 | 0.0044 |

Step 5. Effect b_KCNA7 is removed. The model contains the following effects:

diff b_FIGO b_KCNH6

Convergence Status

Convergence criterion (GCONV=1E-8) satisfied.

Model Fit Statistics

| Criterion | Without Covariates | With Covariates |
|---|---|---|
| -2 LOG L | 173.827 | 136.527 |
| AIC | 173.827 | 142.527 |
| SBC | 173.827 | 145.661 |

Testing Global Null Hypothesis: BETA=0

| Test | Chi-Square | DF | Pr > ChiSq |
|---|---|---|---|
| Likelihood Ratio | 37.2999 | 3 | <.0001 |
| Score | 49.1107 | 3 | <.0001 |
| Wald | 34.0344 | 3 | <.0001 |

Type 3 Tests

| Effect | DF | Wald Chi-Square | Pr > ChiSq |
|---|---|---|---|
| diff | 1 | 5.8668 | 0.0154 |
| b_FIGO | 1 | 15.7018 | <.0001 |
| b_KCNH6 | 1 | 8.5779 | 0.0034 |

**TABLE 3.4: Multivariate diseae-free survival analysis**

The PHREG Procedure

Analysis of Maximum Likelihood Estimates

| Parameter | | DF | Parameter Estimate | Standard Error | Chi-Square | Pr > ChiSq | Hazard Ratio | 95% Hazard Ratio Confidence Limits | |
|---|---|---|---|---|---|---|---|---|---|
| diff | medium-high | 1 | -1.43018 | 0.59046 | 5.8668 | 0.0154 | 0.239 | 0.075 | 0.761 |
| b_FIGO | III-IV | 1 | 2.23855 | 0.56493 | 15.7018 | <.0001 | 9.380 | 3.100 | 28.383 |
| b_KCNH6 | normal | 1 | -1.90193 | 0.64939 | 8.5779 | 0.0034 | 0.149 | 0.042 | 0.533 |

Analysis of Maximum Likelihood Estimates

| Parameter | | Label |
|---|---|---|
| diff | medium-high | diff medium-high |
| b_FIGO | III-IV | b_FIGO III-IV |
| b_KCNH6 | normal | b_kcnh6 normal |

Analysis of Effects Eligible for Removal

| Effect | DF | Wald Chi-Square | Pr > ChiSq |
|---|---|---|---|
| diff | 1 | 5.8668 | 0.0154 |
| b_FIGO | 1 | 15.7018 | <.0001 |
| b_KCNH6 | 1 | 8.5779 | 0.0034 |

Analysis of Effects Eligible for Entry

| Effect | DF | Score Chi-Square | Pr > ChiSq |
|---|---|---|---|
| b_ageyr | 1 | 0.1649 | 0.6847 |
| histo | 1 | 0.7614 | 0.3829 |
| b_KCNA7 | 1 | 0.7807 | 0.3769 |
| b_LHCGR | 1 | 0.0366 | 0.8483 |
| b_HERG1 | 1 | 0.0476 | 0.8272 |

Residual Chi-Square Test

| Chi-Square | DF | Pr > ChiSq |
|---|---|---|
| 1.5032 | 5 | 0.9127 |

NOTE: No (additional) effects met the 0.05 level for entry into the model.

Summary of Stepwise Selection

| Step | Effect Entered | Effect Removed | DF | Number In | Score Chi-Square | Wald Chi-Square | Pr > ChiSq |
|---|---|---|---|---|---|---|---|
| 1 | | b_LHCGR | 1 | 7 | | 0.0645 | 0.7995 |
| 2 | | b_HERG1 | 1 | 6 | | 0.1095 | 0.7407 |
| 3 | | b_ageyr | 1 | 5 | | 0.1443 | 0.7040 |
| 4 | | histo | 1 | 4 | | 0.4636 | 0.4959 |
| 5 | | b_KCNA7 | 1 | 3 | | 0.7725 | 0.3795 |

# OVERALL SURVIVAL ANALYSIS

**TABLE 4.1: Overall survival by type of cohort**

| Variable | N | Number failed | 3-yr survival | Log-rank test p-value | Hazard ratio (95% CI) |
|---|---|---|---|---|---|
| Cohort | . | . | . | | |
| excluded | 11 | 2 | 0.8750 | 0.777 | 1 (ref.) |
| included | 101 | 17 | 0.7520 | | 1.24 (0.28-5.39) |

**TABLE 4.2: Overall survival of included cohort by clinical and biological characteristics**

| Variable | N | Number failed | 3-yr survival | Log-rank test p-value | Hazard ratio (95% CI) |
|---|---|---|---|---|---|
| Age | . | . | . | | |
| <=65 yrs | 50 | 6 | 0.8249 | 0.099 | 1 (ref.) |
| >65 yrs | 51 | 11 | 0.6900 | | 2.37 (0.82-6.83) |
| Histology | . | . | . | | |
| endometroid | 83 | 7 | 0.8734 | <0.001 | 1 (ref.) |
| non endometroid | 18 | 10 | 0.1717 | | 13.43 (4.65-38.76) |
| Differentiation | . | . | . | | |
| low | 40 | 13 | 0.4570 | <0.001 | 1 (ref.) |
| medium-high | 61 | 4 | 0.9361 | | 0.13 (0.04-0.44) |
| FIGO | . | . | . | | |
| I-II | 81 | 5 | 0.9113 | <0.001 | 1 (ref.) |
| III-IV | 20 | 12 | 0.1881 | | 18.27 (5.77-57.80) |
| FIGO | . | . | . | | |
| I | 67 | 5 | 0.8997 | <0.001 | 1 (ref.) |
| II | 14 | 0 | 1.0000 | | 0.00 (0.00-.) |
| III | 15 | 10 | 0.1795 | | 17.17 (5.31-55.55) |
| IV | 5 | 2 | 0 | | 11.35 (1.98-64.98) |
| Nodes | . | . | . | | |
| negative | 80 | 7 | 0.8539 | <0.001 | 1 (ref.) |
| positive | 12 | 8 | . | | 15.01 (5.12-44.05) |
| Ploidy | . | . | . | | |
| aneuploid | 26 | 7 | 0.5578 | 0.040 | 1 (ref.) |
| diploid | 57 | 6 | 0.8366 | | 0.34 (0.11-1.00) |
| b_KCNA7 | . | . | . | | |
| hyperexpressed | 80 | 10 | 0.8195 | 0.005 | 1 (ref.) |
| normal | 21 | 7 | 0.4829 | | 3.81 (1.41-10.30) |
| b_LHCGR | . | . | . | | |
| hyperexpressed | 56 | 13 | 0.6463 | 0.047 | 1 (ref.) |
| normal | 45 | 4 | 0.8706 | | 0.34 (0.11-1.04) |
| LHCGR / KCNA7 | . | . | . | | |
| - / - | 14 | 3 | 0.6713 | <0.001 | 1 (ref.) |
| + / - | 7 | 4 | 0 | | 5.58 (1.19-26.13) |
| - / + | 31 | 1 | 0.9565 | | 0.12 (0.01-1.15) |
| + / + | 49 | 9 | 0.7219 | | 0.77 (0.20-2.89) |

combi represents the combination of LHCGR and KCNA7, respectively

**TABLE 4.2: Overall survival of included cohort by clinical and biological characteristics**

| Variable | N | Number failed | 3-yr survival | Log-rank test p-value | Hazard ratio (95% CI) |
|---|---|---|---|---|---|
| b_KCNH6 | . | . | . | | |
| hyperexpressed | 73 | 13 | 0.7219 | 0.603 | 1 (ref.) |
| normal | 28 | 4 | 0.8045 | | 0.74 (0.24-2.31) |
| b_HERG1 | . | . | . | | |
| hyperexpressed | 91 | 14 | 0.7779 | 0.351 | 1 (ref.) |
| normal | 10 | 3 | 0.6000 | | 1.80 (0.51-6.35) |

**TABLE 4.3: Overall survival analysis: interaction between LHCGR and KCNA7**

The PHREG Procedure

Model Information

| | |
|---|---|
| Data Set | WORK.ENDOM |
| Dependent Variable | dos |
| Censoring Variable | los |
| Censoring Value(s) | 0 |
| Ties Handling | BRESLOW |

| | |
|---|---|
| Number of Observations Read | 101 |
| Number of Observations Used | 101 |

Class Level Information

| Class | Value | Design Variables |
|---|---|---|
| b_KCNA7 | hyperexpressed | 0 |
| | normal | 1 |
| b_LHCGR | hyperexpressed | 0 |
| | normal | 1 |

Summary of the Number of Event and Censored Values

| Total | Event | Censored | Percent Censored |
|---|---|---|---|
| 101 | 17 | 84 | 83.17 |

Convergence Status

Convergence criterion (GCONV=1E-8) satisfied.

Model Fit Statistics

| Criterion | Without Covariates | With Covariates |
|---|---|---|
| -2 LOG L | 131.934 | 116.436 |
| AIC | 131.934 | 122.436 |
| SBC | 131.934 | 124.936 |

Testing Global Null Hypothesis: BETA=0

| Test | Chi-Square | DF | Pr > ChiSq |
|---|---|---|---|
| Likelihood Ratio | 15.4976 | 3 | 0.0014 |
| Score | 24.5768 | 3 | <.0001 |
| Wald | 14.8925 | 3 | 0.0019 |

Type 3 Tests

| Effect | DF | Wald Chi-Square | Pr > ChiSq |
|---|---|---|---|
| b_KCNA7 | 1 | 9.4908 | 0.0021 |
| b_LHCGR | 1 | 3.0680 | 0.0798 |
| b_KCNA7*b_LHCGR | 1 | 0.0114 | 0.9149 |

**TABLE 4.3: Overall survival analysis: interaction between LHCGR and KCNA7**

The PHREG Procedure

Analysis of Maximum Likelihood Estimates

| Parameter | | | DF | Parameter Estimate | Standard Error | Chi-Square | Pr > ChiSq |
|---|---|---|---|---|---|---|---|
| b_KCNA7 | normal | | 1 | 1.98534 | 0.64444 | 9.4908 | 0.0021 |
| b_LHCGR | normal | | 1 | -1.85948 | 1.06160 | 3.0680 | 0.0798 |
| b_KCNA7*b_LHCGR | normal | normal | 1 | 0.14063 | 1.31628 | 0.0114 | 0.9149 |

Analysis of Maximum Likelihood Estimates

| Parameter | | | Hazard Ratio | 95% Hazard Ratio Confidence Limits | | Label |
|---|---|---|---|---|---|---|
| b_KCNA7 | normal | | . | . | . | b_KCNA7 normal |
| b_LHCGR | normal | | . | . | . | b_LHCGR normal |
| b_KCNA7*b_LHCGR | normal | normal | . | . | | b_KCNA7 normal * b_LHCGR normal |

Hazard Ratios for b_LHCGR

| Description | Point Estimate | 95% Wald Confidence Limits | |
|---|---|---|---|
| b_LHCGR normal vs hyperexpressed At b_KCNA7=hyperexpressed | 0.156 | 0.019 | 1.248 |
| b_LHCGR normal vs hyperexpressed At b_KCNA7=normal | 0.179 | 0.038 | 0.840 |

Hazard Ratios for b_KCNA7

| Description | Point Estimate | 95% Wald Confidence Limits | |
|---|---|---|---|
| b_KCNA7 normal vs hyperexpressed At b_LHCGR=hyperexpressed | 7.282 | 2.059 | 25.750 |
| b_KCNA7 normal vs hyperexpressed At b_LHCGR=normal | 8.381 | 0.869 | 80.786 |

**TABLE 4.4: Multivariate overall survival analysis**

The PHREG Procedure

Model Information

| | |
|---|---|
| Data Set | WORK.ENDOM |
| Dependent Variable | dos |
| Censoring Variable | los |
| Censoring Value(s) | 0 |
| Ties Handling | BRESLOW |

| | |
|---|---|
| Number of Observations Read | 101 |
| Number of Observations Used | 101 |

Class Level Information

| Class | Value | Design Variables |
|---|---|---|
| b_ageyr | <=65 yrs | 0 |
| | >65 yrs | 1 |
| histo | endometroid | 0 |
| | non endometroid | 1 |
| diff | low | 0 |
| | medium-high | 1 |
| b_FIGO | I-II | 0 |
| | III-IV | 1 |
| b_KCNA7 | hyperexpressed | 0 |
| | normal | 1 |
| b_LHCGR | hyperexpressed | 0 |
| | normal | 1 |
| b_KCNH6 | hyperexpressed | 0 |
| | normal | 1 |
| b_HERG1 | hyperexpressed | 0 |
| | normal | 1 |

Summary of the Number of Event and Censored Values

| Total | Event | Censored | Percent Censored |
|---|---|---|---|
| 101 | 17 | 84 | 83.17 |

Step 0. The model contains the following effects:

b_ageyr histo diff b_FIGO b_KCNA7 b_LHCGR b_KCNH6 b_HERG1

Convergence Status

Convergence criterion (GCONV=1E-8) satisfied.

Model Fit Statistics

| Criterion | Without Covariates | With Covariates |
|---|---|---|
| -2 LOG L | 131.934 | 88.565 |
| AIC | 131.934 | 104.565 |
| SBC | 131.934 | 111.231 |

**TABLE 4.4: Multivariate overall survival analysis**

The PHREG Procedure

Testing Global Null Hypothesis: BETA=0

| Test | Chi-Square | DF | Pr > ChiSq |
|---|---|---|---|
| Likelihood Ratio | 43.3681 | 8 | <.0001 |
| Score | 70.5907 | 8 | <.0001 |
| Wald | 32.7540 | 8 | <.0001 |

Type 3 Tests

| Effect | DF | Wald Chi-Square | Pr > ChiSq |
|---|---|---|---|
| b_ageyr | 1 | 0.3465 | 0.5561 |
| histo | 1 | 1.1034 | 0.2935 |
| diff | 1 | 0.0009 | 0.9760 |
| b_FIGO | 1 | 9.6752 | 0.0019 |
| b_KCNA7 | 1 | 2.7872 | 0.0950 |
| b_LHCGR | 1 | 0.7441 | 0.3884 |
| b_KCNH6 | 1 | 0.4287 | 0.5126 |
| b_HERG1 | 1 | 0.6866 | 0.4073 |

Analysis of Maximum Likelihood Estimates

| Parameter | | DF | Parameter Estimate | Standard Error | Chi-Square | Pr > ChiSq | Hazard Ratio | 95% Hazard Ratio Confidence Limits | |
|---|---|---|---|---|---|---|---|---|---|
| b_ageyr | >65 yrs | 1 | 0.43073 | 0.73175 | 0.3465 | 0.5561 | 1.538 | 0.367 | 6.456 |
| histo | non endometroid | 1 | 1.00067 | 0.95262 | 1.1034 | 0.2935 | 2.720 | 0.420 | 17.598 |
| diff | medium-high | 1 | -0.02862 | 0.95040 | 0.0009 | 0.9760 | 0.972 | 0.151 | 6.260 |
| b_FIGO | III-IV | 1 | 2.66552 | 0.85694 | 9.6752 | 0.0019 | 14.375 | 2.680 | 77.099 |
| b_KCNA7 | normal | 1 | 1.11663 | 0.66885 | 2.7872 | 0.0950 | 3.055 | 0.823 | 11.331 |
| b_LHCGR | normal | 1 | -0.69001 | 0.79992 | 0.7441 | 0.3884 | 0.502 | 0.105 | 2.406 |
| b_kcnh6 | normal | 1 | -0.45412 | 0.69354 | 0.4287 | 0.5126 | 0.635 | 0.163 | 2.472 |
| b_HERG1 | normal | 1 | -0.76518 | 0.92341 | 0.6866 | 0.4073 | 0.465 | 0.076 | 2.842 |

Analysis of Maximum Likelihood Estimates

| Parameter | | Label |
|---|---|---|
| b_ageyr | >65 yrs | b_ageyr >65 yrs |
| histo | non endometroid | histo non endometroid |
| diff | medium-high | diff medium-high |
| b_FIGO | III-IV | b_FIGO III-IV |
| b_KCNA7 | normal | b_KCNA7 normal |
| b_LHCGR | normal | b_LHCGR normal |
| b_KCNH6 | normal | b_kcnh6 normal |
| b_HERG1 | normal | b_HERG1 normal |

Analysis of Effects Eligible for Removal

| Effect | DF | Wald Chi-Square | Pr > ChiSq |
|---|---|---|---|
| b_ageyr | 1 | 0.3465 | 0.5561 |
| histo | 1 | 1.1034 | 0.2935 |
| diff | 1 | 0.0009 | 0.9760 |
| b_FIGO | 1 | 9.6752 | 0.0019 |
| b_KCNA7 | 1 | 2.7872 | 0.0950 |
| b_LHCGR | 1 | 0.7441 | 0.3884 |
| b_KCNH6 | 1 | 0.4287 | 0.5126 |
| b_HERG1 | 1 | 0.6866 | 0.4073 |

Step 1. Effect diff is removed. The model contains the following effects:

b_ageyr histo b_FIGO b_KCNA7 b_LHCGR b_KCNH6 b_HERG1

**TABLE 4.4: Multivariate overall survival analysis**

The PHREG Procedure

Convergence Status

Convergence criterion (GCONV=1E-8) satisfied.

Model Fit Statistics

| Criterion | Without Covariates | With Covariates |
|---|---|---|
| -2 LOG L | 131.934 | 88.566 |
| AIC | 131.934 | 102.566 |
| SBC | 131.934 | 108.399 |

Testing Global Null Hypothesis: BETA=0

| Test | Chi-Square | DF | Pr > ChiSq |
|---|---|---|---|
| Likelihood Ratio | 43.3672 | 7 | <.0001 |
| Score | 68.7636 | 7 | <.0001 |
| Wald | 32.7422 | 7 | <.0001 |

Type 3 Tests

| Effect | DF | Wald Chi-Square | Pr > ChiSq |
|---|---|---|---|
| b_ageyr | 1 | 0.3487 | 0.5548 |
| histo | 1 | 1.5544 | 0.2125 |
| b_FIGO | 1 | 11.1919 | 0.0008 |
| b_KCNA7 | 1 | 2.8226 | 0.0929 |
| b_LHCGR | 1 | 0.7625 | 0.3825 |
| b_KCNH6 | 1 | 0.4284 | 0.5128 |
| b_HERG1 | 1 | 0.6892 | 0.4064 |

Analysis of Maximum Likelihood Estimates

| Parameter | | DF | Parameter Estimate | Standard Error | Chi-Square | Pr > ChiSq | Hazard Ratio | 95% Hazard Ratio Confidence Limits | |
|---|---|---|---|---|---|---|---|---|---|
| b_ageyr | >65 yrs | 1 | 0.43152 | 0.73074 | 0.3487 | 0.5548 | 1.540 | 0.368 | 6.448 |
| histo | non endometroid | 1 | 1.01562 | 0.81461 | 1.5544 | 0.2125 | 2.761 | 0.559 | 13.629 |
| b_FIGO | III-IV | 1 | 2.67489 | 0.79957 | 11.1919 | 0.0008 | 14.511 | 3.028 | 69.548 |
| b_KCNA7 | normal | 1 | 1.11399 | 0.66307 | 2.8226 | 0.0929 | 3.046 | 0.831 | 11.174 |
| b_LHCGR | normal | 1 | -0.68548 | 0.78499 | 0.7625 | 0.3825 | 0.504 | 0.108 | 2.347 |
| b_KCNH6 | normal | 1 | -0.45278 | 0.69176 | 0.4284 | 0.5128 | 0.636 | 0.164 | 2.467 |
| b_HERG1 | normal | 1 | -0.76229 | 0.91823 | 0.6892 | 0.4064 | 0.467 | 0.077 | 2.822 |

Analysis of Maximum Likelihood Estimates

| Parameter | | Label |
|---|---|---|
| b_ageyr | >65 yrs | b_ageyr >65 yrs |
| histo | non endometroid | histo non endometroid |
| b_FIGO | III-IV | b_FIGO III-IV |
| b_KCNA7 | normal | b_KCNA7 normal |
| b_LHCGR | normal | b_LHCGR normal |
| b_KCNH6 | normal | b_KCNH6 normal |
| b_HERG1 | normal | b_HERG1 normal |

Analysis of Effects Eligible for Removal

| Effect | DF | Wald Chi-Square | Pr > ChiSq |
|---|---|---|---|
| b_ageyr | 1 | 0.3487 | 0.5548 |
| histo | 1 | 1.5544 | 0.2125 |
| b_FIGO | 1 | 11.1919 | 0.0008 |
| b_KCNA7 | 1 | 2.8226 | 0.0929 |

TABLE 4.4: Multivariate overall survival analysis

The PHREG Procedure

Analysis of Effects Eligible for Removal

| Effect | DF | Wald Chi-Square | Pr > ChiSq |
|---|---|---|---|
| b_LHCGR | 1 | 0.7625 | 0.3825 |
| b_KCNH6 | 1 | 0.4284 | 0.5128 |
| b_HERG1 | 1 | 0.6892 | 0.4064 |

Step 2. Effect b_ageyr is removed. The model contains the following effects:

histo b_FIGO b_KCNA7 b_LHCGR b_kcnh6 b_HERG1

Convergence Status

Convergence criterion (GCONV=1E-8) satisfied.

Model Fit Statistics

| Criterion | Without Covariates | With Covariates |
|---|---|---|
| -2 LOG L | 131.934 | 88.920 |
| AIC | 131.934 | 100.920 |
| SBC | 131.934 | 105.919 |

Testing Global Null Hypothesis: BETA=0

| Test | Chi-Square | DF | Pr > ChiSq |
|---|---|---|---|
| Likelihood Ratio | 43.0134 | 6 | <.0001 |
| Score | 68.6730 | 6 | <.0001 |
| Wald | 31.9506 | 6 | <.0001 |

Type 3 Tests

| Effect | DF | Wald Chi-Square | Pr > ChiSq |
|---|---|---|---|
| histo | 1 | 1.8053 | 0.1791 |
| b_FIGO | 1 | 12.4582 | 0.0004 |
| b_KCNA7 | 1 | 2.4400 | 0.1183 |
| b_LHCGR | 1 | 1.0020 | 0.3168 |
| b_KCNH6 | 1 | 0.2669 | 0.6054 |
| b_HERG1 | 1 | 1.5454 | 0.2138 |

Analysis of Maximum Likelihood Estimates

| Parameter | | DF | Parameter Estimate | Standard Error | Chi-Square | Pr > ChiSq | Hazard Ratio | 95% Hazard Ratio Confidence Limits | |
|---|---|---|---|---|---|---|---|---|---|
| histo | non endometroid | 1 | 1.07556 | 0.80049 | 1.8053 | 0.1791 | 2.932 | 0.611 | 14.076 |
| b_FIGO | III-IV | 1 | 2.79578 | 0.79209 | 12.4582 | 0.0004 | 16.375 | 3.467 | 77.343 |
| b_KCNA7 | normal | 1 | 1.03841 | 0.66478 | 2.4400 | 0.1183 | 2.825 | 0.768 | 10.395 |
| b_LHCGR | normal | 1 | -0.75293 | 0.75216 | 1.0020 | 0.3168 | 0.471 | 0.108 | 2.057 |
| b_KCNH6 | normal | 1 | -0.33677 | 0.65185 | 0.2669 | 0.6054 | 0.714 | 0.199 | 2.562 |
| b_HERG1 | normal | 1 | -1.02656 | 0.82578 | 1.5454 | 0.2138 | 0.358 | 0.071 | 1.807 |

Analysis of Maximum Likelihood Estimates

| Parameter | | Label |
|---|---|---|
| histo | non endometroid | histo non endometroid |
| b_FIGO | III-IV | b_FIGO III-IV |
| b_KCNA7 | normal | b_KCNA7 normal |
| b_LHCGR | normal | b_LHCGR normal |
| b_KCNH6 | normal | b_KCNH6 normal |

**TABLE 4.4: Multivariate overall survival analysis**

The PHREG Procedure

Analysis of Maximum Likelihood Estimates

| Parameter | | Label |
|---|---|---|
| b_HERG1 | normal | b_HERG1 normal |

Analysis of Effects Eligible for Removal

| Effect | DF | Wald Chi-Square | Pr > ChiSq |
|---|---|---|---|
| histo | 1 | 1.8053 | 0.1791 |
| b_FIGO | 1 | 12.4582 | 0.0004 |
| b_KCNA7 | 1 | 2.4400 | 0.1183 |
| b_LHCGR | 1 | 1.0020 | 0.3168 |
| b_KCNH6 | 1 | 0.2669 | 0.6054 |
| b_HERG1 | 1 | 1.5454 | 0.2138 |

Step 3. Effect b_kcnh6 is removed. The model contains the following effects:

histo b_FIGO b_KCNA7 b_LHCGR b_HERG1

Convergence Status

Convergence criterion (GCONV=1E-8) satisfied.

Model Fit Statistics

| Criterion | Without Covariates | With Covariates |
|---|---|---|
| -2 LOG L | 131.934 | 89.198 |
| AIC | 131.934 | 99.198 |
| SBC | 131.934 | 103.364 |

Testing Global Null Hypothesis: BETA=0

| Test | Chi-Square | DF | Pr > ChiSq |
|---|---|---|---|
| Likelihood Ratio | 42.7352 | 5 | <.0001 |
| Score | 68.5341 | 5 | <.0001 |
| Wald | 32.2803 | 5 | <.0001 |

Type 3 Tests

| Effect | DF | Wald Chi-Square | Pr > ChiSq |
|---|---|---|---|
| histo | 1 | 2.0005 | 0.1572 |
| b_FIGO | 1 | 12.4520 | 0.0004 |
| b_KCNA7 | 1 | 2.5752 | 0.1086 |
| b_LHCGR | 1 | 1.1125 | 0.2915 |
| b_HERG1 | 1 | 1.5907 | 0.2072 |

Analysis of Maximum Likelihood Estimates

| Parameter | | DF | Parameter Estimate | Standard Error | Chi-Square | Pr > ChiSq | Hazard Ratio | 95% Hazard Ratio Confidence Limits | |
|---|---|---|---|---|---|---|---|---|---|
| histo | non endometroid | 1 | 1.14431 | 0.80904 | 2.0005 | 0.1572 | 3.140 | 0.643 | 15.333 |
| b_FIGO | III-IV | 1 | 2.69330 | 0.76325 | 12.4520 | 0.0004 | 14.780 | 3.311 | 65.972 |
| b_KCNA7 | normal | 1 | 1.05165 | 0.65534 | 2.5752 | 0.1086 | 2.862 | 0.792 | 10.341 |
| b_LHCGR | normal | 1 | -0.80554 | 0.76372 | 1.1125 | 0.2915 | 0.447 | 0.100 | 1.996 |
| b_HERG1 | normal | 1 | -1.03501 | 0.82064 | 1.5907 | 0.2072 | 0.355 | 0.071 | 1.774 |

**TABLE 4.4: Multivariate overall survival analysis**

The PHREG Procedure

Analysis of Maximum Likelihood Estimates

| Parameter | | Label |
|---|---|---|
| histo | non endometroid | histo non endometroid |
| b_FIGO | III-IV | b_FIGO III-IV |
| b_KCNA7 | normal | b_KCNA7 normal |
| b_LHCGR | normal | b_LHCGR normal |
| b_HERG1 | normal | b_HERG1 normal |

Analysis of Effects Eligible for Removal

| Effect | DF | Wald Chi-Square | Pr > ChiSq |
|---|---|---|---|
| histo | 1 | 2.0005 | 0.1572 |
| b_FIGO | 1 | 12.4520 | 0.0004 |
| b_KCNA7 | 1 | 2.5752 | 0.1086 |
| b_LHCGR | 1 | 1.1125 | 0.2915 |
| b_HERG1 | 1 | 1.5907 | 0.2072 |

Step 4. Effect b_LHCGR is removed. The model contains the following effects:

histo b_FIGO b_KCNA7 b_HERG1

Convergence Status

Convergence criterion (GCONV=1E-8) satisfied.

Model Fit Statistics

| Criterion | Without Covariates | With Covariates |
|---|---|---|
| -2 LOG L | 131.934 | 90.351 |
| AIC | 131.934 | 98.351 |
| SBC | 131.934 | 101.684 |

Testing Global Null Hypothesis: BETA=0

| Test | Chi-Square | DF | Pr > ChiSq |
|---|---|---|---|
| Likelihood Ratio | 41.5824 | 4 | <.0001 |
| Score | 66.7394 | 4 | <.0001 |
| Wald | 31.9970 | 4 | <.0001 |

Type 3 Tests

| Effect | DF | Wald Chi-Square | Pr > ChiSq |
|---|---|---|---|
| histo | 1 | 6.7222 | 0.0095 |
| b_FIGO | 1 | 12.7007 | 0.0004 |
| b_KCNA7 | 1 | 1.8980 | 0.1683 |
| b_HERG1 | 1 | 1.3835 | 0.2395 |

**TABLE 4.4: Multivariate overall survival analysis**

The PHREG Procedure

Analysis of Maximum Likelihood Estimates

| Parameter | | DF | Parameter Estimate | Standard Error | Chi-Square | Pr > ChiSq | Hazard Ratio | 95% Hazard Ratio Confidence Limits | |
|---|---|---|---|---|---|---|---|---|---|
| histo | non endometroid | 1 | 1.68072 | 0.64825 | 6.7222 | 0.0095 | 5.369 | 1.507 | 19.130 |
| b_FIGO | III-IV | 1 | 2.51188 | 0.70483 | 12.7007 | 0.0004 | 12.328 | 3.097 | 49.074 |
| b_KCNA7 | normal | 1 | 0.84435 | 0.61288 | 1.8980 | 0.1683 | 2.326 | 0.700 | 7.734 |
| b_HERG1 | normal | 1 | -0.93817 | 0.79760 | 1.3835 | 0.2395 | 0.391 | 0.082 | 1.868 |

Analysis of Maximum Likelihood Estimates

| Parameter | | Label |
|---|---|---|
| histo | non endometroid | histo non endometroid |
| b_FIGO | III-IV | b_FIGO III-IV |
| b_KCNA7 | normal | b_KCNA7 normal |
| b_HERG1 | normal | b_HERG1 normal |

Analysis of Effects Eligible for Removal

| Effect | DF | Wald Chi-Square | Pr > ChiSq |
|---|---|---|---|
| histo | 1 | 6.7222 | 0.0095 |
| b_FIGO | 1 | 12.7007 | 0.0004 |
| b_KCNA7 | 1 | 1.8980 | 0.1683 |
| b_HERG1 | 1 | 1.3835 | 0.2395 |

Step 5. Effect b_HERG1 is removed. The model contains the following effects:

histo b_FIGO b_KCNA7

Convergence Status

Convergence criterion (GCONV=1E-8) satisfied.

Model Fit Statistics

| Criterion | Without Covariates | With Covariates |
|---|---|---|
| -2 LOG L | 131.934 | 91.865 |
| AIC | 131.934 | 97.865 |
| SBC | 131.934 | 100.365 |

Testing Global Null Hypothesis: BETA=0

| Test | Chi-Square | DF | Pr > ChiSq |
|---|---|---|---|
| Likelihood Ratio | 40.0683 | 3 | <.0001 |
| Score | 65.0175 | 3 | <.0001 |
| Wald | 31.6119 | 3 | <.0001 |

Type 3 Tests

| Effect | DF | Wald Chi-Square | Pr > ChiSq |
|---|---|---|---|
| histo | 1 | 7.8982 | 0.0049 |
| b_FIGO | 1 | 11.9497 | 0.0005 |
| b_KCNA7 | 1 | 0.7307 | 0.3926 |

**TABLE 4.4: Multivariate overall survival analysis**

The PHREG Procedure

Analysis of Maximum Likelihood Estimates

| Parameter | | DF | Parameter Estimate | Standard Error | Chi-Square | Pr > ChiSq | Hazard Ratio | 95% Hazard Ratio Confidence Limits | |
|---|---|---|---|---|---|---|---|---|---|
| histo | non endometroid | 1 | 1.78603 | 0.63551 | 7.8982 | 0.0049 | 5.966 | 1.717 | 20.731 |
| b_FIGO | III-IV | 1 | 2.28625 | 0.66137 | 11.9497 | 0.0005 | 9.838 | 2.691 | 35.964 |
| b_KCNA7 | normal | 1 | 0.46749 | 0.54688 | 0.7307 | 0.3926 | 1.596 | 0.546 | 4.662 |

Analysis of Maximum Likelihood Estimates

| Parameter | | Label |
|---|---|---|
| histo | non endometroid | histo non endometroid |
| b_FIGO | III-IV | b_FIGO III-IV |
| b_KCNA7 | normal | b_KCNA7 normal |

Analysis of Effects Eligible for Removal

| Effect | DF | Wald Chi-Square | Pr > ChiSq |
|---|---|---|---|
| histo | 1 | 7.8982 | 0.0049 |
| b_FIGO | 1 | 11.9497 | 0.0005 |
| b_KCNA7 | 1 | 0.7307 | 0.3926 |

Step 6. Effect b_KCNA7 is removed. The model contains the following effects:

histo b_FIGO

Convergence Status

Convergence criterion (GCONV=1E-8) satisfied.

Model Fit Statistics

| Criterion | Without Covariates | With Covariates |
|---|---|---|
| -2 LOG L | 131.934 | 92.583 |
| AIC | 131.934 | 96.583 |
| SBC | 131.934 | 98.250 |

Testing Global Null Hypothesis: BETA=0

| Test | Chi-Square | DF | Pr > ChiSq |
|---|---|---|---|
| Likelihood Ratio | 39.3501 | 2 | <.0001 |
| Score | 62.3724 | 2 | <.0001 |
| Wald | 30.1892 | 2 | <.0001 |

Type 3 Tests

| Effect | DF | Wald Chi-Square | Pr > ChiSq |
|---|---|---|---|
| histo | 1 | 9.1779 | 0.0024 |
| b_FIGO | 1 | 14.0694 | 0.0002 |

**TABLE 4.4: Multivariate overall survival analysis**

The PHREG Procedure

Analysis of Maximum Likelihood Estimates

| Parameter | | DF | Parameter Estimate | Standard Error | Chi-Square | Pr > ChiSq | Hazard Ratio | 95% Hazard Ratio Confidence Limits | |
|---|---|---|---|---|---|---|---|---|---|
| histo | non endometroid | 1 | 1.86941 | 0.61707 | 9.1779 | 0.0024 | 6.484 | 1.935 | 21.733 |
| b_FIGO | III-IV | 1 | 2.39921 | 0.63963 | 14.0694 | 0.0002 | 11.014 | 3.144 | 38.585 |

Analysis of Maximum Likelihood Estimates

| Parameter | | Label |
|---|---|---|
| histo | non endometroid | histo non endometroid |
| b_FIGO | III-IV | b_FIGO III-IV |

Analysis of Effects Eligible for Removal

| Effect | DF | Wald Chi-Square | Pr > ChiSq |
|---|---|---|---|
| histo | 1 | 9.1779 | 0.0024 |
| b_FIGO | 1 | 14.0694 | 0.0002 |

Analysis of Effects Eligible for Entry

| Effect | DF | Score Chi-Square | Pr > ChiSq |
|---|---|---|---|
| b_ageyr | 1 | 0.1456 | 0.7028 |
| diff | 1 | 0.1617 | 0.6876 |
| b_KCNA7 | 1 | 0.7397 | 0.3898 |
| b_LHCGR | 1 | 0.5282 | 0.4674 |
| b_KCNH6 | 1 | 0.5508 | 0.4580 |
| b_HERG1 | 1 | 0.3897 | 0.5325 |

Residual Chi-Square Test

| Chi-Square | DF | Pr > ChiSq |
|---|---|---|
| 4.3071 | 6 | 0.6352 |

NOTE: No (additional) effects met the 0.05 level for entry into the model.

Summary of Stepwise Selection

| Step | Effect Entered | Effect Removed | DF | Number In | Score Chi-Square | Wald Chi-Square | Pr > ChiSq |
|---|---|---|---|---|---|---|---|
| 1 | | diff | 1 | 7 | | 0.0009 | 0.9760 |
| 2 | | b_ageyr | 1 | 6 | | 0.3487 | 0.5548 |
| 3 | | b_KCNH6 | 1 | 5 | | 0.2669 | 0.6054 |
| 4 | | b_LHCGR | 1 | 4 | | 1.1125 | 0.2915 |
| 5 | | b_HERG1 | 1 | 3 | | 1.3835 | 0.2395 |
| 6 | | b_KCNA7 | 1 | 2 | | 0.7307 | |

**ACKNOWLEDGMENTS**

I thank Annarosa Arcangeli, Ivo Noci, Luca Boni, Helga B. Salvesen, Massimo D'Amico, Elena Morelli, Pasquale Laise, Serena Pillozzi, Marika Masselli, Luca Gasparoli, Sara Falsini, Alberto Magi and Olivia Crociani.